A complex system approach to assess the beef cattle industry robustness against biosecurity threats

by

Qihui Yang

B.S., Harbin Institute of Technology, 2012

M.S., Harbin Institute of Technology, 2015

M.S., Delft University of Technology, 2017

AN ABSTRACT OF A DISSERTATION

submitted in partial fulfillment of the
requirements for the degree

DOCTOR OF PHILOSOPHY

Mike Wiegers Department of Electrical and Computer Engineering
Carl R. Ice College of Engineering

KANSAS STATE UNIVERSITY
Manhattan, Kansas

2021

Abstract

Modern infrastructure systems have become increasingly interconnected, and this includes those in the agricultural industry. Although this interdependence enables the economic functioning of the interdependent system, it also brings vulnerabilities to the system amplifying disease spreading and natural disaster consequences. With this background, this dissertation aims to investigate behaviors of complex systems facing biosecurity challenges from different perspectives.

First, we develop an agent-based model simulating the beef cattle production and related transportation services in southwest Kansas, United States. We evaluate the robustness of the interdependent system by constructing hypothetical disruptions in both the cattle industry and the transportation industry. We observe that the system is robust to random failures but vulnerable to the targeted shutdown of cattle premises or truck premises. In addition, disruptions in the trucks serving packers have the worst impact on cattle production, as compared to other transportation disruptions. In disaster preparations, policymakers need to pay particular attention to one of its critical components, meat packers.

Second, we assess the impact of truck contamination and information sharing on the foot-and-mouth disease transmission. Scenario analyses results show that including indirect contact routes between premises via truck movements can significantly increase the amplitude of disease spread, compared with equivalent scenarios that only consider animal movement. We find that mitigation strategies informed by information sharing can effectively mitigate epidemics, highlighting the benefit of promoting information sharing in the cattle industry.

Third, we examine the impact of human behavior factors on a hypothetical foot-and-mouth disease outbreak. The simulation results indicate that heterogeneity of individuals regarding risk attitudes significantly affects the epidemic dynamics, and human-behavior factors need to be considered for improved epidemic forecasting. With the same initial

biosecurity status, the number of infected producer locations and cattle losses can be more effectively reduced with an increase in the percentage of risk-averse producers selecting large producers first compared to randomly selecting producers. In addition, the reduction in epidemic size caused by the shifting of producers' risk attitudes towards risk-aversion is heavily dependent on the distribution of the initial biosecurity level.

Fourth, we study the robustness of supply chain networks against cascading failures. The simulation results show that the system is relatively robust against load fluctuations but is more fragile to demand shocks. For the underload-driven model without the recovery process, we find the existence of a discontinuous phase transition. Compared to other systems studied under overload cascading failures, this system is more robust for power-law distributions than uniform distributions of the lower bound parameter for the studied scenarios.

Finally, it is critical to prevent the 2019 novel coronavirus disease spread, which has left significant economic consequences to the U.S. beef industry. Several slaughterhouses were forced to stop operations temporarily due to outbreaks identified among meat-processing workers, causing sharp disruptions in beef production. We use network-based modeling to examine the impact of non-pharmaceutical interventions on the coronavirus disease spreading with various scenarios. Although the method is applied to simulate the early stage of epidemic dynamics in Hubei province, China, the model developed can be easily adapted to other regions. The simulation results show that without continued control measures, the epidemic in Hubei Province could have become persistent. Only by continuing to decrease the infection rate through protective measures and social distancing can the actual epidemic trajectory that happened in Hubei Province be reconstructed in simulation.

In summary, we develop several computational models for robustness assessment and epidemic prediction and control in this dissertation. The outcomes are expected to raise awareness of vulnerabilities in the interconnected systems and benefit existing disaster preparedness.

A complex system approach to assess the beef cattle industry robustness against biosecurity threats

by

Qihui Yang

B.S., Harbin Institute of Technology, 2012

M.S., Harbin Institute of Technology, 2015

M.S., Delft University of Technology, 2017

A DISSERTATION

submitted in partial fulfillment of the
requirements for the degree

DOCTOR OF PHILOSOPHY

Mike Wiegers Department of Electrical and Computer Engineering
Carl R. Ice College of Engineering

KANSAS STATE UNIVERSITY
Manhattan, Kansas

2021

Approved by:

Co-Major Professor
Caterina Scoglio

Approved by:

Co-Major Professor
Don Gruenbacher

Copyright

Abstract

Modern infrastructure systems have become increasingly interconnected, and this includes those in the agricultural industry. Although this interdependence enables the economic functioning of the interdependent system, it also brings vulnerabilities to the system amplifying disease spreading and natural disaster consequences. With this background, this dissertation aims to investigate behaviors of complex systems facing biosecurity challenges from different perspectives.

First, we develop an agent-based model simulating the beef cattle production and related transportation services in southwest Kansas, United States. We evaluate the robustness of the interdependent system by constructing hypothetical disruptions in both the cattle industry and the transportation industry. We observe that the system is robust to random failures but vulnerable to the targeted shutdown of cattle premises or truck premises. In addition, disruptions in the trucks serving packers have the worst impact on cattle production, as compared to other transportation disruptions. In disaster preparations, policymakers need to pay particular attention to one of its critical components, meat packers.

Second, we assess the impact of truck contamination and information sharing on the foot-and-mouth disease transmission. Scenario analyses results show that including indirect contact routes between premises via truck movements can significantly increase the amplitude of disease spread, compared with equivalent scenarios that only consider animal movement. We find that mitigation strategies informed by information sharing can effectively mitigate epidemics, highlighting the benefit of promoting information sharing in the cattle industry.

Third, we examine the impact of human behavior factors on a hypothetical foot-and-mouth disease outbreak. The simulation results indicate that heterogeneity of individuals regarding risk attitudes significantly affects the epidemic dynamics, and human-behavior factors need to be considered for improved epidemic forecasting. With the same initial

biosecurity status, the number of infected producer locations and cattle losses can be more effectively reduced with an increase in the percentage of risk-averse producers selecting large producers first compared to randomly selecting producers. In addition, the reduction in epidemic size caused by the shifting of producers' risk attitudes towards risk-aversion is heavily dependent on the distribution of the initial biosecurity level.

Fourth, we study the robustness of supply chain networks against cascading failures. The simulation results show that the system is relatively robust against load fluctuations but is more fragile to demand shocks. For the underload-driven model without the recovery process, we find the existence of a discontinuous phase transition. Compared to other systems studied under overload cascading failures, this system is more robust for power-law distributions than uniform distributions of the lower bound parameter for the studied scenarios.

Finally, it is critical to prevent the 2019 novel coronavirus disease spread, which has left significant economic consequences to the U.S. beef industry. Several slaughterhouses were forced to stop operations temporarily due to outbreaks identified among meat-processing workers, causing sharp disruptions in beef production. We use network-based modeling to examine the impact of non-pharmaceutical interventions on the coronavirus disease spreading with various scenarios. Although the method is applied to simulate the early stage of epidemic dynamics in Hubei province, China, the model developed can be easily adapted to other regions. The simulation results show that without continued control measures, the epidemic in Hubei Province could have become persistent. Only by continuing to decrease the infection rate through protective measures and social distancing can the actual epidemic trajectory that happened in Hubei Province be reconstructed in simulation.

In summary, we develop several computational models for robustness assessment and epidemic prediction and control in this dissertation. The outcomes are expected to raise awareness of vulnerabilities in the interconnected systems and benefit existing disaster preparedness.

Table of Contents

List of Figures

List of Tables

Acknowledgments

First and foremost, I would like to express my sincere gratitude to my advisors, Dr. Don Gruenbacher and Dr. Caterina Scoglio, for their continuous support, encouragement, trust, and patience. What I have learned from them over these years will accompany me for the rest of my life. I am extremely grateful to my committee members, Dr. Jessica Heier Stamm and Dr. David Amrine, for their precious time and constructive comments on my work. I also want to thank Dr. Daniel Andresen for serving as the outside chairperson of the examining committee for this doctoral degree.

I am incredibly grateful to Dr. Gary Brase and Dr. Scott DeLoach for their support and guidance on my research work. Special thanks to Dr. Martin de Jong and Dr. Haiyan Lu at TU Delft for collaborating on 'A network-based approach to model the development of city branding in China,' which is my first journal publication. I want to thank my friends, Xin Li, Haotian Wu, Xinya Wang, Wenting Ma, Sheng Cang, Yun Wang, Wenji Zhang, Lawryn Edmonds, Hang Zhang, Futing Fan, Junyao Kuang, Chunlin Yi, and many others for all the happy times we spent together.

Lastly, I owe gratitude to my family members for their endless love throughout my life. Without encouragement from my parents, it would be impossible for me to complete this doctoral degree. They are the best friends in my life, with whom I share my happiness and sorrow every day during this long journey.

Dedication

To my beloved daughter Iris.

Preface

This dissertation, "A complex system approach to assess the beef cattle industry robustness against biosecurity threats," is submitted for the degree of Doctor of Philosophy in the Department of Electrical and Computer Engineering at Kansas State University. The research was conducted under the supervision of Professors Caterina Scoglio and Don Gruenbacher.

To the best of my knowledge, this work is original, except where acknowledgements and references are indicated. Most of the work has been presented in the following published or submitted peer-reviewed journals:

- Qihui Yang, Don Gruenbacher, Jessica L Heier Stamm, Gary L Brase, Scott A DeLoach, David E Amrine, and Caterina Scoglio. Developing an agent-based model to simulate the beef cattle production and transportation in southwest Kansas. Physica A: Statistical Mechanics and its Applications, 526:120856, 2019.

- Qihui Yang, Don M Gruenbacher, Jessica L Heier Stamm, David E Amrine, Gary L Brase, Scott A DeLoach, and Caterina M Scoglio. Impact of truck contamination and information sharing on foot-and-mouth disease spreading in beef cattle production systems. PLoS ONE, 15(10):e0240819, 2020.

- Qihui Yang, Don M Gruenbacher, Gary L Brase, Jessica L Heier Stamm, Scott A DeLoach, Caterina M Scoglio. Simulating human behavioral changes in livestock production systems during an epidemic: the case of the US beef cattle industry. Submitted.

- Qihui Yang, Caterina M Scoglio, and Don M Gruenbacher. Robustness of supply chain networks against underload cascading failures. Physica A: Statistical Mechanics and its Applications, 563:125466, 2021.

- Qihui Yang, Chunlin Yi, Aram Vajdi, Lee W Cohnstaedt, Hongyu Wu, Xiaolong Guo, and Caterina M Scoglio. Short-term forecasts and long-term mitigation evaluations for the COVID-19 epidemic in Hubei province, China. Infectious Disease Modelling, 5:563-574,2020.

Simulated cattle and truck movement date sets which can be useful for the community studying interconnected complex systems are published in the following data repository :

- Qihui Yang, Caterina Scoglio, Don Gruenbacher. EAGER: SSDIM: Data Generation for the Coupled System Composed of the Beef Cattle Production Infrastructure and the Transportation Services Infrastructure in Southwestern Kansas. DesignSafe-CI, 2019. https://doi.org/10.17603/ds2-3ft2-0441.

This research is supported by the National Science Foundation, USA, under Grant Award CMMI-1744812.

Chapter 1

Introduction

1.1 Motivation

The U.S. food and agriculture systems, which account for roughly one-fifth of the nation's economic activity, face many biosecurity threats such as natural hazards and animal disease outbreaks. Here, biosecurity is a term broadly defined as a strategic and integrated approach to analyzing and managing relevant risks to plant health, animal health, human health, and the environment[1]. These four different sectors are not isolated, and biosecurity hazards existing in one sector can potentially spread to other sectors[2]. For instance, the ongoing coronavirus disease 2019 (COVID-19) pandemic has dramatically impacted people's normal activities and left significant economic consequences to industries, among which the livestock production industries are one of the most negatively impacted sectors[3;4]. In the United States, outbreaks identified among meat-processing workers led to the closure of several meat-processing plants, causing sharp disruptions in livestock production. Shutdowns of restaurants and schools led to a 12–15% reduction in the total demand for dairy[5]. Peel et al.[6] suggested that COVID-19 could result in $13.6 billion of economic losses to the U.S. beef industry, highlighting the fragility of today's intensive livestock production industries.

In modern society, livestock production systems have become increasingly interconnected with other infrastructure systems, including transportation systems. The interdependencies among infrastructure systems can cause a high systemic vulnerability within the overall U.S. economic system[7]. Livestock production heavily relies upon transportation services for the timely delivery of animals. It can suffer substantial financial losses due to disruptions in transportation infrastructure caused by natural disasters and movement restrictions during disease outbreaks. On the other hand, disruptions in livestock production would likely undermine the profitability of regional truck companies due to underutilized capital assets and employee layoffs. For example, the 2001 U.K. foot-and-mouth disease outbreak required the slaughter of approximately 6.5 million animals to contain the epidemic. Shutdowns of farm activities left significant impacts on the meat and dairy production and local communities that rely on these industries, resulting in severe economic losses totaling more than £2.8 billion[8;9].

The examples above illustrated the necessity to examine the systemic-level behavior that goes beyond a single component behavior to address biosecurity concerns in complex systems. Scholars have conducted extensive studies on the cascading failure phenomenon and network robustness of complex systems[10–18]. The failures in these models are often overload-driven. For example, power outages can lead to load redistribution across the power system and result in more failures due to the power flows exceeding the line capacity. Failures in a critical fraction of nodes could lead to a failure cascade and complete breakdown of the interdependent systems[10]. However, few works have focused on the interdependence between livestock production systems with other infrastructure systems.

Industrial livestock production is characterized by intensive and high-throughput systems, with all parts of the chain from birth to slaughter nearly always operating at full capacity. Disruptions that initially occur at one part of the chain can immediately impact both upstream and downstream aspects due to entities' demand-supply relationships. Such impacts could be amplified and propagated throughout the supply chain[5]. Several studies have utilized the above overload failure models to analyze the cascading failures in supply chains[19;20]. In supply chain networks, nodes refer to supply chain entities, and links represent interaction and connections among the entities. However, cascading failures in supply chains are mostly caused by insufficient load, and only a few works have considered such failures[21–24], which are referred as underload cascading failures hereafter. When entities cannot fulfill the expected production requirement to overcome fixed production costs, they will fail to gain profit and possibly exit the market. When a node is disrupted, its downstream and upstream neighbors will be affected due to supply shortage and demand losses, respectively.

Among the disruptions, animal disease outbreaks are a major threat to livestock production supply chains. In view of livestock producers, biosecurity is referred to as implementing control measures to decrease the chance of animal disease spreading[25]. Over the past few years, simulation models have been widely used to analyze control strategies for farm-to-farm disease transmission. While disease transmission through the movement of infected cattle has been extensively studied in previous works[26–28], indirect contact through fomites such as contaminated equipment and vehicles has recently gained attention. Only a few studies have focused on indirect contact via livestock transporters, one of the most at-risk operator categories[29;30]. In addition, most these herd-level models are based on static networks and rely on accurate estimates of the contact frequency and distance distribution between livestock operations[8;31]. As possible outbreak sizes may be overestimated in static networks, recent work has increasingly focused on temporal network measures[32]. However, most simulation models are built without slaughterhouses, the inspection at which is the most effective surveillance component for early epidemic detection[33]. Moreover, human factors such as farmers' risk perception and disease experience of neighboring farmers are likely to influence farmers' willingness to comply with biosecurity protocols, but most animal disease models do not account for human behavioral changes, which could lead to substantial bias in the predicted epidemic trajectory[34–37].

Computational modeling offers a practical method to simulate complex systems, in which the non-linear interaction effects among individuals could be highly heterogeneous. Agent-based modeling (ABM), also called individual-based modeling, is one computational method that has been used in various disciplines, including economics, agriculture, logistics, and healthcare[38–44]. In these models, autonomous agents maintain behaviors characterized by a set of simple rules[45]. ABM is a more general term than the individual-based model, which is most commonly used in ecology[46]. As alternatives to classical mathematical tools, ABMs developed for disease prediction can simulate the disease transmission among individuals in a more fine-confined way[47]. There are a number of ABMs developed in the context of livestock production to study the policies and human decision factors in social-ecological systems[48–53]. However, none of these previous research explicitly models livestock production and the associated transportation industry as two distinct but interdependent industries.

Although extensive studies have been conducted to ensure biosecurity in complex systems, there are various topics in this field that remain to be explored. In this dissertation, we aim to advance our knowledge of 1) the robustness of interconnected beef cattle production and transportation systems, 2) the impact of information sharing and indirect contact on animal disease spreading, 3) the interplay between human behavior and animal disease spreading, 4) the robustness of supply chain networks, and 5) mitigation measures for the COVID spreading.

1.2 Background

In this section, we introduce beef cattle systems, which are the main focus of this dissertation. The U.S. beef industry contributes significantly to the global meat supply chain, accounting for 20.3% of the world's beef production by January 2020[54]. As the most critical component in U.S. agricultural industries, cattle production accounts for $66.2 billion in cash receipts and represents about 18 percent of the $374 billion in total cash receipts forecast for agricultural commodities in 2019[55]. The region of southwest Kansas provides a great context to study beef cattle production systems. Kansas ranks third in the U.S., with 2.5 million head of cattle on feed as of January 1, 2021, according to the USDA's National Agricultural Statistics Service. The beef cattle sector provides 38,973 jobs to the Kansas agriculture industry and contributes approximately $8.7 billion to the Kansas economy[56].

Modern beef cattle production in the U.S. is a highly specialized system that spans from cow-calf ranches, to stockers, to feedlots, to packers. There are several terms used to describe cattle based on their gender and life stages. "Calves" are young cattle of both genders. "Cows" are female cattle that have had a calf. "Steers" are castrated male cattle, and "heifers" are female cattle before having calves. In cow-calf ranches, cows produce a new generation of calves that are fed until around 450 pounds, and will be sold directly or via auction markets to stockers. At approximately 650 pounds, cattle raised in stocker operations will be sold directly or via auction markets to feedlots. Once heifers and steers in feedlots achieve 1250 pounds and 1350 pounds, respectively, they will be moved to the final meat-processing facilities, the slaughterhouses. Slaughterhouses are also called packers in U.S. beef production systems, and these two terms are used interchangeably in Chapters 2–4. In addition, the beef slaughter industry in the U.S. is heavily concentrated, with only four firms in Kansas accounting for more than 80% of the total beef slaughter capacity [57].

1.3 Research questions and contributions

In this dissertation, we use computational methods to model behaviors of complex systems in the face of biosecurity challenges. Although this dissertation mainly focuses on beef supply chains, our methods can be applied to other livestock production systems.

The first question we explore in this dissertation is how the interdependence between cattle production and transportation systems can affect the system performance under disruptions. In addition, we aim to generate realistic cattle and truck movement data for southwest Kansas. The outcome will significantly raise awareness of vulnerabilities in the interconnected system and benefit existing disaster preparedness.

The second question is how truck contamination and information sharing can impact the foot-and-mouth disease virus transmission in the beef cattle systems. The findings are expected to promote mitigation strategies informed by data sharing among cattle premises.

In the third question, we examine how human behavioral changes around biosecurity could affect the animal disease spread. The outcomes are expected to deepen our understanding of the link between disease transmission dynamics and human behavioral changes, and improve animal disease management.

The fourth question we investigate in this dissertation is whether an abrupt breakdown would emerge in supply chain systems against underload cascading failures. We examine the fraction of failed entities under load decrease and load fluctuation scenarios through numerical simulations. We also provide analytic results based on the assumption of equal load redistribution upon failures. The outcomes are expected to shed light on the qualitative behavior of real-world supply chain systems that policymakers can consider to avoid systemic failure risks.

In our final study, we test the effectiveness of non-pharmaceutical interventions on COVID spreading in Hubei Province, China. Understanding the impact of non-pharmaceutical interventions on the epidemic dynamics is crucial for decision-makers to take proper actions to contain the pandemic. The findings can be a reference for policy recommendations regarding the epidemic in other countries.

My major contributions in this dissertation are summarized as follows:

- Develop an agent-based model for the interdependent beef production and associated transportation systems[58;59].

- Identify meat-packers as critical components of the beef production system as disruptions in trucks serving packers have the worst impact on cattle production. The interdependent system is robust to random failures but vulnerable to the targeted shutdown of cattle premises or truck premises. Realistic cattle and truck movement data sets are provided for the community studying interconnected complex systems[58].

- Reveal that including indirect contact routes through contaminated trucks can significantly increase the disease spread amplitude, compared with equivalent scenarios that only consider direct contact routes via animal movement. Enabling information infrastructure on producers and packers reduces the median number of infected producers in the producer isolation scenario by 90.28%, suggesting it is imperative to promote information sharing in the cattle industry for rapid disease detection and containment[59].

- Quantify the impact of human behavior factors on epidemic dynamics. Shifting 40% of producers towards greater risk-averse behavior can lead to a sharp decrease in the median number of infected producers, from 102 to 31, assuming that producers initially have low compliance for biosecurity protocols.

- Discover numerically and analytically the existence of a discontinuous phase transition in supply chain networks facing disruptions. Unlike other systems studied under overload cascading failures, the supply chain system is more robust for power-law distributions than uniform distributions of the lower bound load parameter[60].

- Reveal that the epidemic in Hubei Province could have become persistent without continued control measures, using an individual-level network-based model. Only by continuing to decrease the infection rate through strict protective measures and social distancing measures, the COVID spreading dynamics would peak at around mid-February and approximate the actual epidemic trajectory in March 2020[61].

1.4 Dissertation structure

The dissertation is organized as follows. Chapter 1 introduces the background, research questions and contributions of this dissertation. Chapter 2 introduces the agent-based model we developed for the beef cattle industry in southwest Kansas and analyzes the interdependence between the cattle and transportation systems. Chapter 3 simulates the foot-and-mouth disease spreading through the movement of infected animals and fomite, and evaluates the effectiveness of different mitigation strategies. Chapter 4 demonstrates the impact of human behavior factors on animal disease transmission in livestock production systems. Chapter 5 proposes an underload cascade failure model for supply chain networks, and examines the network robustness under disruptions both analytically and numerically. Chapter 6 assesses the effectiveness of non-pharmaceutical interventions on the epidemic dynamics in Hubei Province through network-based modeling. Finally, Chapter 7 presents the key conclusions, reflects on the limitations, and suggests directions for future research.

Chapter 2

Robustness of interdependent cattle production and transportation systems[1]

2.1 Introduction

Critical infrastructure systems (CIS) such as power grids and water supply systems provide reliable flows of products and services vital to society. They can be disrupted by technological failures such as the 2003 Northeast American power blackout and 2021 Texas power outages, by natural hazards like hurricanes and by deliberate attacks like the cyber-attack on the Ukrainian electrical distribution system[62–65]. These disruptions are more than inconveniences; the cumulative costs from damage due to natural disaster events in the U.S. reached $306 billion in 2017[66]. Studies have been conducted extensively on individual networks to enhance network resilience[67–70]. However, modern infrastructure systems no longer exist in isolation but have become mutually interdependent. For example, the food and agriculture sector, which accounts for roughly one-fifth of the nation's economic activity, exhibits particular interconnectedness with other CIS sectors, including transportation systems[71].

[1] This chapter is a slightly modified version of our published article[58].

Disruptions of components in one system may propagate and cause elements in the other system to fail. Several studies have focused on enhancing the robustness of interdependent networks under random failures and targeted attacks[10–12;20]. But to our knowledge, no such exercise has been undertaken to analyze the interdependence between food production and transportation systems.

The region of southwest Kansas (SW KS) provides a great context to study the interdependence of the beef cattle production industry, one component of the food and agriculture sector, with the transportation industry. Incapacitation or destruction in either cattle production or transportation would almost certainly cripple the regional economy. Disruptions in cattle production would likely undermine the profitability of regional truck companies due to underutilized capital assets and employee layoffs. On the other hand, lack of transportation services could lead to delays in cattle movement between premises.

Although the interconnectedness between these two industries has not been systematically studied, as has been done with other infrastructure systems, several studies have focused on the main factors affecting the stability of the cattle system. The cattle production system can be influenced by fluctuations in weather. For instance, drought may cause premature termination of the grazing season and force producers to sell cattle early due to limited feed reserves, resulting in lower cattle production and higher mortality rates[57;72]. Additionally, disease outbreaks can cause disruptions in cattle production. Schroeder et al. estimated that a foot-and-mouth disease outbreak in the central U.S. would result in the loss of as many as 7,000–8,000 livestock herds and 16–18 million animals[73].

A successful beef cattle system heavily relies upon timely delivery and proper handling of cattle for transportation. Consider that the prices paid for slaughter cattle in the U.S. are influenced by age, quality grade, yield grade, and weight. Among these cattle production parameters, the USDA quality grade and cattle finishing diet have the greatest impact on beef flavor profiles[74]. Animals that deposit excessive fat can lead to discounted prices accordingly. In cattle transportation, the loading density, trailer environment, transport duration, and animal condition are substantially related to animal welfare, carcass and meat quality[75–77]. Transportation may be a potential stressor and decrease beef cattle welfare, resulting in substantial financial losses to the beef industry[78;79]. However, natural disasters such as heavy snowstorms and tornados may lead to disruptions in transportation infrastructure. Bai et al.[80] studied the transportation mode of meat-related industries in SW KS and provided county-level cattle transportation data, which will be used to validate our model.

Previous research reveals that beef cattle production and transportation infrastructures are interrelated, but no study has evaluated the interdependence between these two industries. In this work, we will assess the robustness of the interdependent cattle production and transportation systems under different node failure conditions. Removal of nodes representing animals or premises is often conducted to examine the likely effects of implementing trade restrictions or vaccinations during disease outbreaks[81–83]. Similarly, we will simulate the removal of cattle to mimic the loss of supply due to disease outbreaks. In scenarios depicting transportation disruptions, trucks will be removed to represent vehicle shortage caused by deliberate attacks.

Of course, understanding the interdependent cattle production and transportation systems requires the availability of movement data and cooperation among private operators. Animal movement tracking systems in Europe have contributed significantly to the analysis of livestock movements and disease spread patterns there[31;84–86]. However, the adoption of a traceability system is not compulsory for U.S. beef cattle operations, and producer organizations have been against such systems for confidential concerns. To address this challenge, questionnaire-based methods have been used in some studies to examine livestock movements in the U.S.[29;87]. Other studies try to estimate movement based on Interstate Certificate of Veterinary Inspection data, but these only capture the interstate movement patterns[88;89]. Therefore, this chapter first generates cattle and truck movement data among production locations in normal conditions using agent-based modeling (ABM).

ABM offers a practical method to model the complex cattle system. Prior agent-based simulations regarding the beef cattle industry have focused on disease prediction and control measures[90–95]. Other research has studied the risk management strategies in reaction to disease outbreaks, agricultural policy interventions, and market dynamics[48–53]. However, none of these studies explicitly model both the cattle industry and the associated transportation industry as two distinct but interdependent industries. This work thus adds a new element to this domain. Based on the eighty-five ABM frameworks[96] and additional research on modeling and simulation capabilities, we selected AnyLogic as an appropriate simulation toolkit for this study.

In this chapter, we develop an agent-based model that builds the business operations of both the beef cattle industry and the associated transportation services. This model is employed to generate cattle movement data among premises under normal conditions and then to assess the system robustness under different node failure conditions. The next section illustrates our approach to develop the model and assess the system robustness.

2.2 Model

In this section, we first introduce the operating principles of the beef cattle industry and the transportation industry. Assumptions are made based on prior research and field studies. Then we illustrate the model design guided by the Organization Model for Adaptive Computational Systems (OMACS) framework. In the end, implementation details in AnyLogic are briefly described.

2.2.1 Conceptual model of the interdependent system

Besides the literature review above, we consulted beef cattle experts and performed field studies in a local auction market and a finishing feedlot. According to the main findings from these activities, the operation processes and assumptions are summarized as the following.

Operating principles and model assumptions of the beef cattle industry

In the model, the beef cattle system mainly consists of three components: live production, entry point, and packer. Market conditions are assumed to be stable, and price fluctuations are not included for simplification reasons. In the cattle trading process, the buyers randomly select sellers to purchase cattle, and operators in each production stage make decisions to move cattle mainly based on the animals' weight. The model structure is depicted in Fig. 2.1. Calves raised in ranches are sold to stockers either through direct sales or auction markets. Similarly, feedlot operators source cattle either directly from stockers or through auction markets. Here, auction markets refer to the physical sale barns and are seen as aggregated points for cattle movement.

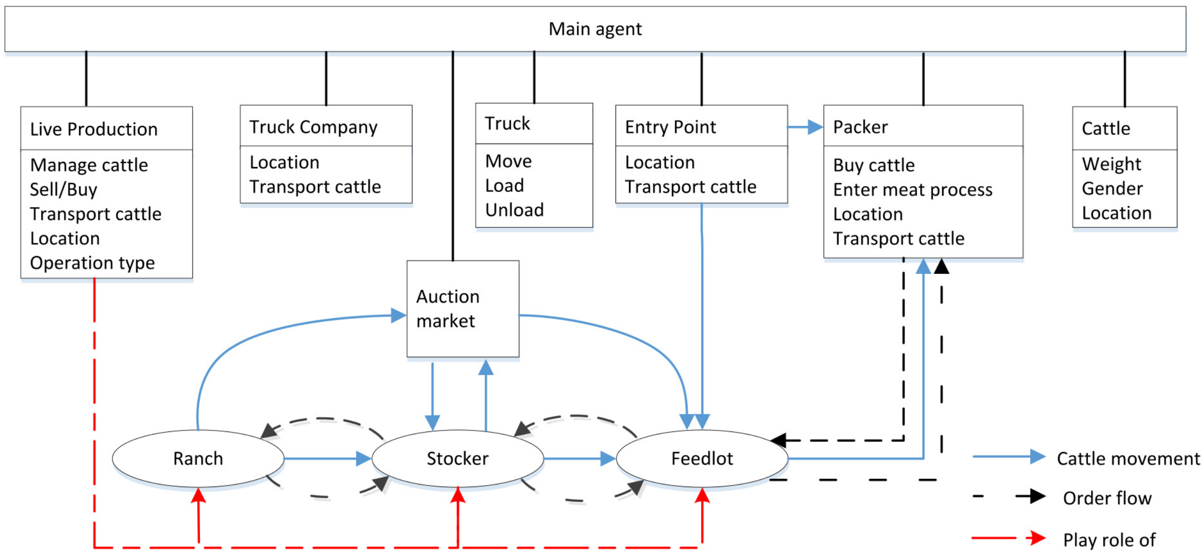

Figure 2.1: *The model structure of the interdependent cattle and transportation systems*

Live production. The live production locations are cattle premises inside SW KS, namely cow-calf ranches, stockers and feedlots. The latter two categories are referred to as "starter feedlot" and "finishing feedlot" in paper[80]. Cattle producers usually purchase cattle on a weekly basis based on their inventory and cattle flow requirements. They continue buying the available supply of animals until they achieve their maximum size. If the supply inside SW KS cannot provide enough cattle, the producers will purchase cattle from outside SW KS. More specifically, when the available cattle supply within SW KS is below the producer's demand multiplied by the presumed percentage of animals coming from within SW KS (see below), the producer will purchase more cattle from outside SW KS to compensate this shortage. In particular, we assume:

- For a feedlot, around 10–15% of its cattle are purchased from within SW KS, and the remaining 85–90% are sourced from outside the region. The average daily gain is uniformly distributed between 2.6–3.3 pounds per day for heifers and 3–4 pounds per day for steers. Once heifers and steers achieve 1250 pounds and 1350 pounds respectively, they will be moved to the packers. At model initialization, the ratio between heifer and steer is set at 0.6:0.4.

- For a stocker, about 50% of calves originate from SW KS, and the rest come from outside. Both heifers and steers grow at a rate of 2 pounds per day, and they are moved to feedlots for backgrounding once they achieve 650 pounds. At model initialization, the ratio between heifer and steer is 0.6:0.4.

- For a ranch, cattle gain 1.67 pounds per day, and the finishing weight is 450 pounds. Cows are equally likely to give birth to a heifer or steer calf. Based on the ideal distribution of pregnancy for cow-calf herds in paper[97], it is assumed that most calves are born in March and April in the model. We assume 60% of the herd gives birth in the first 21-day interval, 23% in the second 21-day interval, and 7% in the third 21-day interval. Additionally, 5% of calves are born outside this 63-day period. It is assumed that 5% of cows fail to become pregnant and therefore they won't give birth to calves. At model initialization, only cows are set in the ranches.

Entry point. Since there are also cattle coming from outside SW KS, we put 12 entry points on the system boundaries which are located on the major highways into and out of SW KS, as in paper[80]. Cattle and trucks are placed at these entry points to represent those cattle or trucks coming from outside SW KS into the region. The following assumptions are made for the cattle from outside SW KS: (1) Transporting finished cattle from outside SW KS to the packers: 70% of the cattle come from the south, and 10% of cattle come from each of the north, east, and west directions[80]; (2) Transporting feeder cattle from outside SW KS to the feedlots: 30% of the cattle come from each of the north, south, and east directions, and 10% of the cattle come from the west[80]; (3) Transporting calves from outside SW KS to stockers: same as the feedlots; (4) No calves are coming from outside SW KS to the ranches in SW KS; (5) Cattle are evenly distributed among those entry points in the same direction.

Packer. All the cattle fed in SW KS are assumed to be slaughtered in the four major packers in SW KS as consistent with paper[80]. Despite the influence from market conditions, the demand for finished cattle remains relatively constant throughout the year. Each packer operates close to full capacity and slaughters, on average, 6,000 head of cattle per day. From Monday through Friday, the meat processing lasts for 16 hours per day, and the cleaning process goes on in the remaining 8 hours. Buyers from the packers randomly select feedlots to purchase cattle weekly. In 2005, there were 2,539,280 cattle transported from outside SW KS and 3,721,050 finished cattle transported from inside SW KS to the packers[80]. Based on this, we assume that each packer purchase 59% of its cattle from within SW KS and the rest from outside SW KS.

Operating principles and model assumptions of the transportation industry

In reality, cattle movements among premises are highly dynamic and depend on a multitude of factors such as space availability, cattle weight and feed availability. For simplicity, we assume the ratios of total transport activity for each type of transportation flows as in Table 2.1.

Table 2.1: *Transportation flows and percentages of total transport activity*

Transportation flows			Percentages of total transport activity			
Origin	Destination	Type	Owned by producers	Rent from fleets	Owned by packers	From entry points
Ranch	Stocker	Via auction market	10%	90%	-	-
Ranch	Stocker	Via direct sales	90%	10%	-	-
Stocker	Feedlot	Via auction market	10%	90%	-	-
Stocker	Feedlot	Via direct sales	90%	10%	-	-
Feedlot	Packer	Via direct sales	-	-	100%	-
Entry point	Packer	Via direct sales	-	-	100%	-
Entry point	Producer	Via direct sales	-	-	-	100%

After producers (ranch, stocker or feedlot) finish trading cattle, the buyer will transport the cattle either using its trucks or renting from truck companies. More specifically, 90%

of cattle movements through direct sales between producers are via producers' trucks, while the remaining 10% are via trucks from fleets. In comparison, cattle movements via auction market between producers have the opposite percentages of total transport activity. Overall, 34% of the operations purchase cattle from the auction markets[98]. Entry points representing truck premises outside SW KS, use their trucks to move cattle from outside to the region. Packers use their trucks to ship cattle from both inside and outside SW KS.

In the model, vehicles owned by cattle producers are of small capacity, while all the rest are of large size. A large truck can accommodate on average 45 finished cattle or can hold 75 feeder cattle[80]. By similar calculations, it is assumed that small vehicles can carry 38 feeder cattle or 75 calves.

Livestock transportation is subject to federal and state regulations governing drivers' hours of service, as well as animal welfare requirements[99]. Thus, we assume that each truck driver must complete a route within a 14-hour duty period and must rest for ten consecutive hours before going back on duty. Based on this, a vehicle dispatch algorithm is designed to minimize the number of vehicles dispatched and total distance traveled while obeying duty time limits.

2.2.2 Model design

In this section, we illustrate the model design using the OMACS framework. Packer, live production, fleet and entry point agents are all in possessions of trucks and are referred to as *truck premises*. Meanwhile, live production and entry point agents are suppliers of cattle and are indicated as *cattle premises*.

The OMACS framework is proposed to guide multi-agent system design, and its fundamental concepts include agents, goals, and roles[100]. Our model consists of two organizations at the highest level of conception, i.e., the cattle production process and the transportation process. Constructed in agentTool III[101], Fig. 2.2 presents the goal classes that drive the system and the parameters related to these goals. Each goal is labeled as G_i, using the following notation. The top goal consists of two sub-organization goals, i.e., *initialize the* *beef cattle industry* (G_1) and *initialize transport services* (G_2). The top goal indicates that agents need to be appropriately created and located based on the GIS map at model setup.

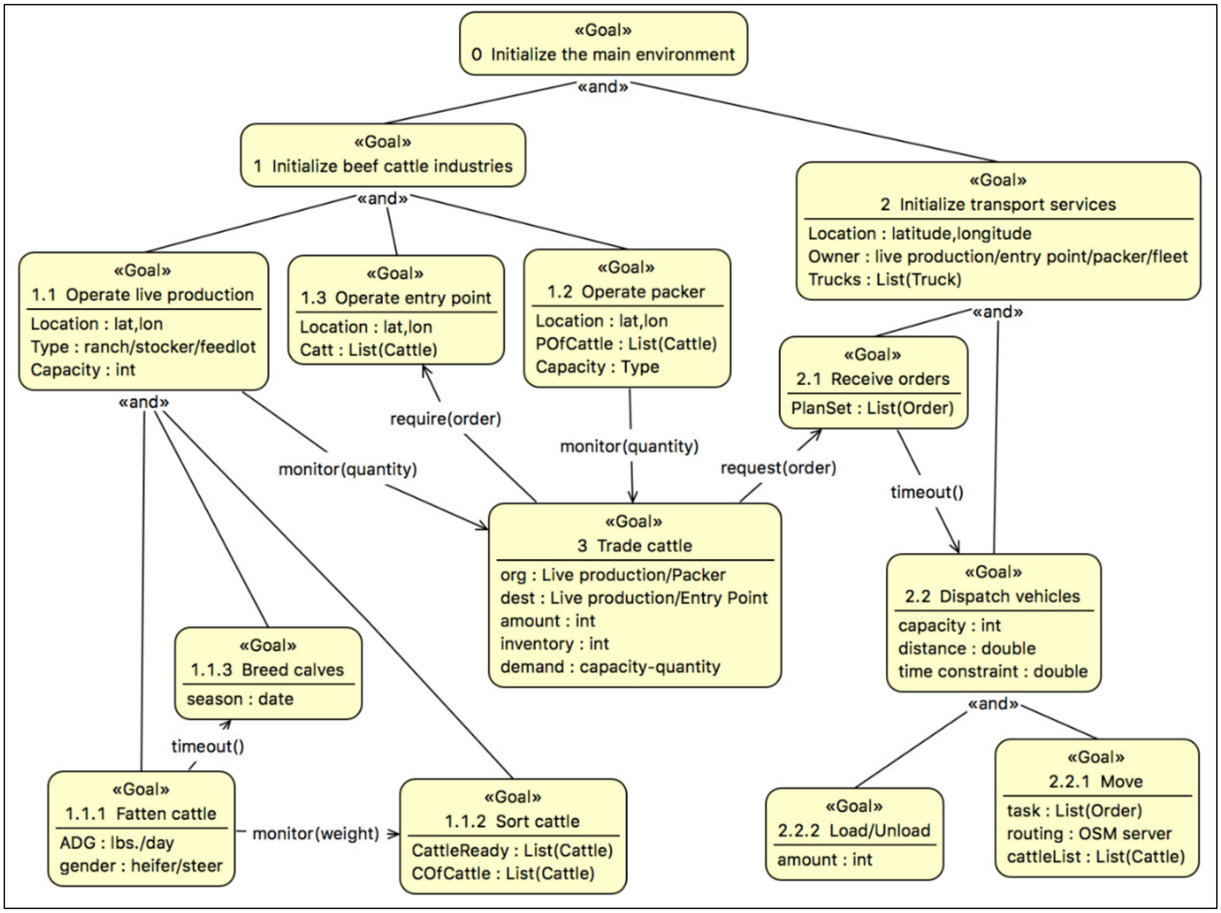

Figure 2.2: *Goal model of the system*

In the cattle industry organization, G_1 is decomposed to three leaf goals ($G_{1.1}$, $G_{1.2}$, $G_{1.3}$) that are assigned to live production, packer and entry point agents, respectively. The sub-goal of $G_{1.1}$, *fatten the cattle* ($G_{1.1.1}$) is the only goal that initially exists, and the rest are triggered by events. When the system starts, $G_{1.1.1}$ is applied to all live production agents, in which cattle weight is based on the average daily gain. Meanwhile, a timeout-event is periodically triggered so that producers periodically sort those cattle above the finishing weight into groups, which are ready to be shipped ($G_{1.1.2}$). Cows in ranches are assigned with $G_{1.1.3}$ *breed the cattle*, which is triggered once a year. G_3 *trade cattle* is a complex goal assigned to live production and packer agents. They periodically count their cattle inventory and will start to purchase cattle once the inventory falls below the capacity (an event is raised to trigger G_3).

In the transportation organization, truck premises need to achieve goals of $G_{2.1}$ *receive orders* and $G_{2.2}$ *dispatch vehicles*. At idle state, the vehicles are placed at the truck premises. After the cattle trade ends (G_3), an event will be triggered to send requests for transport services, which will be received by the truck premises agent ($G_{2.1}$). A time-out event will be triggered so that the truck premises conducts the vehicle dispatch algorithm and sends the trajectory commands to the vehicles ($G_{2.2}$) on the second day. Upon receiving the messages, the truck starts to move to each order's origin to pick up cattle and unload the cattle at the destination ($G_{2.2.1}$ and $G_{2.2.2}$).

OMACS goals are achieved by agents playing specific roles within the corresponding organization. Table 2.2 shows the agent types, the capabilities required and the corresponding roles. For example, the cattle playing the role of heifers give birth to calves each year. Table 2.3 details the interactions between agents or roles.

Table 2.2: *Agent types, capability and roles*

Agent types	Capability possessed	Playable roles
Cattle	Give birth; Grow.	Heifer; Steer.
Truck	Move along the road; Transport cattle; Communication.	Truck.
Fleet	Execute algorithms; Communication.	Truck premises.
Live production	Accommodate cattle; Trade cattle; Communication; Sort cattle periodically.	Cattle premises (ranch, stocker or feedlot); Truck premises.
Packer	Accommodate cattle; Trade cattle; Execute algorithms; Enter meat process; Communication.	Order buyer; Entrance of meat process; Truck premises.
Entry point	Accommodate cattle; Execute algorithms; Communication.	Cattle premises; Truck premises.
Order	Record the origin, destination and the amount of cattle.	Messages in trade process; Tasks of the trucks.

Table 2.3: *Interacting agents and rules*

Interacting agents		rules
Truck	Cattle	Trucks transport cattle according to the amount specified in the order.
	Packer	The packer sends orders to its trucks according to the vehicle dispatch algorithm.
	Fleet	Fleet company sends a sequence of orders to its trucks on the second day of receiving orders.
	Entry point	Entry point agent dispatches trucks on the second day of receiving orders.
	Live production	Live production agent dispatches vehicles on the second day after the trade ends.
Live production	Live production	Producers communicate with each other at random during a week to trade cattle.
	Packer	Packers and live producers (feedlots) trade cattle on each Friday morning.
	Entry point	Live producers (feedlots or stockers) purchase cattle from entry points
Packer	Entry point	Packers purchase cattle from the entry points weekly.

2.2.3 Model implementation

The model was developed in AnyLogic software, with all functions written in Java. The interdependent system includes a total of 301 live production locations, four major packers and 12 entry points for cattle and trucks from outside SW KS. Statistics of the model input are summarized in Table 2.4.

Table 2.4: *Summary input statistics.*

	Ranch	Stocker	Feedlot	Total
Number of farms	18	50	233	301
Cattle Inventory	14,050	79,768	2,819,189	2,913,007

The main agent builds the environment that the other agents share. At model initialization, it creates and locates the agents within a GIS map based on the latitude and longitude of the model input data (Fig. 2.3). The routes are requested from OpenStreetMap server provided by AnyLogic and set with the shortest path method. The live production agents are assigned one of the three industry roles: *ranch*, *stocker*, or *feedlot* based on the input data. Cattle agents are assigned with a weight parameter uniformly distributed between a minimum and a maximum value and located at their cattle premises.

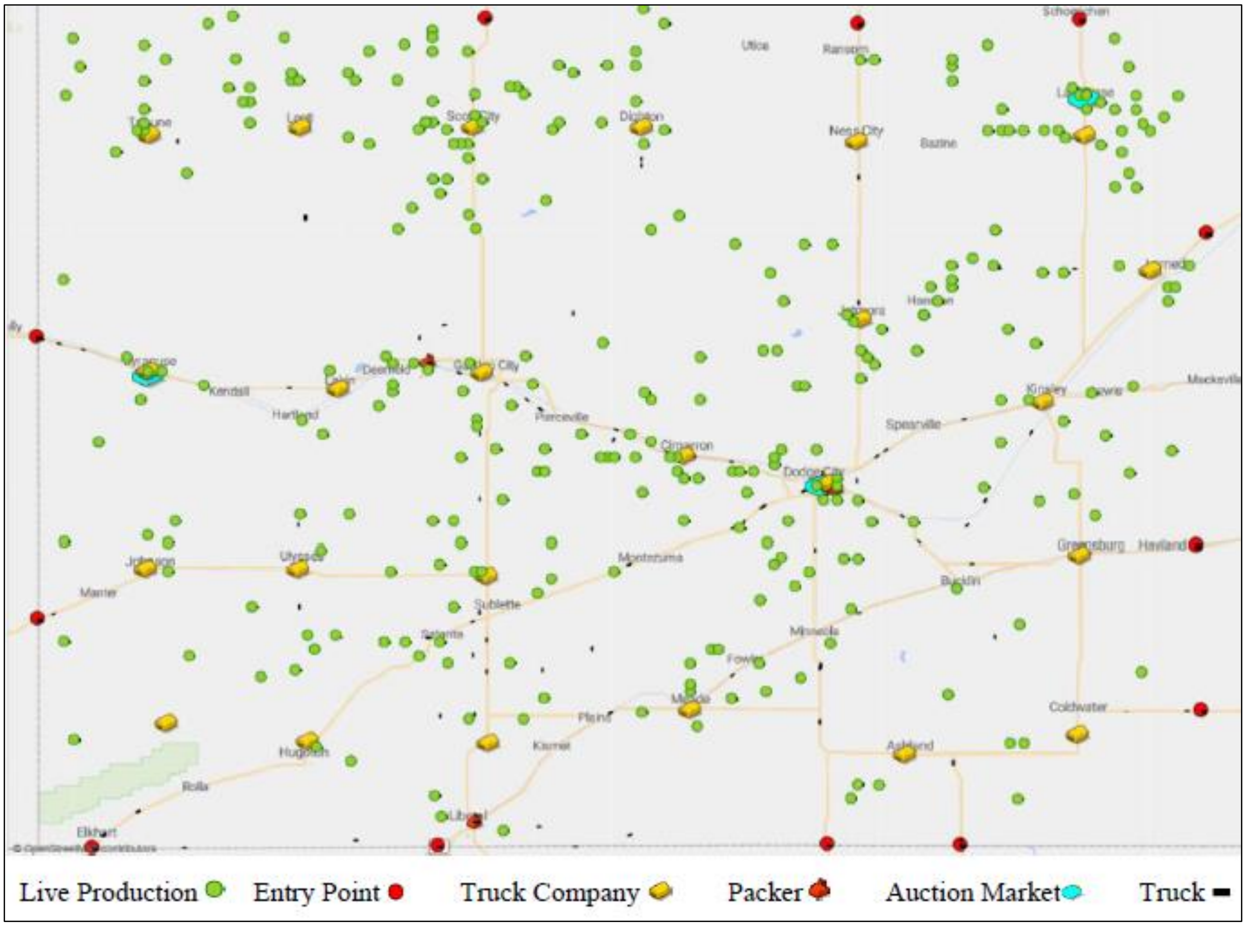

Figure 2.3: *Animation on a GIS map*

The live production agents periodically check whether the cattle achieve the finishing weight and sort them into the group ready to be shipped. On a weekly basis, they communicate with other live production agents and entry point agents to purchase cattle. On the second day after the trade ends, cattle are transported to the next production stage. Packer agents purchase cattle from feedlots within SW KS and entry points each week. The order agent consists of the number of cattle, origin, and destination. Each cattle agent gains weight based on a growth rate determined by its gender and owner (i.e., type of live production agent it belongs to). Heifers in cow-calf ranches breed new calves according to the predetermined fertility rate. The variables deemed necessary for readers to understand the model are shown in Table 2.5.

Table 2.5: *Summary of key variables*

Agent	Variable name	Description
Live production	CofCattle	List of cattle not ready to be sold.
	CattleReady	List of cattle ready to be sold to the next place.
	FSTrucks	List of light trucks belonging to this live production agent.
	PlanSet	List of orders to be fulfilled by the trucks.
Packer	PofCattle	List of cattle physically stay in the packer.
	FBTrucks	List of large trucks belonging to this packer.
	PlanSet	List of orders to be fulfilled by the trucks.
Entry point	Feeders/Finished	List of feeder/finished cattle from outside SW KS.
	PlanSet	List of orders to be fulfilled by the trucks.
	Trucks	List of large trucks from outside SW KS.

The model's time scale is based on dates, generating data from Jan 1st 12:00:00 AM–Dec 31st 11:59:59 PM. For the simulation experiment, the maximum available memory is set as "Custom 56320Mb". "Fixed seed" option is selected for the random number generation, making the results reproducible.

2.2.4 Experimental design

Two experiments were performed to assess the system robustness in response to disruptions. In the first experiment, the removal of trucks refers to the unavailability of vehicles caused by deliberate attacks. In the second experiment, cattle premises are removed to mimic the loss of cattle supply caused by interventions such as trade restrictions or culling during disease outbreaks. For example, the removal of entry point agents considers the possible case, in which cattle are found to be infected outside SW KS and the markets in SW KS are subsequently closed to cattle from that side of the boundary.

During cattle trade, a cattle buyer randomly selects producers to purchase cattle. To model this process, we use a pseudorandom number generator in AnyLogic to generate a sequence of numbers, which are the indexes of the cattle premises. Please note that the sequence of numbers is not truly random and is determined by the seed. Therefore, "fixed seed" option is selected in the simulation setup so that the model will always produce the same results as long as all the other settings remain unchanged. Accordingly, we only run the model once to obtain the results for each simulation scenario. Aside from the removal of the premises, all other parameters remain unchanged for comparison purposes.

A truck premises agent and the population of all the truck premises are denoted as g and $\mathcal{G}$ respectively to explain the simulation process. Truck premises are categorized by agent class, and the population in the k^{th} category is indicated as $\mathcal{G}_k$, where $k = 0, ..., 3$ refer to packer, farm, fleet or entry point respectively. g_i^k is the i^{th} truck premises agent in the k^{th} truck premises category. The fraction of unavailable trucks over all the vehicles is denoted by p.

Disruptions in the transportation industry

To reflect the impact of transportation disruptions on the cattle industry, we defined an indicator, the fraction of demand met, as follows:

$$\text{Fraction of demand met}(\%) = \mathcal{A}/\mathcal{P}, \tag{2.1}$$

where $\mathcal{A}$ and $\mathcal{P}$ are the total headcount of cattle actually moved and expected to be moved regarding all cattle premises respectively.

Each truck premises agent dispatches vehicles using the vehicle dispatch algorithm with input *PlanSet*, a list of orders to be delivered. Facing vehicle shortage problems, the truck premise agent would fail to complete assigning all orders in *PlanSet*. As a result, those orders fulfilled will be placed in the *ActualSet*, and the remaining orders are left at *PlanSet*. Those cattle which need to be moved by the remaining orders are seen as cattle losses, since they will not reach their destination on time. The remaining orders and the new orders coming in will be mixed in *PlanSet* and processed on the next day.

Algorithm 1: Compute the *fraction of demand set*

Input: $g_i^k \in \mathcal{G}_k$ which has *PlanSet* and *ActualSet*, $\mathcal{P}^{t-1}$, $\mathcal{A}^{t-1}$, $\mathcal{L}^{t-1}$

Output: $\mathcal{P}^t, \mathcal{A}^t, \mathcal{L}^t$

Function `calcFDM(`g_i^k, $\mathcal{P}^{t-1}$, $\mathcal{A}^{t-1}$, $\mathcal{L}^{t-1}$`)`**:**

  $\mathcal{A} \longleftarrow \mathcal{A}^{t-1}$, $\mathcal{P} \longleftarrow \mathcal{P}^{t-1}$, $\mathcal{L} \longleftarrow \mathcal{L}^{t-1}$

  for $k \leftarrow 0$ **to** 3 **by** 1 **do**

    $\mathcal{P}_k \longleftarrow 0, \mathcal{A}_k \longleftarrow 0, \mathcal{L}_k \longleftarrow 0$

    foreach $g_i^k \in \mathcal{G}_k$ **do**

      $p_i^k \longleftarrow 0$, $a_i^k \longleftarrow 0$

      foreach *order in* g_i^k*.PlanSet* **do**

        $p_i^k \longleftarrow p_i^k + order.amount$

      end

      foreach *order in* g_i^k*.ActualSet* **do**

        $a_i^k \longleftarrow a_i^k + order.amount$

      end

      $\mathcal{P}_k \longleftarrow \mathcal{P}_k + p_i^k$, $\mathcal{A}_k \longleftarrow \mathcal{A}_k + a_i^k$

    end

    $\mathcal{L}_k \longleftarrow \mathcal{P}_k - \mathcal{A}_k$

    $\mathcal{P} \longleftarrow \mathcal{P} + \mathcal{P}_k$, $\mathcal{A} \longleftarrow \mathcal{A} + \mathcal{A}_k$, $\mathcal{L} \longleftarrow \mathcal{L} + \mathcal{L}_k$

  end

  $\mathcal{A}^t \longleftarrow \mathcal{A}$, $\mathcal{P}^t \longleftarrow \mathcal{P}$, $\mathcal{L}^t \longleftarrow \mathcal{L}$

  return $\mathcal{P}^t, \mathcal{A}^t, \mathcal{L}^t$

End Function

The main agent executes Algorithm 1 on a daily basis to calculate $\mathcal{A}$, $\mathcal{P}$ and the total cattle loss $\mathcal{L}$. We first compute $\mathcal{P}^k$ by summing up the amount of cattle specified in the order agents of PlanSet from $\mathcal{G}_k$, which are all truck premises in the k^{th} truck premises category. Then, $\mathcal{P}$ is the summation of $\mathcal{P}^k$ for all truck premise categories from the first day to the last day (simulation stop time). Similarly, the summation of the cattle quantities specified in *ActualSet* is $\mathcal{A}$. Alternatively, we can count the number of cattle unloaded every time a truck arrives at the destination. Both methods are conducted in the experiment and yield the same results.

Disruptions in the cattle industry

In the cattle transportation industry, the profitability of truck companies or the hauling cost is closely related to the headcount of cattle transported and the distance of each trip. Therefore, the product of headcount and distance are calculated as an indicator for the adverse effects caused by disruptions in cattle industry with the following steps.

Step 1. Live production and entry point agents are removed based on either random or targeted strategy. In the targeted removal strategy, we progressively remove nodes, one after another, in the decreasing order of specific criteria.

Step 2. When the truck t fulfills an order j, the miles traveled (round trip) d_j and the headcount of cattle carried during this trip n_j are recorded.

Step 3. Calculate the travel distance of all cattle in the system, $headcount \times distance$ of the system, which is $\sum_{t \in \mathcal{T}} n_j \cdot d_j$.

The next section will describe the simulation results and implications.

2.3 Results and discussion

In this section, we present results regarding the simulated data generated from the agent-based model. We then evaluate results regarding the system robustness to disruptions in the cattle production and transportation industries.

2.3.1 Data generation under normal conditions

We present the visualization of cattle quantity from the perspective of each producer category and individual cattle premises as follows. Results regarding the total number of cattle located in ranches, stockers, and feedlots within SW KS over a year are shown in Figs. 2.4(a)–(d). The number of new calves born daily is shown in Fig. 2.4(a). In Fig. 2.4(b), the number of cows in the ranches stays stable while the number of calves increases in March and April because of the new births. The new calves remain in the ranches for several months and are then moved to stockers in fall. Therefore, the curve starts to decrease around August. In Fig. 2.4(d), the total number of cattle living in feedlots fluctuates weekly. Packers ship cattle out of feedlots from Monday to Friday, causing the number of cattle in feedlots to decrease. Next, feedlots buy animals from stockers to return to capacity. When the new cattle arrive, the number of cattle in feedlots increases accordingly. In comparison, the number of cattle in stockers fluctuates with a smaller amplitude in Fig. 2.4(c).

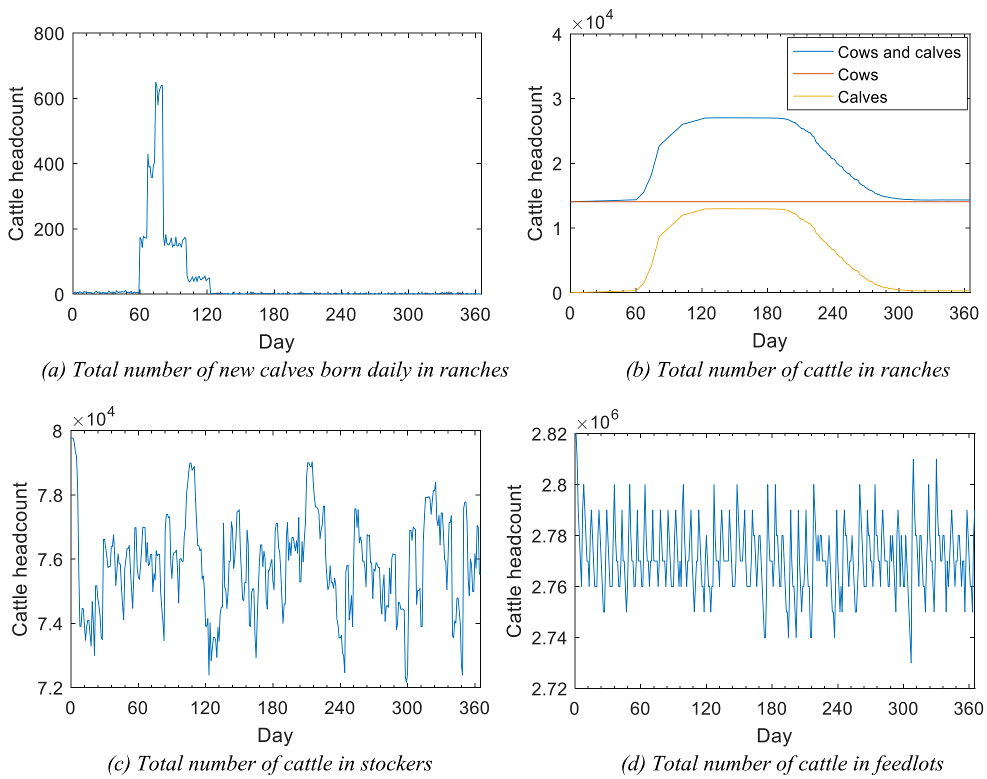

(a) Total number of new calves born daily in ranches

(b) Total number of cattle in ranches

(c) Total number of cattle in stockers

(d) Total number of cattle in feedlots

Figure 2.4: *Statistics of cattle in each production stage within SW KS over a 365-day period.*

Over the annual period, all premises are consistently part of the trade network. With the constant weekly nature of the market chain, there is little variation between the seasons. Births of calves in ranches are seasonal, but the ranches' total capacity constitutes only

0.48% of the total capacity of all live production sites in SW KS according to our input data. Therefore, the model is not strongly affected by seasonality.

Cattle quantities of particular premises in each producer category over time result in similar patterns. Thus, we randomly select one producer agent from each group and present its cattle quantity over a year in Fig. 2.5.

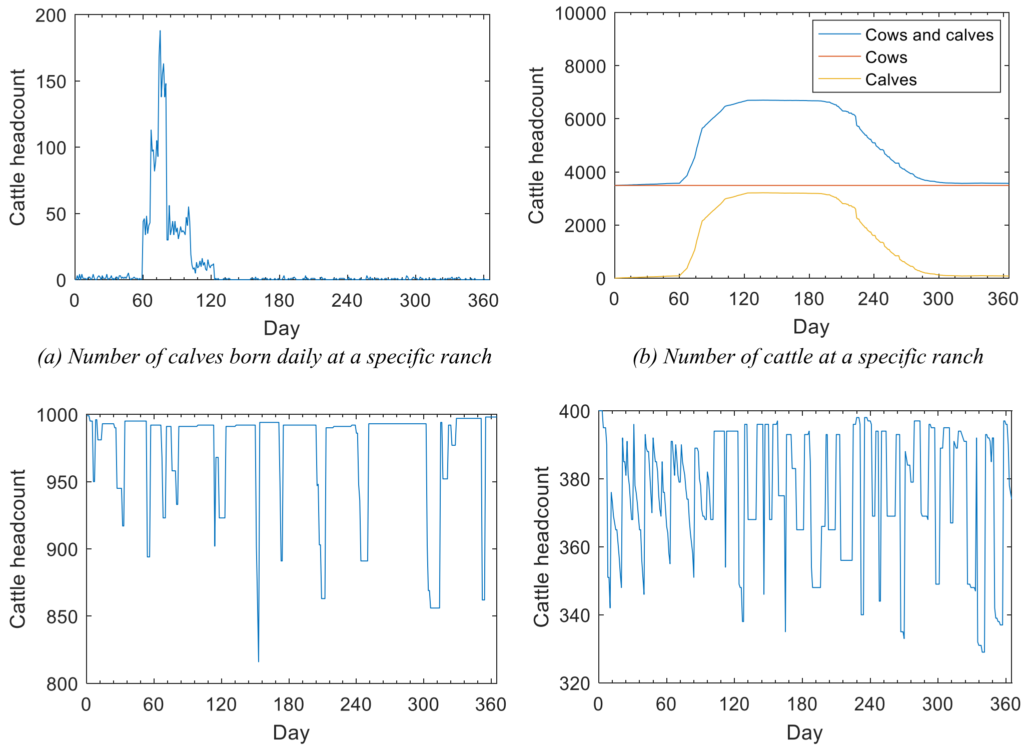

(a) Number of calves born daily at a specific ranch

(b) Number of cattle at a specific ranch

(c) Number of cattle at a specific feedlot

(d) Number of cattle at a specific stocker

Figure 2.5: *Sample plots of cattle quantity in individual producer locations within SW KS over a 365-day period.*

The model output contains details describing every truck and cattle movement among premises, e.g., truck id, cattle id, origin, destination, date. The individual truck movement data, which are generated from the model and aggregated at the county-level, are within a similar range of the county-level data published by Bai et al[80]. Comparisons between these simulated data sets are shown in Table 2.6.

Table 2.6: *Key statistics over a year.*

Statistics	Simulated data in Bai et al.[80]	Author's simulated data	Difference
Total number of finished cattle from feedlots inside SW KS to the packer	3,721,050 head	3,694,270 head	0.72%
Number of cattle coming from outside SW KS to packers	Total: 2,539,280 head; South: 1,777,496 head; North/East/West: 253,928 head	Total: 2,569,225 head; South: 1,798,282 head; North/East/West: 256,868 head	Total: 1.18% South: 1.17% North: 1.16% East: 1.16% West: 1.16%
Packer annual kill capacity	6,260,330 head	6,263,495 head	0.05%
Truck miles traveled for transporting cattle from inside SW KS to packers	13,456,956 miles	10,749,558.7 miles	-
Truck miles traveled for transporting cattle from outside SW KS to packers	10,438,844 miles	10,314,759.3 miles	1.19%
Truck miles traveled for transporting cattle (inside and outside SW KS) to packers	23,895,800 miles	21,064,318 miles	-

2.3.2 Evaluation of system robustness under disaster conditions

In this section, system robustness to disruptions in the beef cattle industry and transportation industry are measured under different scenarios. Since the model results under normal conditions show little variation across seasons, subsequent analysis was conducted just for the first two weeks of the year.

Disruptions in the transportation industry

Removal of trucks over the system. Different removal strategies of truck premises are summarized in Table 2.7. In Fig. 2.6, all the random strategies result in a similar response pattern, revealing the robustness of the network.

For example, 61.1% to 76.5% of the demand can be still met when 50% of trucks become unavailable. In comparison, targeted removal based on a decreasing order of truck quantity

Table 2.7: *Summary of removal strategies.*

Strategy	Description
Random strategy-each premises	For each truck premises agent g_i^k with n_i^k trucks, randomly remove $p \cdot n_i^k$ trucks. In total, $\sum_{g \in \mathcal{G}} p \cdot n_i^k$ trucks are removed, where $\mathcal{G}$ refer to all truck premises agents.
Random strategy-over the system	Randomly remove $p \sum_{g \in \mathcal{G}} n_i^k$ trucks from the whole system.
Random strategy-each premises category	For each category k, randomly remove $p \sum_{g \in \mathcal{G}_k} n_i^k$ trucks. In total, remove $\sum_{k=0}^{3} p \sum_{g \in \mathcal{G}_k} n_i^k$.
Targeted strategy-over the system	In the whole system, intentionally remove $p \sum_{g \in \mathcal{G}} n_i^k$ trucks based on truck premises ranked by number of trucks, from high to low.

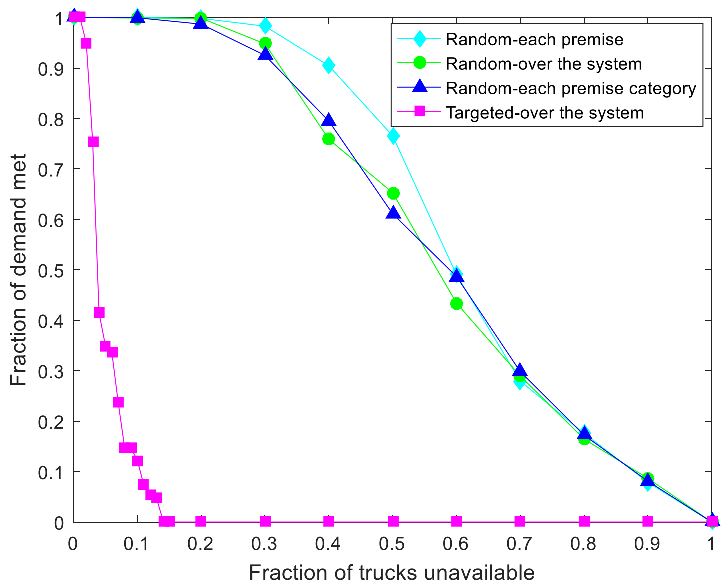

Figure 2.6: *Fraction of demand met over the fraction of trucks removed from the transportation industry under different removal strategies in a two-week period.*

owned by each truck premises leads to a notably faster drop in the fraction of demand met. Among the truck premises, packers possess the largest numbers of trucks. Thus, their trucks will be removed first under the targeted strategy. Packers utilize their vehicles to pick up cattle both from inside and outside SW KS. Once packers lose all their trucks, they are unable to pull cattle from feedlots. Consequently, feedlots will always be at full capacity and will not request cattle from other premises. Similarly, stockers will not purchase animals from other suppliers as well. Therefore, the system's transportation flow quickly stops when the fraction of trucks unavailable reaches around 14%, which is the ratio of the number of packers' vehicles over total truck quantity in the system.

Removal of trucks over each truck premises category. Here we analyze the system robustness with the removal of trucks belonging to each truck premises sector. We continue removing those trucks from the truck premises based on their truck quantity, from high to low, until the number of vehicles removed reaches the product of p and the total truck quantity in the system (see Fig. 2.7).

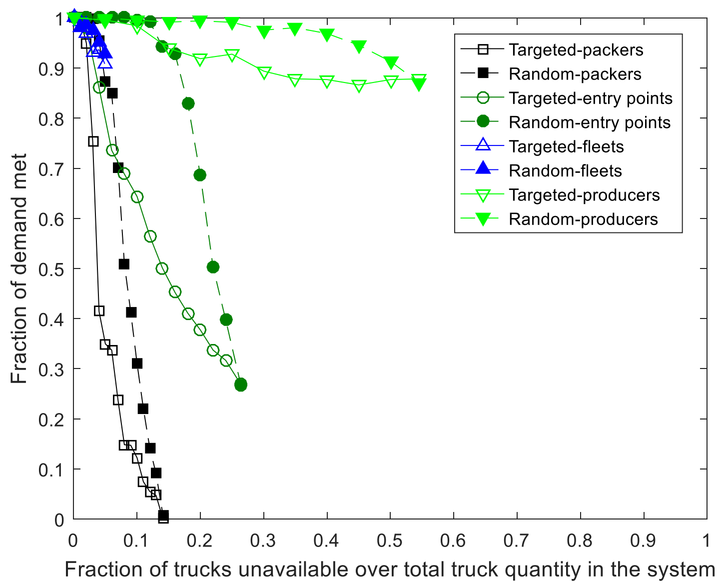

Figure 2.7: *Fraction of demand met over the fraction of trucks removed in transportation industry under strategies differentiated on sectors in a two-week period.*

In Fig. 2.7, both the black curves change abruptly compared with others, indicating that disruptions in the packer sector affect the cattle movement most. Packers are the most demanding truck premises located at the top of the supply chain, making the coupled system more fragile. When 10% of the total truck population is removed under a targeted strategy on packers, the demand met is reduced by about 90%. In comparison, random removal of trucks from the packer sector seems to be slightly less impactful and converges with the targeted strategy at around 14%, which is the maximum portion of all trucks that the packer sector owns. It is worth noting that, although the total trucks from producers constitute around 55% of all trucks in the system, complete removal of the producers' trucks only decreases the fraction of transportation demand met by about 15%. This is probably because there are many feedlots, allowing a relatively robust network.

These findings highlight that packers and regional boundaries represent crucial components of truck industry resiliency. Packers are the premises with the largest number of trucks, followed by the entry points. To mitigate the effects of deliberate transportation attacks on the cattle industry, truck premises should become more resilient by distributing vehicles within a larger geographical area. In the model, we did not consider sharing trucks among different truck premises. Such coordination among truck premises may help decrease the effects of transportation disruptions on cattle production during disasters. For example, if all the trucks become unavailable at a packer, other neighbors' trucks could transport cattle and fulfill its production needs. In this way, cattle production could possibly last for a more extended period when there are disruptions.

Disruptions in the cattle industry

The simulation results of cattle industry disruptions are shown in Fig. 2.8, in which *headcount*$\times$*distance* is normalized based on its value under normal conditions. The results show that the intentional removal of cattle premises changes more sharply compared with the random strategy. During the trade, producers randomly select from the rest of the premises to purchase animals. Arbitrary node removal causes cattle movement in the system to be redistributed, but the system stays relatively robust and self-adaptive. For example, when 50% of cattle premises become unavailable, *headcount*$\times$*distance* is still around 65%. For targeted strategies based on cattle capacity or the number of cattle ready, large producers and entry point agents were removed first. Large cattle suppliers need more transportation services, and once they are removed the distance cattle travel decreases quickly. Targeted removal based on out-degree, which is the number of animals moved out of that premises in a period, does not decrease as much as other targeted strategies after $p = 10\%$. This appears to be because some large-capacity producers did not sell cattle in this period and are not removed at the beginning, so they maintain the functioning of the transportation industry until they are removed in the end.

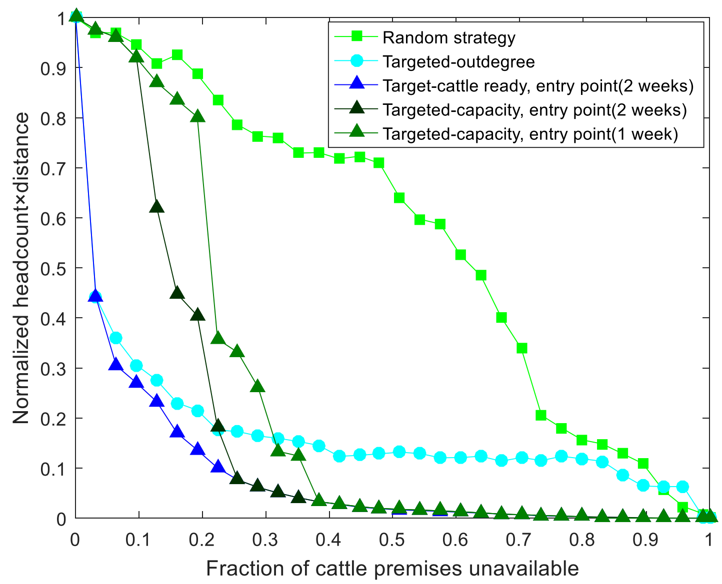

Figure 2.8: *Normalized product of headcount and distance of transportation industry on the fraction of cattle premises removed in a two-week period.*

Two conclusions may be drawn from these findings to help ensure truck premises' profitability and buffer against possible losses caused by dependence on the cattle industry. Regarding disease outbreaks, more focus can be put on communicating control measures for large cattle producers in SW KS and inspection on the regional boundary. In addition, large-capacity producers may distribute their cattle to multiple locations to help enhance the system robustness against targeted attacks.

2.4 Summary

In this chapter, we explicitly model both the cattle industry and transportation services as two distinct but interdependent industries. The model generates cattle and truck movement data among premises based on regular business operating principles and assumed conditions. The data is fine-grained in both time and space, capturing each cattle and truck movement with a labeled id. Due to privacy issues, cattle and truck movement data for SW KS are only available in paper[80] to the authors' knowledge. The cattle and truck movement data generated from the agent-based model are aggregated at the county-level, which are within a similar range of the county-level data in paper[80]. We proceeded to evaluate the interdependent network robustness under disaster conditions. Our results show that the interconnected system is relatively stable against disruptions in either the beef cattle industry or the transportation industry under random failure strategies. For targeted strategies, packers are identified as critical elements of the truck system, since a shortage of packer trucks was shown to inflict the worst impact on the system. In addition, truck premises, especially those that require a larger number of vehicles, need to ensure that they take proper measures to have access to additional trucks in case of deliberate attacks. In this way, the negative effects of vehicle shortage on the cattle production system can be mitigated. However, the best approach to provide additional trucks with greater diversity in physical locations requires more investigation.

In conclusion, the interdependence between the cattle industry and the transportation industry creates vulnerability to the system. The locations and natures of these vulnerabilities need to be fully considered by system planners for making better decisions on disaster preparedness. Due to the complexity of the cattle supply chain, the current model is a simplification of reality, but it does include the most significant elements of cattle production and transportation. In the model, the cattle birth distribution is assumed based on the literature[97], and future data collection efforts may focus on obtaining better cattle birth data.

Chapter 3

Impact of truck contamination and information sharing on foot-and-mouth disease spreading[1]

3.1 Introduction

Foot-and-mouth disease (FMD) is a highly contagious infectious disease that could threaten cloven-hoofed animals worldwide[102]. The 2001 U.K. FMD outbreak resulted in severe economic losses totaling more than £2.8 billion and required the slaughter of approximately 6.5 million animals[8]. Recently, several major outbreaks have occurred in previously FMD-free countries, including South Korea and Japan[103;104]. Although the United States has been free of FMD since 1929, the disease is still prevalent in approximately two-thirds of the world. Concerns about the reintroduction of FMD into the United States have escalated due to increases in international travel and trade[105]. The beef cattle industry is of great importance to the U.S. economy, and an FMD outbreak would produce devastating economic losses as estimated by simulation-based studies. For example, Pendell et al.[106] reported that an FMD virus released from the National Bio and Agro-Defense Facility in Kansas could cause $16

[1]This chapter is a slightly modified version of our published article[59].

billion–\$140 billion in damages. Schroeder et al.[73] estimated that a hypothetical FMD outbreak in the midwestern United States could result in \$56 billion–\$188 billion of producer and consumer losses.

The FMD virus can be transmitted between farms through animal movement (direct contact) and via fomites such as contaminated equipment and vehicles (indirect contact)[29;107;108]. Its transmission routes also include local area spread and airborne spread. While disease transmission through the movement of infected cattle has been extensively studied in previous works[26–28], indirect contact through fomites has recently gained attention, especially after the 2001 U.K. FMD outbreak, in which new cases occurred for several months after early implementation of an animal movement ban[86]. The spread of FMD stopped only after strict biosecurity measures targeting the movement of contaminated equipment and personnel were implemented[109]. This study focused on indirect contact via livestock transporters, one of the most at-risk operator categories[29;30].

Only a few studies have considered truck movements to be indirect contact routes for the spread of disease among farms. Thakur et al.[110] developed a farm-level model to simulate the spread of porcine reproductive and respiratory syndrome virus through animal movement and truck sharing. Their results of using static links between farms highlighted the significant role indirect contact played in spreading the disease. Wiltshire[111] developed a model to heuristically generate a dynamic hog production system while accounting for truck contamination, demonstrating that producer specialization can increase system vulnerability to disease outbreaks. Bernini et al.[8] developed a two-layer temporal network to model disease transmission through cattle exchanges and transportation and compared epidemic size under full or partial knowledge of daily truck itineraries. Their work concluded that an accurate description of indirect contact is essential for precise prediction of epidemic spreading dynamics. However, no previous studies have included trucks as independent epidemiological units, as is emphasized in this research.

Simulation models have been widely used to mimic FMD transmission among farms and analyze various control strategies. Bate et al.[105] simulated FMD transmission in a three-county area in California, demonstrating the effectiveness of preemptive culling of highest-risk herds and ring vaccination. This model was widely used and later adapted to analyze FMD mitigation strategies in other countries, including Sweden[112] and Denmark[107]. Other stochastic, state-transition simulation models included the NAADSM[113], AusSpread[114], InterSpreadPlus[115], and AADIS[116], which involve multiple animal species and pathways for disease spreading. However, these herd-level models rely on accurate estimates of the contact frequency and distance distribution between livestock operations and do not consider actual contact sequences that occur between farms[8]. In addition, the number of animals is often assumed to be constant over time in each herd in these models.

Suggested animal movement traceability systems in the United States have faced opposition from beef producer organizations due to privacy issues, resulting in contact rates used for most FMD simulation models being based on expert opinions and questionnaires. Though the inspection at slaughterhouses is the most effective surveillance component for early epidemic detection[33], most FMD simulation models are built without including slaughterhouses. In addition, they are often based on static networks and ignore the system's time-varying structure, which is crucial for simulating the dynamics of highly contagious diseases[31]. In this study, the structures of both cattle movement and truck movement networks vary over time based on cattle trading among farms. Recent work has focused increasingly on temporal network measures, showing that possible outbreak sizes may be overestimated in a static view of the network[32]. Sterchi et al.[117] concluded that information about transport sequences could change the contact network topology and that consideration of truck sharing and contamination could increase network connectivity and individual connectedness of farms. Liu et al.[90] built a spatially explicit cattle-level agent-based model for two counties in Kansas, in which producers made decisions on cattle trade based on cattle weights and market conditions. Their work emphasized the influence of trading dynamics on the disease transmission through cattle movement.

Traceability programs, however, have become common in the global beef market, and lack of such programs may decrease export markets for the U.S. beef industry[118]. For example, if 25% of beef products became unacceptable in international trade, then the U.S. economy would experience an estimated $6.65 billion loss[119]. An improved information infrastructure with traceability systems would yield many benefits, including targeted and timely product recalls after a foodborne illness outbreak and increased brand value for products due to quality assurance. Several pilot projects have recently developed and tested purpose-built cattle disease traceability infrastructures. In these projects, cattle movement information is uploaded to a secure third-party database through radio frequency identification tags or similar devices. Since the acceptance of such traceability programs depends on the trust among stakeholders, these pilot programs have focused on persuading operators to participate. New technologies such as Blockchain, which has been increasingly studied[120–123], are expected to build trust among food partners, promote livestock traceability, and enhance food safety.

In response to potential FMD outbreaks, governmental agencies in the United States have designed control measures and preparedness plans. According to the U.S. Department of Agriculture, the depopulation of clinically affected and in-contact susceptible animals (stamping-out) is typically applied with other emergency vaccination strategies depending on the circumstances and epidemic sizes of FMD outbreaks[124]. In Kansas, for example, the Kansas Animal Health Commissioner would issue a state-wide stop movement order to all animal and related product movement if an FMD case occurred in North America. This movement restriction would remain in effect until the situation was deemed safe for the Kanas livestock industry, and producers would have to provide documents such as normal health status for animals on the production site for the previous 14 days to request a movement permit from the Kansas Department of Agriculture[125].

In this chapter, we aims to *examine the potential impact of truck contamination and information sharing for FMD virus transmission in the beef cattle production system in southwest Kansas (SW KS), United States.* We simulate a hypothetical FMD transmission through cattle movement and truck movement with major expansions relative to the model[58], including state transition models embedded in cattle agent, truck agent, producer agent, and packer agent. In order to enable information-sharing functionality, each producer/packer agent stores time-stamped trade information and can inform their trade partners during an outbreak. Scenario analysis is conducted to evaluate the effect of various control strategies on the spread of the epidemic, and sensitivity analysis is implemented to examine the outcomes affected by different input parameters.

3.2 Model

In this section, we describe the agent-based model developed for the simulations and the design for scenario analysis and sensitivity analysis.

3.2.1 Model description

In this work, an agent-based, stochastic, cattle-level simulation model is developed in AnyLogic software based on the agent-based model developed in Chapter 2. Agent functionalities are altered to enable FMD transmission through both direct and indirect contact routes and information-sharing functionality.

Model structure

The model simulates the behaviors of the interdependent beef cattle production and transportation systems in SW KS, which can be regarded as dynamic cattle movement and truck movement networks. The model structure is shown in Figure 3.1.

As shown in Fig 3.1, the main agent builds the environment in which other agents live. All premises are located based on their latitude and longitude, and trucks move cattle on the roads within the GIS map. Producer agents play the role of cow-calf ranches, stockers, and feedlots. In ranches, cows produce a new generation of calves that are fed until around 450 pounds, and will be sold directly or via auction markets to stockers. At approximately 650 pounds, cattle raised in stocker operations will be sold directly or via auction markets to feedlots. Once heifers and steers in feedlots achieve 1250 pounds and 1350 pounds respectively, they will be moved to the final meat-processing facilities, the packers. Please note that slaughterhouses are also called packers in U.S. beef production systems, and these two terms are used interchangeably in this paper. When producers from inside SW KS request cattle from the outside, cattle coming from outside SW KS are generated at entry point agents,

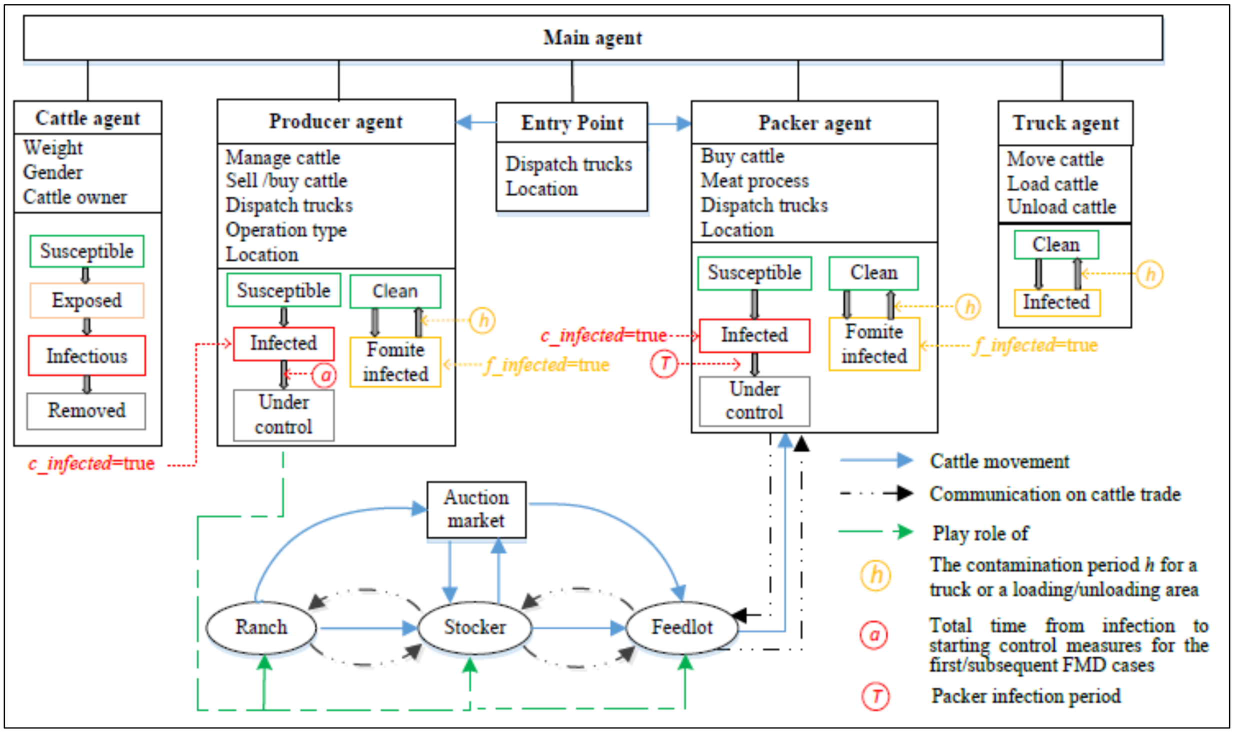

Figure 3.1: *Structure of the agent-based epidemic model.*

which are located on the major highways into and out of SW KS. Trucks are dispatched by their owner to transport cattle among premises following the amounts specified in the order agents, which are set up during the cattle trade process.

The parameters used for simulation are presented in Table 3.1.

Epidemic initialization

All the cattle in the system are in the susceptible state before the epidemic is initialized. For each simulation run, one randomly selected animal from outside SW KS will enter the infectious state on the 9th day at midnight, and will be brought to a stocker inside the region on the 10th day. If there are no cattle at the border at this time, the simulation will stop and start the next simulation run. In different simulation runs, the recipient stocker of the first infectious animal will be different due to the stochasticity of the model.

Table 3.1: *Parameters used for simulating the FMD spread*

Parameters	Value	References
Probability of transmission when an infected cattle agent contacts a susceptible cattle agent	0.95	Boklund et al.[107]
Length of the cattle latent period (days) [Pert distribution]	Pert(1.2, 1.2, 2.4)	Yadav et al.[126]
Length of the cattle infectious period (days) [Normal distribution]	Normal(11.4, 1.1)	Yadav et al.[126]
Total time from infection to starting control measures for the first infected FMD case [Triangular distribution]	$\mu = 8.6; 6.0 \leq x \leq 12.8$	Walz et al.[127]
Total time from infection to starting control measures for subsequent FMD cases [Triangular distribution]	$\mu = 6.6; 4.5 \leq x \leq 10.5$	Walz et al.[127]
The contamination period h for a truck or a loading/unloading area of premises (days)	14	Rossi et al.[128]
Length of the packer infection period (days) [triangular distribution]	$\mu = 5; 0 \leq x \leq 10$	Wiltshire et al.[111]
Probability that truck will be contaminated upon visiting an infected producer/packer	0.15	Wiltshire et al.[111]
Probability that contaminated truck will infect the subsequent producer/packer it will visit	0.15	Wiltshire et al.[111]
Probability that infected cattle will contaminate packer/producer receiving area	0.75	Wiltshire et al.[111]
Number of days to trace back and forward during the information sharing process (days)	14	Assumed

Spread of the disease

In this section, we describe major functions added to the base model to enable FMD transmission.

(1) Cattle agent

Each cattle agent is associated with a Susceptible-Exposed-Infectious-Removed compartment model. Compared to the cattle in the infectious state, cattle agents in the exposed state have been infected by the FMD disease, but are not contagious yet. Animals in the removed state have been infected before, and become dead or immune, or are culled by the producers. More specifically, in contact with an animal in the infectious state, a susceptible cattle agent has a 95% chance to become infected and transition to the exposed state. After a latent period, the cattle agent will transition to the infectious state during which it contacts and infects other cattle of the same premises. Then, the cattle agent enters the removed state after an infectious period.

Considering computational efficiency, we use a scaling factor of 10 to change all the parameters related to the number of cattle, e.g., truck capacity and cattle capacity of each producer, such that one cattle agent represents ten cattle. We assume that each cattle agent contacts, on average, 20 cattle agents in a day. 20 cattle agents correspond to 200 cattle due to the scaling factor, indicating the approximate number of cattle in a group. Accordingly, during the infectious state, each cattle agent can infect on average 20×0.95 cattle agents per day, where 0.95 is the probability of transmission when infected cattle contact susceptible cattle.

(2) Producer agent

When an infectious cattle agent occurs in the producer agent, the producer will transition from the susceptible state to the infected state ($c\_infected$ = true). If there is no control strategy implemented on the producer premises level, the infected producers will not transition to the under-control state. Otherwise, the producer agent will enter the under-control state after a total time from infection to starting control measures. As the producer agent enters the under-control state, all its cattle will transition to the removed state, simulating that the producer depopulates its cattle. In addition, various control strategies are implemented, and more details will be described in the scenario analysis section.

When all infected cattle of an infected producer enter the removed state, the *c_infected* variable is set to be false. On the other hand, when a producer becomes infected by fomite, the variable *f_infected* becomes true and will last for 14 days (the contamination period h in Table 3.1).

(3) Packer agent

Once a cattle agent in the infectious state arrives at the packer, the packer agent will transition to the infected state ($c\_infected$=true), and after a packer infection period T, the packer goes to the under-control state, in which the packer stops requesting and transporting cattle from other producers to its location. To be more realistic, we assume that more infectious cattle arriving at the packer will speed up FMD detection. For example, if there are infectious cattle coming in on day d_1 and day d_2, the model will generate two numbers, ct and ct', respectively, according to the distribution with a mean of 5 days in Table 3.1. The smaller value between ct' and ct will be assigned as the contamination period T, as shown in Fig 3.1. On the other hand, once the packer is infected by fomite, its cattle receiving area will remain contaminated (*f_infected* = true) for 14 days based on the contamination period h.

(4) Truck agent

Following a clean-infected-clean cycle, trucks move to the origin premises to pick up cattle and then move the animals to the destination premises to unload. With direct contact infection probability set as 1.0[110;128], when at least one infectious cattle agent is moved and received at the destination premises, the destination becomes infected with *c_infected* set as true. For indirect contact, trucks may become contaminated by visiting fomite-infected premises, and then remain contaminated for a contamination period h, during which time the infection may spread to other premises.

More specifically, when the truck arrives at the origin premises, if there are infectious cattle loaded to the truck at the origin premises, then there is a 75% probability that the receiving area of the origin producer will become infected via fomite (*f_infected* = true). If the origin producer is fomite-infected and the truck is not contaminated, the truck may become contaminated with a 15% probability; however, if the truck is contaminated and the origin producer is not fomite-infected (*f_infected* = false), the truck will cause the producer to become fomite-infected with a 15% probability.

When the truck arrives at the destination premises, if there are infectious cattle unloaded, there is a 75% probability that the destination premises will become fomite-infected. Meanwhile, if the destination is fomite-infected and the truck is clean, there is a 15% probability that the truck may become contaminated. However, if the truck is infected and the destination is not fomite-infected, the truck may cause the destination to become fomite-infected. Note that at the time the origin or destination producer becomes fomite-infected, we will randomly select one cattle agent from the premises to become infected.

3.2.2 Scenario analysis

In this section, ten different scenarios are constructed based on three attributes: (1) the two FMD virus transmission routes, namely by direct contact only or by both direct and indirect contact; (2) the implementation of movement bans; and (3) the involvement of information infrastructure. The combination of these factors is described in Table 3.2, and all the parameters follow the values described in Table 3.1 in the scenario analysis. Five hundred iterations of each scenario are run to generate a distribution of the outcomes. A 200-day simulation duration is selected such that all producers already reach the steady-state in the end regarding disease transmission, i.e., no new infections occur.

Table 3.2: *Description of the scenarios*

Scenario number and name	Spread by direct contact	Spread by indirect contact	Movement ban on infected producers	Information infrastructure enabled on producers	Information infrastructure enabled on packers	Movement ban in the whole region
1 DI	Yes	No	No	No	No	No
2 DI_B	Yes	No	Yes	No	No	No
3 DI_B_P	Yes	No	Yes	Yes	No	No
4 DI_B_PP	Yes	No	Yes	Yes	Yes	No
5 DI_RB	Yes	No	No	No	No	Yes
6 D&IN	Yes	Yes	No	No	No	No
7 D&IN_B	Yes	Yes	Yes	No	No	No
8 D&IN_B_P	Yes	Yes	Yes	Yes	No	No
9 D&IN_B_PP	Yes	Yes	Yes	Yes	Yes	No
10 D&IN_RB	Yes	Yes	Yes	No	No	Yes

DI: direct contact only, D&IN: direct and indirect contact, B: movement ban on infected producers, P: information infrastructure on producers, PP: information infrastructure on both producers and packers. RB: region-wide movement ban.

In scenarios 1 and 6, there is no control strategy implemented on the producer premises level. In all the other scenarios, once a producer/packer is in the under-control state, it will be under movement restrictions. Here we assume that any movement ban was effective with 100% compliance, meaning that all movements to and from the producer/packer would stop, once the movement ban is enacted. Therefore, both direct and indirect contacts related to these premises are stopped, since trucks will no longer move cattle to or from these premises. To enable information-sharing functionality, each producer/packer agent stores time-stamped trade information with its trade partners. During outbreaks, the producer/packer agent can trace back and forward its trade record in the past 14 days to inform their trade partners about its infection by disease. This time-interval of 14 days will be referred as the number of days to trace back and forward in the sensitivity analysis section.

- For scenarios with a movement ban on infected producers, or called producer isolation (scenarios 2 and 7), a movement ban will be introduced to the infected producer once the producer is in the under-control state.

- For scenarios with a region-wide movement ban (scenarios 5 and 10), the movement ban will be enacted for all the producers and packers inside the region as long as there is one infected producer in the under-control state.

- For scenarios with information-sharing functionality enabled only on producers and not on packers (scenarios 3 and 8), the producer in the under-control state will notify those producers with which it has traded in the past 14 days (both its suppliers and customers). Once those producers receive notification from the information sender, they will go to the under-control state and notify their trading partners as well.

- For scenarios that information-sharing functionality is enabled on both producers and packers (scenarios 4 and 9), the producer will notify both producers and packers with which it has traded in the past 14 days. In addition, once an infected packer enters the under-control state, it will immediately notify its trade partner producers. On the other hand, if a producer in the under-control state notifies a packer not in the under-control state that it has the potential to be infected, the packer will also go to the under-control state.

3.2.3 Sensitivity analysis

To evaluate how changes in parameters can impact the simulation results, we perform sensitivity analyses for different scenarios by creating variations in a single input parameter while keeping other simulation settings unchanged. First, sensitivity analyses of the number of days to trace back and forward during the information-sharing process are conducted under scenarios D&IN_B_PP (information infrastructure enabled on producers and packers) and D&IN_B_P (information infrastructure enabled on only producers). The number of days to trace back and forward is selected for sensitivity analyses, as it is assumed as 14 days based on expert opinion, and it is likely to influence the epidemic control effectiveness during the information-sharing process. Second, parameters related to indirect contact routes: (a) indirect contact transmission probability, and (b) contamination period h for a truck or a loading/unloading area of premises are altered, and their impact on the number of infected producers are evaluated under scenario D&IN_B. In this work, we set indirect contact transmission probability as 0.15[111], but Bate et al.[105] assume distributions for the high-risk and low-risk indirect contact probability as BetaPert(0.1, 0.5, 0.9) and BetaPert(0.05, 0.175, 0.35), respectively. Accordingly, we compare the number of infected producers under different values of the indirect contact transmission probability, varying from 0.05 to 0.5 with an interval of 0.05. In addition, we conduct sensitivity analyses on the contamination period h, ranging from 1 day to 22 days with an interval of 3 days. For all variations, 500 iterations of each scenario are simulated for 200 days.

3.3 Results

3.3.1 Scenario analysis

Fig. 3.2 shows the distributions of numbers of infected producers and cattle agents removed for the ten scenarios. Overall, the epidemic size is smaller for scenarios that model only direct contact (scenarios 1–5) when compared to equivalent scenarios that incorporate both direct and indirect contact (scenarios 6–10). For example, the median number of infected producers changes from 12 in scenario 1 (direct contact only) to 86 in scenario 6 (direct and indirect contact). Findings indicate that including indirect contact through truck contamination has a considerable impact on the FMD spread among producers. Since contaminated trucks can travel to multiple places, truck contamination can aggravate the disease spread between those who do not have direct contact (animal movement in between), thereby enlarging the scale of epidemic spreading.

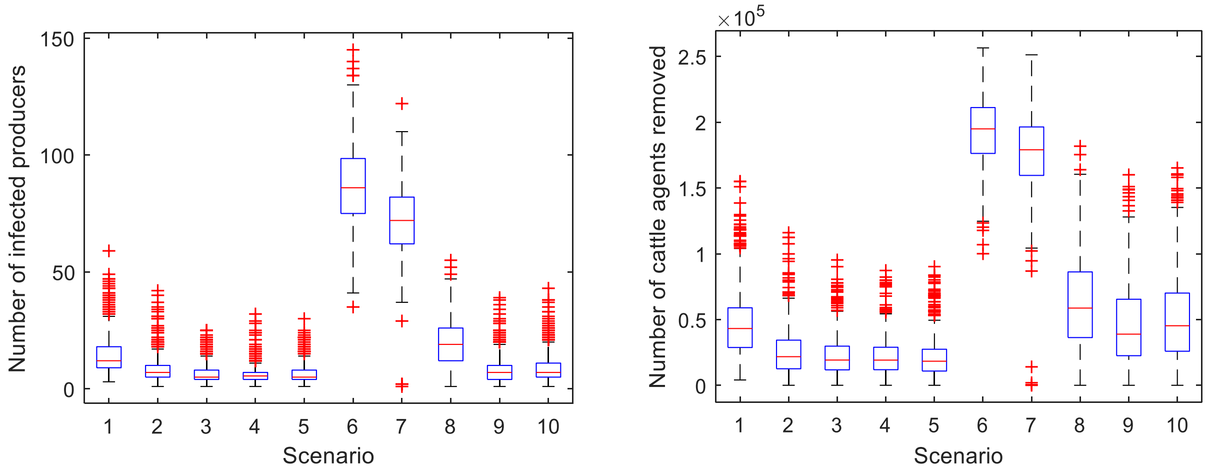

(a) Number of infected producers *(b) Number of cattle agents removed*

Figure 3.2: *Distributions of numbers of infected producers and cattle agents removed.*

More specifically, for scenarios 1–5, scenarios 2–5 result in a smaller and similar epidemic size compared to scenario 1 (no premises-level control strategies implemented). For scenarios 6–10, scenario 6 (no premises-level control strategies implemented) results in the largest epidemic size, followed by scenario 7 (producer isolation), and then scenario 8 (information infrastructure enabled on producers), while scenarios 9 (information infrastructure enabled on producers and packers) and 10 (regional movement ban) result in the smallest and similar epidemic sizes. There is a slight difference in terms of the median size between scenarios 6 and 7, indicating that merely implementing movement bans on infected producers cannot effectively contain the epidemic when indirect contact is considered. Information sharing can significantly reduce the epidemic size, compared to scenario 6. Particularly, the number of infected producers is larger in scenario 8 is with median 19 and interquartile range 12–26, compared with scenarios 9 and 10 in Fig. 3.2(a). This is because information-sharing functionality is not enabled on packers in scenario 8, and these infected packers can spread the infection by their contaminated trucks to other producers in some simulation runs.

As additional information for the epidemic dynamics, Figs. 3.3–3.4 show the numbers of cattle agents in each compartment and newly infected producers over time for scenarios 2, 7 and 8–9. In Fig. 3.3, both the epidemic size and epidemic duration is larger in scenario 7 compared with scenario 2, indicating that truck contamination can aggravate the spread of epidemics. Comparing Fig. 3.4 with Fig. 3.3, it is shown that the addition of information-sharing functionality reduces the number of cattle agents removed during the outbreak. Particularly, there is a larger variance in terms of new infected producers in scenario 8 compared to scenario 9, indicating that the system is more robust when information-sharing functionality is enabled in both producers and packers.

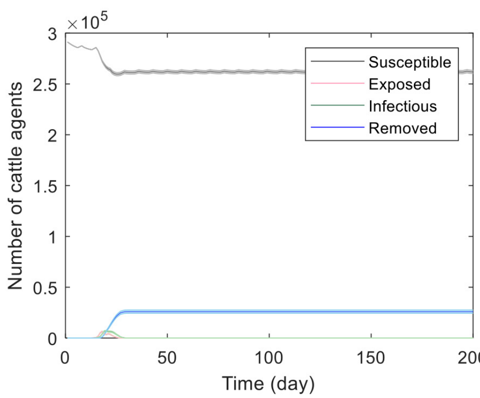

(a) Number of cattle agents in scenario 2

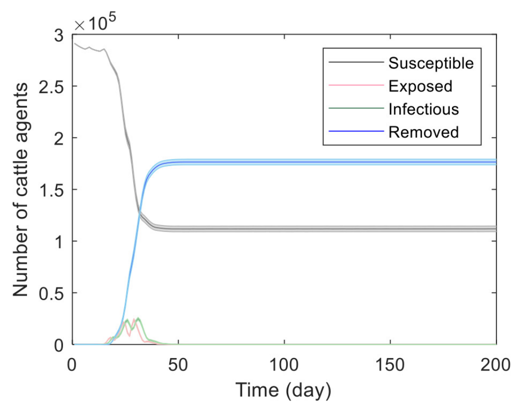

(b) Number of cattle agents in scenario 7

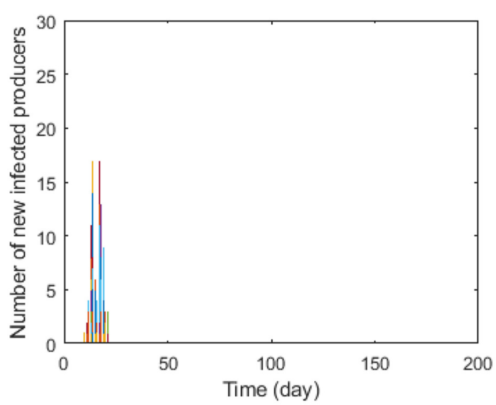

(c) Number of infected producers in scenario 2

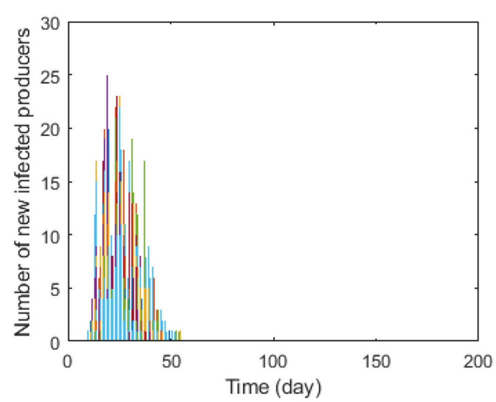

(d) Number of infected producers in scenario 7

Figure 3.3: *Comparison between scenario 2 and scenario 7. In Fig. 3.3(c–d), various colors represent the number of new infected producers in different runs. Five hundred iterations of each scenario are simulated for 200 days.*

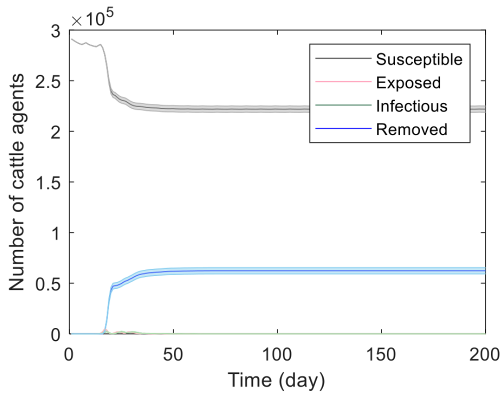

(a) Number of cattle agents in scenario 8

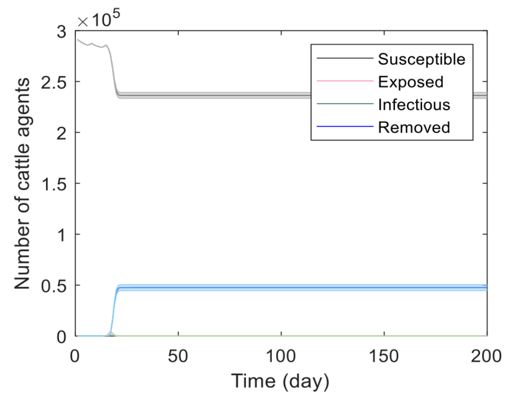

(b) Number of cattle agents in scenario 9

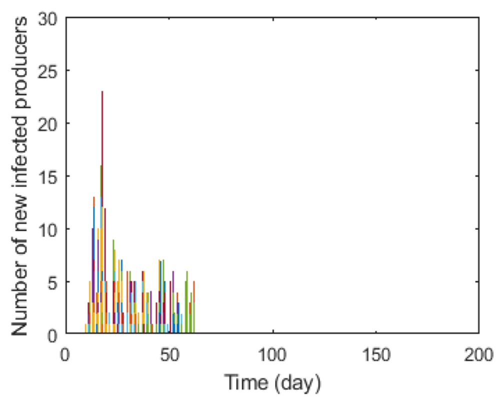

(c) Number of infected producers in scenario 8

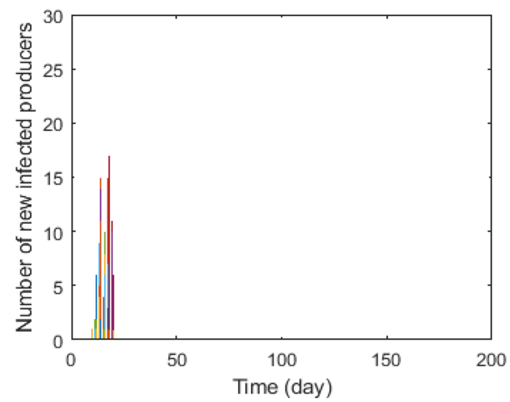

(d) Number of infected producers in scenario 9

Figure 3.4: *Comparison between scenario 8 and scenario 9. In Fig. 3.4(c–d), various colors represent the number of new infected producers in different runs. Five hundred iterations of each scenario are simulated for 200 days.*

In the cattle supply chain, cattle flows are essentially driven by the normal operation of packers to meet steady demand, so the total number of cattle in the system during the simulation period is strongly affected by the packers' operation time. With infected cattle coming in, the packer will go to the under-control state after a infection period, and then will stop receiving cattle from feedlots both inside and outside the region. As a result, feedlots will stop requesting cattle from other premises, which will impact the number of cattle stocker operations will request. Therefore, the system's cattle flow quickly stops once packers are in the under-control state, affecting the total number of cattle agents in the system. As the producers and packers gain revenues by marketing their cattle or cattle-related products, the total number of cattle agents in the system, which include the cattle that are marketed and being prepared to be marketed, can be seen as a measure for the economic impact of the control strategies on the cattle industry. In each simulation run, we calculate the total packer operating time by summing the four packers' operating time during the 200-day simulation period. Distributions of the total number of cattle agents that exist in the system and total packer operating time are shown in Fig. 3.5.

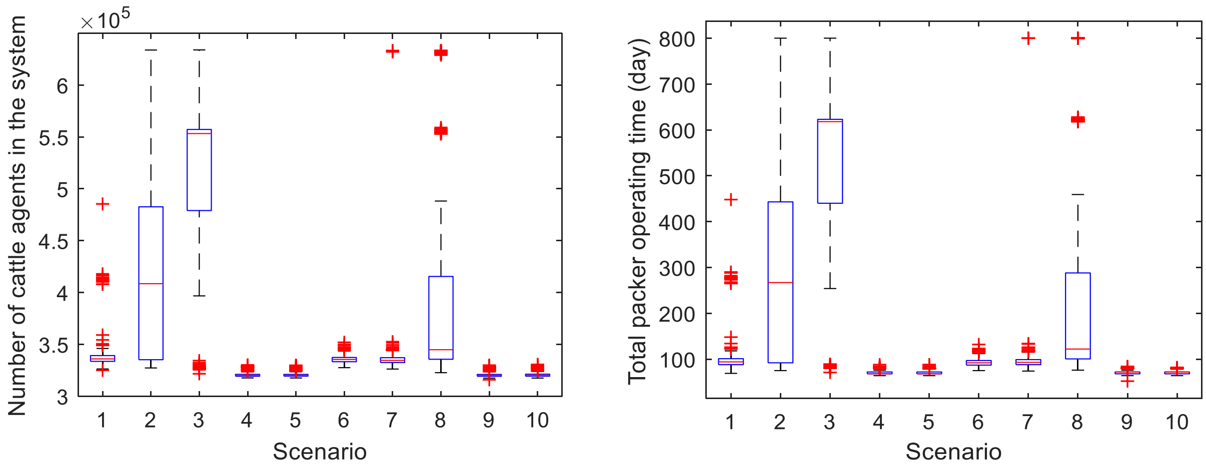

(a) Number of cattle agents in the system *(b) Total packer operating time (day)*

Figure 3.5: *Distributions of the total number of cattle agents and total packer operating time.*

In Fig 3.5, scenarios 3 results in the largest median number of cattle agents (Fig 3.5(a)) and packer operating time (Fig. 3.5(b)), followed by scenario 2 (producer isolation), and all the other scenarios are with a similar value. In scenario 3 (information-sharing functionality enabled only on producers), the infected producers and their trading partner producers become isolated in the system quickly, but the packers can continue to request cattle from other uninfected producers, thereby sustaining regular operations for a longer time. Compared with scenario 1 (no farm-level control strategies implemented), the median number of cattle agents of scenario 2 is larger because producer isolation is already effective to contain the epidemic, resulting in less infected packers and an increased packer operation time. However, the infected producers will be in the under-control state more quickly in scenario 3 with information-sharing among producers, so packers can sustain regular operations for a longer time, and the median number of cattle agents in scenario 3 is higher compared to scenario 2.

When information sharing is enabled for both producers and packers (scenarios 4 and 9), once infected feedlots occur, the four packers are much more likely to have traded with these producers and will quickly transition to the under-control state, resulting in a lower number of cattle agents over the system. Though information-sharing on all premises and region-wide movement ban (scenarios 4–5, 9–10) are both very effective regarding the epidemic containment, these two relatively protective strategies have a greater economic impact with a higher loss in cattle. It indicates that determining the appropriate control strategy is a tradeoff between multiple factors, including the economic effect and effectiveness of the epidemic control. Based on these simulations, placing control measures on packers has a large impact on the business discontinuity to the system based on decreased packer operating time and number of cattle agents. These control decisions need to be based on additional criteria not considered in the current setting, where a packer comes under control only because one of its trading partners is under control.

3.3.2 Sensitivity analysis

The number of days to trace back and forward during the information-sharing process

The distribution of the number of infected producers under scenarios D&IN_B_P (information infrastructure enabled on producers) and D&IN_B_PP (information infrastructure enabled on producers and packers) is shown in Fig 3.6. The modeled outcomes are sensitive to the variation in the number of days to trace back and forward. For instance, a decrease from 14 days to 1 day in scenario D&IN_B_P (scenario 8) results in an increase of 2.47 times in the median number of infected producers. A small number of days to trace back and forward is not enough to contain the epidemic, but a larger value can lead to more premises in the under-control state, resulting in a larger economic impact. This implies that the number of days to trace back and forward is an important parameter during the information-sharing process and should be paid much attention in practice. Besides, the variation regarding the epidemic size in scenario D&IN_B_PP (scenario 9) is smaller than scenario D&IN_B_P, indicating that it is necessary to include the critical component packers into the information-sharing infrastructure.

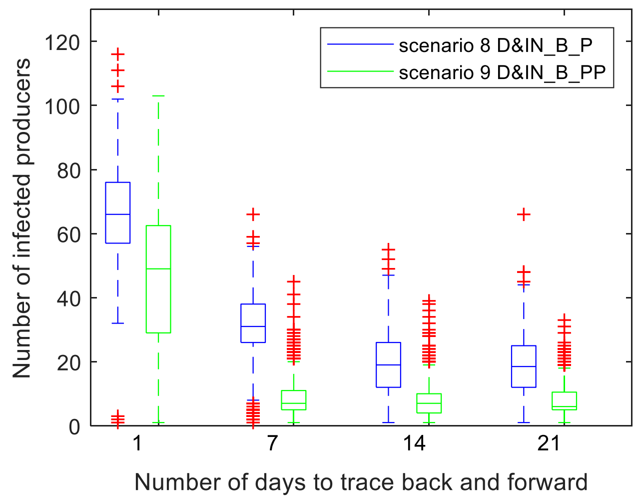

Figure 3.6: *The sensitivity of the number of days to trace back and forward during information sharing .*

Indirect transmission probability and contamination period h

The indirect transmission probability used in the scenario analysis equals 0.15, referring to the probability that a truck will become contaminated upon visiting an infected producer/packer, and the probability that a contaminated truck will infect the subsequent producer/packer. Results in Fig. 3.7 are both sensitive to the indirect contact transmission probability and the contamination period h for scenario D&IN_B (producer isolation). For example, an increase of indirect transmission probability from 0.15 to 0.2, the median number of infected producers changes from 72 to 97. The results suggest that a more accurate estimation of these parameters related to indirect contact routes are critical to epidemic modeling. Since these two parameters are closely tied to the biosecurity status of cattle premises, these premises should be vigilant and follow guidelines for proper cleaning and disinfection of vehicles and cattle loading/unloading areas, such to limit the impact of indirect contacts on disease spread between premises.

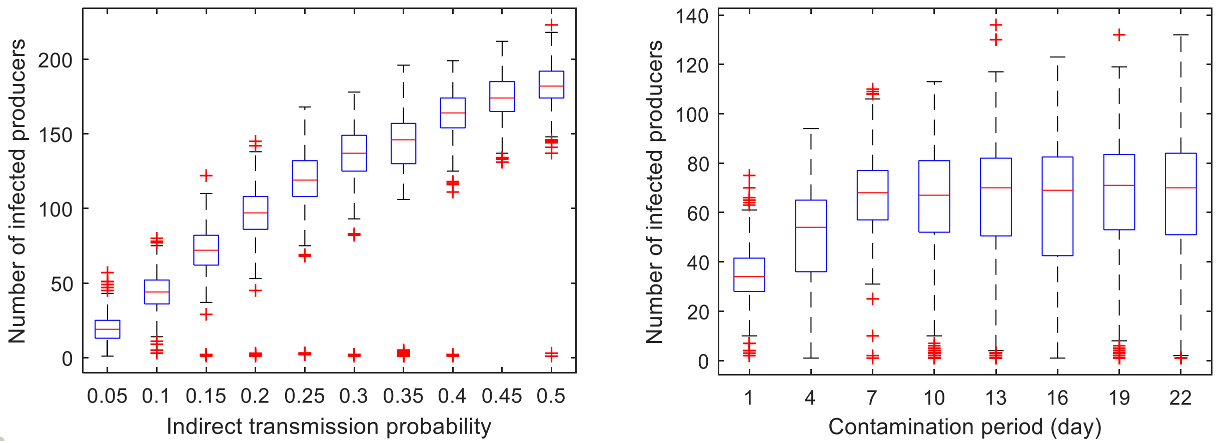

(a) Sensitivity of indirect transmission probability

(b) Sensitivity of contamination period

Figure 3.7: *The sensitivity of indirect transmission probability and contamination period under scenario D&IN_B.*

3.4 Comparison with previous FMD models

The model developed in chapter makes several advances over previous epidemic models on the spread of FMD virus. Many epidemiological studies consider only direct contacts[27;31]. Existing models such as the North American Animal Disease Spread Model[113] and InterSpread Plus[115] include the indirect contact transmission route, but do not consider the sequence of contacts occurring between farms. In this work, cattle are transported by trucks based on premises locations and regular business operating principles, which can be regarded as temporal cattle and truck movement networks. More specifically, the number of connections between pairs of farms and the strength of each connection varies over time, as each transaction between farms involves various cattle order volumes and each truck can transport a variable number of animals. What's more, these models take each farm as an epidemiological unit and ignore the modeling of disease spread within a farm. In contrast, each cattle agent follows its Susceptible-Exposed-Infectious-Removed compartment and is with heterogeneous parameters such as weight and gender in our model. The Australian Animal Disease model[116] predicts the fraction of animals in each state of each herd, but the number of animals in each herd is constant over time, whereas ours changes according to the cattle trade information. In addition, these FMD simulation models only include producers, whereas our work includes also packers, which are sinks for cattle transported through the production system and behave as hubs that can facilitate disease spreading. Natale et al.[129] simulate a hypothetical outbreak in dairy production systems, including slaughter plants, but they only include direct contact through cattle movement, whereas ours simulates indirect contact routes resulting from loading/unloading areas of premises, and trucks transporting cattle.

3.5 Summary

This study examines the potential impact of truck contamination and information sharing on epidemic dynamics, with a particular focus on indirect contacts due to cattle movements. Our simulation results reveal that including the truck movement (indirect contact) can significantly exacerbate the disease spread in the system, compared with equivalent scenarios that only consider animal movement (direct contact). For example, the median [interquartile range] number of infected producers is 7 [5–10] vs. 72 [62–82] in scenarios DI_B (direct contact only) and D&IN_B (direct and indirect contact) respectively. This finding is consistent with recent studies[110;128;130], which all highlighted the substantial effect of indirect contacts on the ability of farms to potentially spread diseases. Focusing on dairy farms, Rossi et al.[85] applied network analysis techniques and showed that indirect contacts through on-farm visits by veterinarians produced a more connected network compared to direct contact only. Considering the sharing of vehicles for shipment of swine, Thakur et al.[110] concluded that indirect contact significantly played a role in further spreading the infection, which is not directly connected regardless of the types of network structures.

Different from prior works, the findings provided in this study add new insights to the works related to the supply chain with a focus on sharing information during epidemics. Our simulation results showed that including information-sharing functionality on producers and packers can dramatically reduce the epidemic size; for instance, the median number of infected producers in scenario D&IN_B (producer isolation) reduces by 90.28% in scenario D&IN_B_PP (information infrastructure enabled on producers and packers). Policymakers may focus more on promoting the development of new mitigation strategies informed by information sharing based on novel cyber-infrastructure for rapid detection and containment.

Particularly, the number of days to trace back and forward during information sharing has a significant influence on the simulation outcome and is worth further studying considering the economic impacts of the related mitigation strategies. These findings supported previous theoretical studies that showed the effectiveness of information awareness or information diffusion in suppressing disease spreading using multilayer networks[131–134]. In these studies, individuals become alerted and adopt preventive measures when sensing the infection in their neighbors.

Chapter 4

Impact of human behavior on animal disease spreading

4.1 Introduction

As livestock production has suffered substantial losses from many prior unexpected events such as foot-and-mouth disease (FMD) outbreaks and swine fever in the past, the number of sophisticated models developed for livestock diseases has surged. However, many of these epidemiological frameworks did not model human behavioral changes during epidemics[35]. A proper understanding of animal disease dynamics depends not only on accurate epidemiological parameter estimates and an appropriate underlying movement network, but also on the disease-related human behavior factors. Not accounting for human behavioral changes in epidemiological models could lead to a substantial bias. Thus, exploring the potential impact of behavioral changes on disease epidemics is vital to shedding light on future disease management[135;136].

Several projects have applied multiplex networks to study the interplay between human behavior factors and epidemic dynamics[131;133;137;138]. The substantial influence of human behavior factors such as risk attitudes has drawn scholars' attention during the current global pandemic. Studies have found that more risk-averse attitudes were related to a dramatic decline in human mobility and were significantly related to adherence to the recommended behaviors[139;140]. In the context of livestock production, biosecurity is referred to as implementing control measures to decrease the chance of animal disease spreading[25]. Several studies have analyzed the factors that are likely to influence farmers' willingness to comply with biosecurity protocols, and examples of such factors include knowledge of disease prevalence, farmers' risk perception, and disease experience of neighboring farmers[34–36]. Mendes et al.[37] emphasized the importance of controlling chronic livestock disease considering farmers' different responses to the perceived risk. Tago et al.[141] illustrated how farmers' strategic behavior can considerably reduce the efficacy of movement restriction policy for disease spread in a French cattle trade network.

This chapter aims at investigating *how human behavioral changes around biosecurity could affect disease transmission dynamics in livestock production systems*. We will apply an agent-based modeling (ABM) approach, which allows simulating interactions among heterogeneous individuals in complex systems. As a bottom-up approach, ABM has been widely applied to diverse areas, including economics, agriculture, transportation, and healthcare[142]. Abdulkareem et al.[143], for example, used an agent-based approach to compare the effects of individual and group learning on the decision-making process regarding risk appraisal and protective decisions. Their results showed that behavioral changes could lead to different epidemic durations and sizes. Bucini et al.[144] found that shifting 37.5% of the producer agents toward a risk-averse position could result in a significantly sharp decrease in the epidemic size of the porcine epidemic diarrhea virus. Sok and Fischer[145] modeled farmers' vaccination decisions over bluetongue disease, taking risk perception and social pressure into account. Their results suggested that a risk communication strategy has an advantage over financial compensation in increasing vaccination uptake. To the best of the authors' knowledge, few works have examined human behavioral changes on animal disease transmission. This work adds a new element to this domain with a focus on the following perspectives: (i) random or targeted selection in risk communication audiences, and (ii) initial biosecurity status.

We will model beef cattle production systems in southwest Kansas, the United States, as a case study and examine the impact of human behavior factors on a hypothetical FMD spreading. FMD could spread so quickly through cattle herds that a delay of even a few days would be devastating, resulting in losses in both animals and export markets. The modeled beef cattle production chain spans from cow-calf ranches to stockers, to feedlots, to packers. We consider disease spreading through direct and indirect contact routes, i.e., movement of infected animals and contaminated fomites. In addition, the model associates risk attitude categories to individuals, including producer agents, packer agents, and fleet companies, and takes the biosecurity level as an indicator to reflect human behavioral change during epidemics. We assume that individuals in the risk-averse category are likely to increase their biosecurity levels more promptly when facing a rise in the regional disease incidence than those with risk-tolerant attitudes. Here, biosecurity level indicates individual's compliance to biosecurity protocols, which are designed to reduce the risks of introducing disease agents to the premises. For example, a producer with a high biosecurity level will strictly follow the cleaning and disinfection guidelines of vehicles.

Resources for risk communication can be limited; for example, lack of employees may exist during the crisis. Therefore, it is necessary to design an effective risk communication strategy to protect livestock production. In scenario analyses, we change the percentage of producers in the risk-tolerant category in the total producer population under both random and targeted selection strategies. In the random strategy, producers are randomly selected as risk-averse or risk-tolerant. In the targeted strategy, producers are selected as risk-averse in descending order of their cattle capacity and the rest are assigned as risk-tolerant. In other words, risk communication resources will be allocated to large producers first, given the limited resources. In addition, we explore the impact of individuals' initial biosecurity levels on the epidemic dynamics. The outcomes are expected to deepen our understanding of the link between disease transmission dynamics and human behavioral changes, and improve disease management in livestock production, from on-farm management to the transportation of animals.

4.2 Model

In this section, we present details about the agent-based model added with the human behavior component.

4.2.1 Model description

The model was built on top of the agent-based model developed in Chapters 2–3. The added features integrated the human behavioral changes around biosecurity with the epidemic spreading process. The model structure is shown in Fig 4.1.

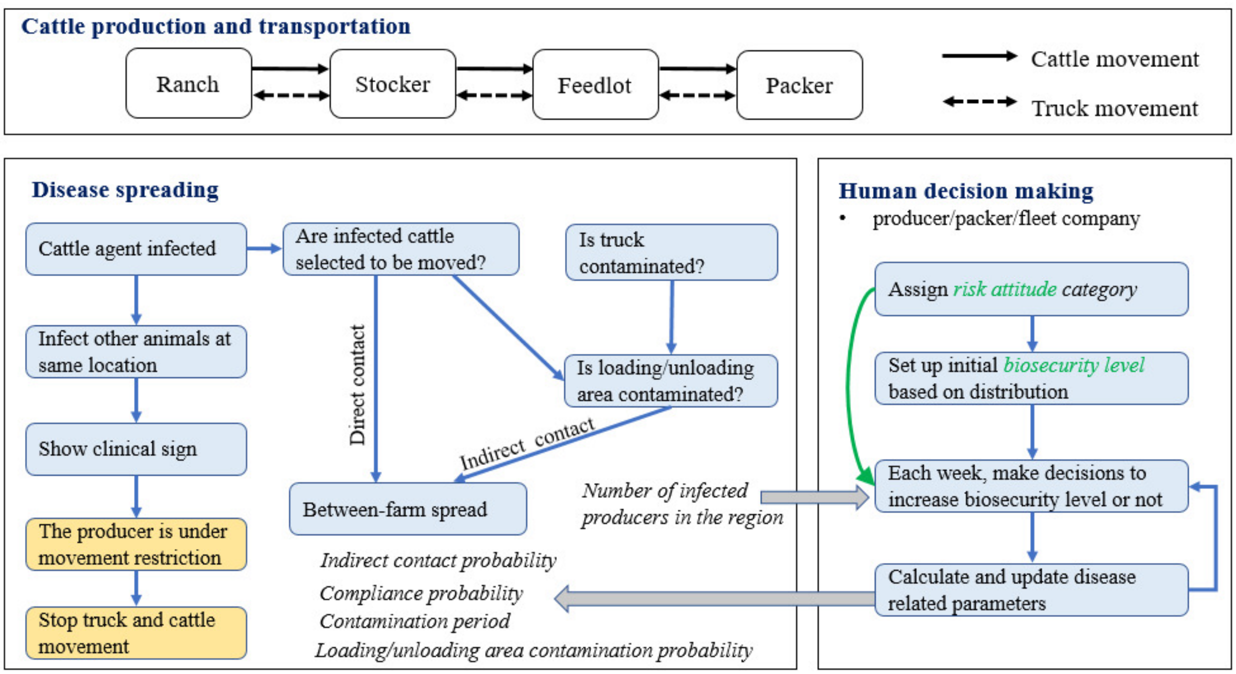

Figure 4.1: *Structure of the agent-based model added with human behavior factors.*

The model explicitly simulates business operations of the beef cattle industry and the associated transportation services on a GIS map. For a hypothetical FMD outbreak, we simulate disease transmission through the movement of infected cattle (direct contact) and the movement of contaminated fomites (indirect contact). Each cattle agent may transition among states of susceptible, exposed, infectious, and removed. Each truck follows a clean-infected-clean cycle and may become contaminated by visiting a fomite-infected location on its route. Contaminated trucks may further spread the infection to subsequent locations visited. A producer agent will transition to the infected state once it has infectious cattle. Then, after a total time from infection to starting control measures, the producer agent will depopulate all its cattle and follow movement restrictions. The producer agent includes three categories, namely ranches, stockers, and feedlots. For the sake of computational efficiency, a scaling factor of 15 is used for parameters related to the number of cattle such that one cattle agent represents fifteen physical animals. Information about the study population and parameters is shown in Table 4.1.

Table 4.1: *Model parameters*

Parameters	Value	References
Probability of transmission when an infected cattle agent contacts a susceptible cattle agent	0.95	Boklund et al.[107]
Length of cattle latent period (days) [Pert distribution]	Pert(1.2, 1.2, 2.4)	Yadav et al.[126]
Length of cattle infectious period (days) [Normal distribution]	Normal(11.4, 1.1)	Yadav et al.[126]
Total time from infection to beginning control measures for the first FMD case (days)[Triangular distribution]	$\mu = 8.6;\ 6.0 \leq x \leq 12.8$	Walz et al.[127]
Total time from infection to beginning control measures for subsequent FMD cases [Triangular distribution]	$\mu = 6.6;\ 4.5 \leq x \leq 10.5$	Walz et al.[127]
Contamination period H_{base} for a truck or a loading/unloading area of premises (days)	14	Rossi et al.[128]
Length of packer infection period (days) [Triangular distribution]	$\mu = 5; 0 \leq x \leq 10$	Wiltshire[111]
Indirect transmission probability P_{ind_base}	0.35	Bucini et al.[144]
Probability that infected cattle will contaminate packer/producer receiving area P_{inLoad_base}	0.75	Wiltshire[111]
Probability to comply with movement restrictions P_{mr_base}	1.0	Assumed

4.2.2 The human decision-making process

In the model, we incorporate the feature of risk attitude into each individual to influence its decision to increase biosecurity level, thereby indirectly affecting the disease transmission in the system. Here we assume that the biosecurity level will never decrease during the disease outbreaks, similar to Bucini et al.[144]. We consider two risk attitude categories, namely risk-averse and risk-tolerant, which will influence individuals' compliance with the biosecurity protocols.

As shown in Fig 4.1, each individual i is associated with variables of risk attitude category Att^i and biosecurity level bs_t^i. First, we initialize the value of Att^i for individual i, which will remain unchanged during the simulation. Then, for each type of the agent population (producer/packer/fleet agent), we set the initial biosecurity level ($bs_{t_0}^i$) for individual i according to the assumed distributions. The biosecurity level bs_t^i will change over time.

Each week, individual i makes a decision on whether to increase its biosecurity level based on equation 4.1 according to Bucini et al.[144].

$$bs_t^i = bs_{t-1}^i + \Delta bs \cdot \psi\left(Att^i, NI_t\right) \tag{4.1}$$

The biosecurity increase Δbs is a constant positive value and is assumed to be 2.5; bs_t^i is assumed to range between [0, 8]; and $\psi\left(Att^i, NI_t\right) = \begin{cases} 0, \text{ if } s > P_{increase} \\ 1, \text{ if } s < P_{increase} \end{cases}, s \in U(0,1)$. $P_{increase}$ is the probability of increasing biosecurity level and is calculated by equation 4.2.

$$P_{increase} = \frac{1}{1 + e^{m(NI_t - rI_0)}} \tag{4.2}$$

NI_t equals the number of infected producers in southwest Kansas at time t; $m = -0.95$ and $rI_0 = 0.18$ for a risk-averse category; and $m = -0.8$ and $rI_0 = 16$ for a risk-tolerant category. The relationship between $P_{increase}$ and NI_t is presented in Fig. 4.2. It shows how the increase in biosecurity level bs_t^i is influenced by the regional disease prevalence and an individual's risk attitude. As the number of infected producers increases, risk-averse individuals may be more prompt to make changes in the biosecurity practices than the risk-tolerant ones.

The model uses the biosecurity level bs_t^i in logistic functions (equation 4.3) to calculate the human-behavior related disease parameters, including indirect transmission probability P_{ind}^i, the contamination period H^i, compliance probability with movement restrictions P_{mr}^i,

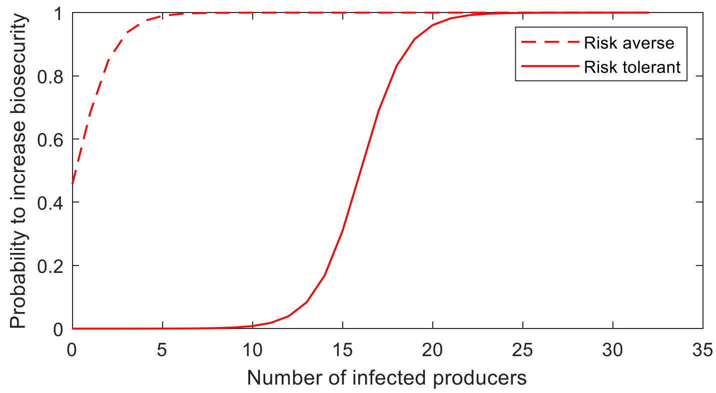

Figure 4.2: *Probability to increase biosecurity as a function of the number of infected farms driven by risk attitude.*

and the probability that infected cattle will contaminate the packer/producer receiving area P^i_{inLoad}. In equation 4.3, $bs_0 = 4.0$ and $m = 1.3$ according to Bucini et al.[144]. Values of P_{ind_base}, H_{base}, P_{mr_base}, P_{inLoad_base} are set according to Table 4.1.

$$\begin{cases} P^i_{ind} = P_{ind\_base}\frac{1}{1+e^{m\left(bs^i_t - bs_0\right)}} \\ H^i = H_{base}\frac{1}{1+e^{m\left(bs^i_t - bs_0\right)}} \\ P^i_{mr} = P_{mr\_base}\frac{1}{1+e^{m\left(bs^i_t - bs_0\right)}} \\ P^i_{inLoad} = P_{inLoad\_base}\frac{1}{1+e^{m\left(bs^i_t - bs_0\right)}} \end{cases} \tag{4.3}$$

From equation 4.3, a high biosecurity level will result in a low infection likelihood, indicating the high effectiveness of biosecurity measures. For example, vehicles can be cleaned and disinfected more frequently between subsequent shipments, leading to a shorter contamination period H^i. FMD outbreaks would lead to movement restrictions in the region. Individuals of higher biosecurity level will stop all movement of animals and vehicles with a higher compliance probability P^i_{mr}. Producers can invest facilities and equipment for washing and disinfecting vehicles entering the managed premises, which may lead to a smaller value of P^i_{ind}. Cattle loading/unloading areas should be kept clean, suggesting a lower P^i_{inLoad}.

4.2.3 Scenario analysis

During initialization, η percentage of the packer/fleet population are randomly selected as risk-averse ($Att^i = 0$), and the rest are characterized as risk-tolerant ($Att^i = 1$). Within each risk attitude category, we set up the initial biosecurity value ($bs^i_{t_0}$) for each packer/fleet agent i according to the following initial biosecurity distribution[144]: 50% of the total population with initial biosecurity $bs^i_{t_0} = 0$, 40% with $bs^i_{t_0} = 2.7$, 10% with $bs^i_{t_0} = 5.3$, 0% with $bs^i_{t_0} = 8$.

In Table 4.2, three simulation sets are designed based on different combinations of two factors in the producer population: (a) random or targeted selection strategy for risk-averse producers, and (b) distribution of initial biosecurity levels. In the targeted selection strategy, we progressively select producers to be risk-averse, one after another, in the decreasing order of their cattle capacity, and the rest will be set as risk-tolerant. In the random selection strategy, producers are randomly selected as risk-averse or risk-tolerant.

Table 4.2: *Description of the simulation sets*

Simulation set	Risk-averse producer selection	Initial biosecurity distribution
I	Random strategy	bs_{t_0} for risk-averse/risk-tolerant category: [0, 2.7, 5.3, 8]—[50%, 40%, 10%, 0]
II	Random strategy	bs_{t_0} for risk-averse/risk-tolerant category: [0, 2.7, 5.3, 8]—[0, 40%, 10%, 50%]
III	Targeted strategy	bs_{t_0} for risk-averse/risk-tolerant category: [0, 2.7, 5.3, 8]—[50%, 40%, 10%, 0]

In simulation sets I and III, producers within each risk category follow the same distribution as packers and fleet companies. In simulation set II, the highest biosecurity levels are assigned to 50% of the producers. Regarding risk category selection, we randomly select risk-averse producers in simulation sets I and II but perform a targeted strategy in simulation set III. Within each simulation set, each scenario represents a different proportion of risk-averse producer agents in the total producer population (η) varied between 0 and 100% with an interval of 20%. We record the number of infected producers/packers and the number of infected cattle over time for each simulation. We perform 1000 simulation runs for each scenario, and the simulation period for each run is 200 days.

4.3 Results and discussion

This section presents and compares the simulation results among the three simulation sets to evaluate the impact of risk attitudes on epidemic dynamics.

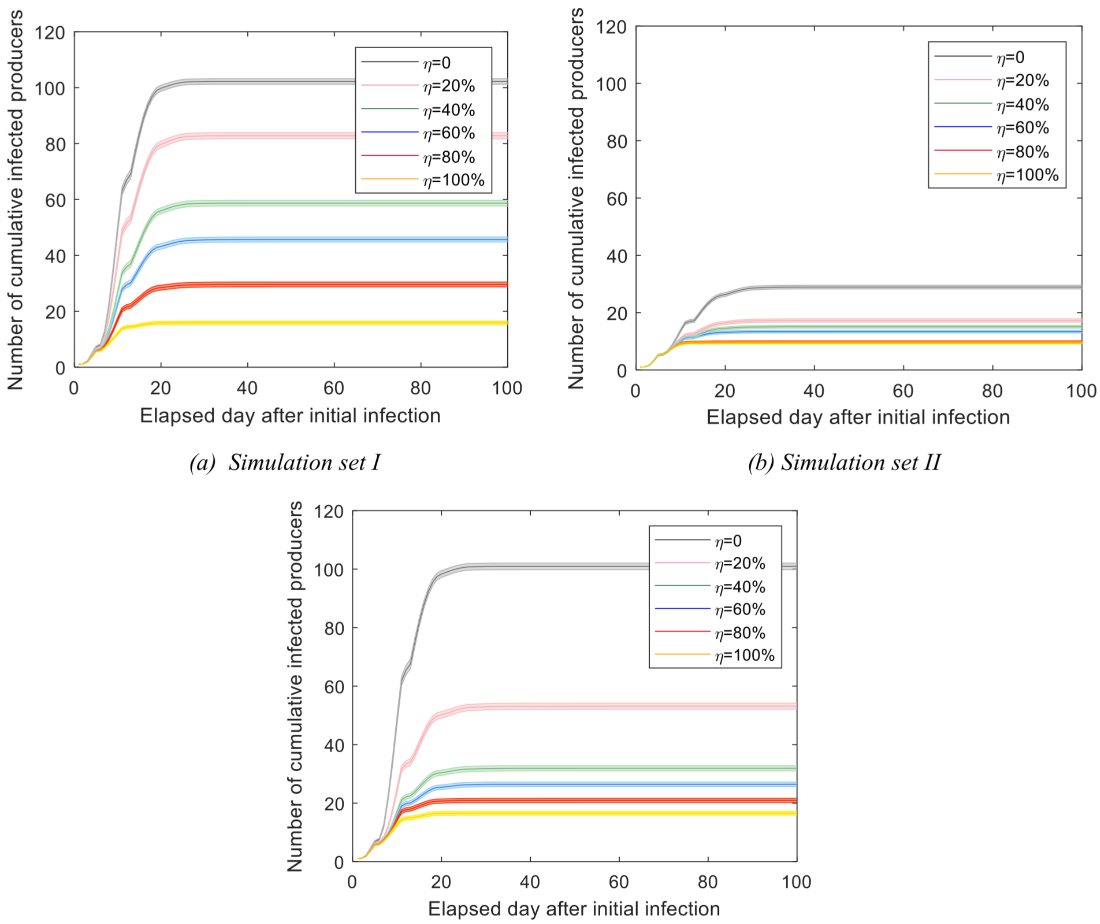

(a) Simulation set I *(b) Simulation set II*

(c) Simulation set III

Figure 4.3: *The number of cumulative infected producers over time. Simulation results are averaged over 1000 runs and associated with 95% confidence intervals.*

Fig. 4.3–4.4 show the average number of cumulative infected producers and the number of currently infected producers over time with 95 percent confidence intervals. In Fig. 4.3 (a), as the percentage of risk-averse producer agents (η) increases from 0 to 100% with 20% as an interval, the final average number of cumulative infected producers gradually decreases with intervals ranging between 13.01–24.13. In Fig. 4.3 (b), 20% of producers in the risk-averse category can achieve a relatively good performance in reducing epidemic

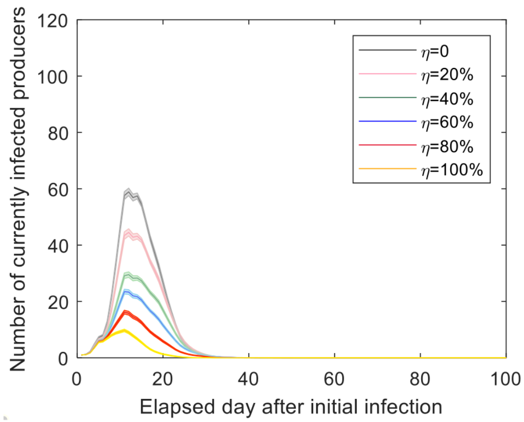

(a) Simulation set I

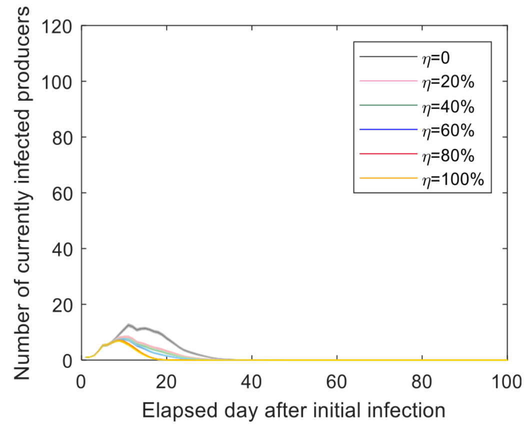

(b) Simulation set II

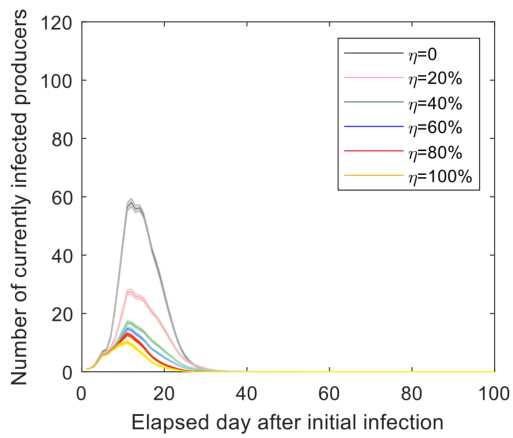

(c) Simulation set III

Figure 4.4: *The number of currently infected producers over time. Simulation results are averaged over 1000 runs and associated with 95% confidence intervals.*

size, and after 20%, the epidemic size reduces more slowly. In Fig. 4.3 (c), the final average number of cumulative infected producers reduces sharply from 100.94 to 31.92 as η varies between 0–40%, and then decreases gradually with smaller gaps, ranging between 4.39–5.50. It suggests that the system needs at least 40% of the producer population as risk-averse to achieve a significantly steeper decrease in the epidemic size under a targeted strategy. In comparison, the number of cumulative infected producers under a random strategy at $\eta = 40\%$ is 58.67 (95% CI: 57.65–59.69) in Fig. 4.3(a).

Similar patterns are observed in the number of currently infected producers in Fig. 4.4. In addition, simulation set II has the lowest peak in terms of producer infection as its overall initial biosecurity level is the highest among the three simulation sets.

Figs. 4.5–4.9 present boxplots of the distributions of simulation results obtained from ABM for the three simulation sets.

(1) Impact of risk attitudes on producers

Fig. 4.5 shows that increasing the percentage of producers in the risk-averse category can reduce the number of infected producers for all simulation sets.

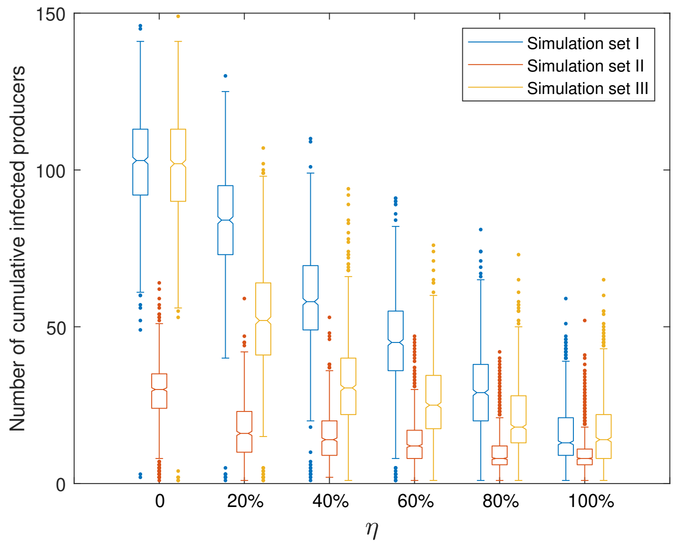

Figure 4.5: *Distributions of the number of cumulative infected producers.*

For simulation set I (blue) and η ranging from 0 to 100%, the median [interquartile range] number of cumulative infected producers decreases dramatically from 103 [92–113] to 13 [9–21]. Compared to simulation set I, the number of cumulative infected producers decreases much less sharply in simulation set II, which is associated with a higher initial biosecurity level. More specifically, when η changes from 0 to 80%, the number of cumulative infected farms changes from 30 [24–35] to 8 [6–12] and then remains almost unchanged between $\eta = 80\%$ and $\eta = 100\%$. It indicates that when the overall biosecurity level is relatively low, changing individuals' risk attitudes towards risk-averse can lead to a significant reduction in the epidemic size, which enhances the effectiveness of control measures.

The epidemic size for simulation set III (targeted selection) is smaller than that under simulation set I (random selection). For example, for $\eta = 40\%$, the median number of infected producers under random selection (58 [49–70]) is almost twice that under targeted selection, which is 31 [22–40]. It indicates that risk communication based on a targeted strategy is more effective than the random strategy to contain the epidemic. A similar pattern of epidemic duration is observed in Fig. 4.6.

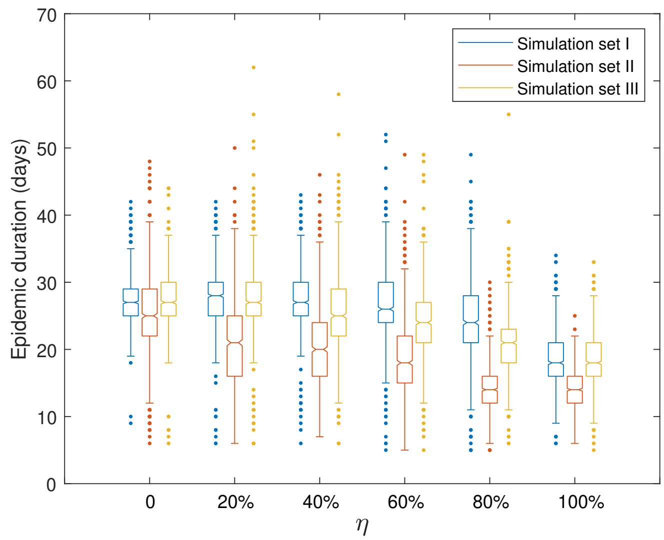

Figure 4.6: *Distributions of the epidemic duration.*

(2) Impact of risk attitudes on cattle losses

In the simulation, when the producer agent detects an infection, it will depopulate its cattle (all cattle transition to the removed state). Fig. 4.7 shows the distributions of the number of cattle removed, reflecting the cattle losses. For simulation set I, when η varies between 0–100%, the median [interquartile range] number of cattle removed ranges changes from 2,199,045 [2,065,838–2,319,615] to 439,215 [270,210–702,540]. For simulation set II, as η increases from 0–100%, cattle losses reduced from 848,640 [658,853–1,028,588] to 262,748 [166,830–385,223]. Comparing results in simulation sets I and III, we can conclude that with the same initial biosecurity distributions, targeted selection of producers to a more risk-averse behavior can yield fewer cattle losses than the random strategy. For instance, the number of cattle removed is 739,778 [502,935–1,015,755] under a targeted selection and 1,519,763 [1,275,960–1,744,928] under a random selection at $\eta = 40\%$.

(3) Impact of risk attitudes on packers

As packers are a critical component of the food production system, we visualize the

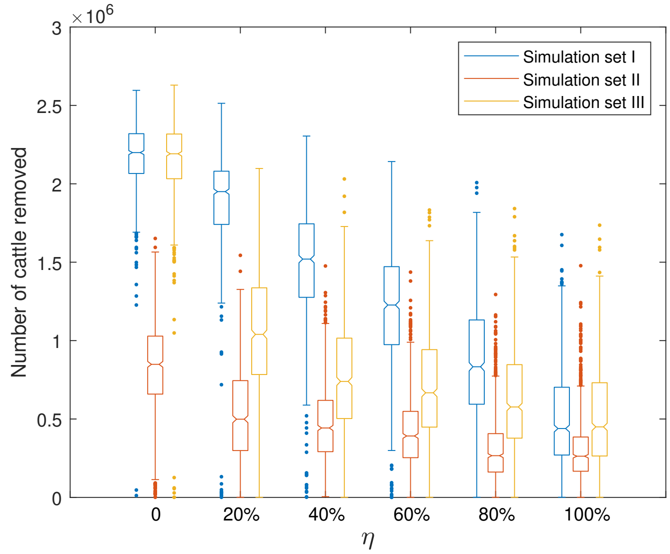

Figure 4.7: *Distributions of the number of cattle removed.*

distribution characteristics across scenarios in Figs. 4.8 and 4.9. As the simulation period for each run is 200 days, the maximum possible value of the total packer operating time is 800 days.

In Fig. 4.8, the median number of infected packers is 4 for all scenarios in simulation sets I and III. For simulation set II, the median number of infected packers is 4 for $\eta \leq 60\%$, and becomes 3 for $\eta > 60\%$. Similarly, in Fig. 4.9, the median total packer operating time across all scenarios for simulation sets I and III ranges between 89–96 days and 90–95 days, respectively. For simulation set II, the range of the medium total packer operating time is 94–99 days for $\eta \leq 60\%$, and is 262–264 days for $\eta > 60\%$.

In summary, the overall patterns of the indicators across scenarios are consistent over the three simulation sets. A more risk-averse population can reduce the number of infected producers/packers and cattle losses. Notably, a targeted selection of producers is more effective than the random strategy under the same initial biosecurity levels.

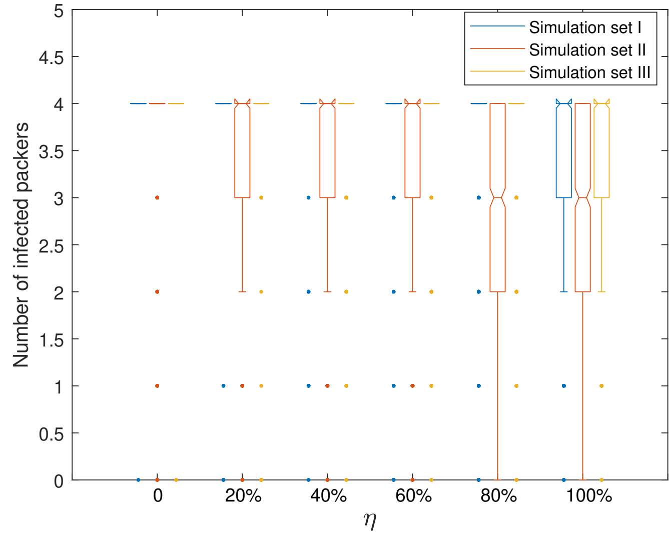

Figure 4.8: *Distributions of the number of infected packers.*

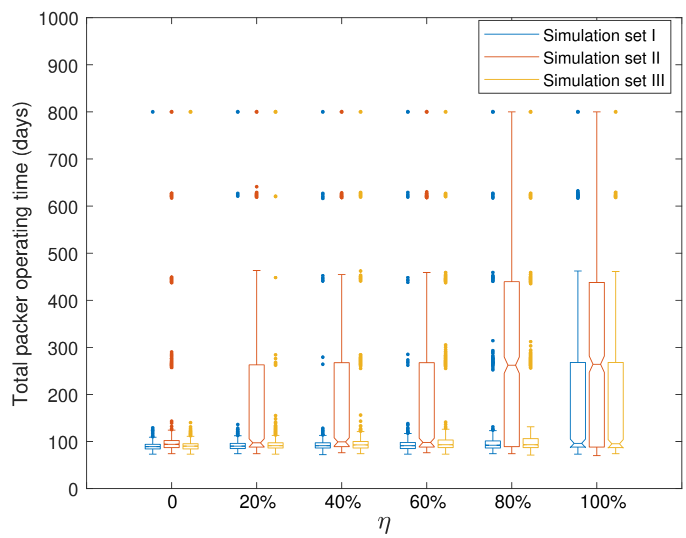

Figure 4.9: *Distributions of the total packer operating time.*

4.4 Summary

In this chapter, an agent-based model was developed to simulate the human decision-making process during epidemics, a factor which is often ignored in conventional livestock disease models. A case study of southwest Kansas was performed to demonstrate the model's ability to simulate the human decision-making process around biosecurity practices as disease dynamics change. The assumptions relevant to the disease-related decision-making process enable the model to capture the complicated interactions between disease spreading and individuals' responsiveness on biosecurity measures, considering individuals' heterogeneous risk attitudes. The model developed can be used by policymakers to examine the effectiveness of various control measures and identify important human behavior factors related to epidemiological parameters in disease transmission dynamics.

The simulation results show that human behavioral responses to biosecurity events, operationalized as risk attitude, substantially affect the epidemic dynamics and the effectiveness of movement restrictions. Additionally, knowing the relevant stakeholders' initial biosecurity level is vital for cost-effective risk communication. When the initial biosecurity level is relatively low, nudging producers' risk attitudes towards greater risk-aversion can significantly reduce the cumulative number of infected producer locations. When the initial biosecurity level is high, communication to increase risk-aversion will lead to a smaller reduction in the final epidemic size. For instance, shifting 40% of producers towards being more risk-averse can lead to a sharp decrease in the median number of infected producers, from 102 to 31, for a low initial biosecurity level (simulation set III). In comparison, the same shift towards risk-aversion reduces the median number of infected producers from 30 to 14 for a high initial biosecurity level context (simulation set II). We also highlighted the advantage of a targeted strategy based on producers' capacity in selecting audiences for communications that promote more risk-aversion over a random selection strategy. For example, when 40% of the producers are risk-averse, the number of cumulative infected producers under the random strategy (simulation set I) is almost twice that under a targeted strategy (simulation III). In terms of packer operations, there is little difference between the random and targeted strategies for a low initial biosecurity level. This implies that risk communication on producers towards risk-aversion regardless of their biosecurity status cannot effectively protect the packers. Packers are the critical components in the system, and it's significant to ensure overall high compliance to biosecurity level in the region to minimize the risk of disease outbreaks.

Chapter 5

Robustness of supply chain networks against underload cascading failures[1]

5.1 Introduction

Cascading failures and network robustness have been studied extensively in real-world networks such as power systems and traffic networks[13–18;146;147]. Failures in these models are often overload-driven. Pahwa et al.[18] built a simple but realistic overload cascade model for power systems and studied its emergent behavior against power outages, which can lead to the load redistribution across the network and result in more failures due to the power flows exceeding the line capacity. They observed a sudden breakdown of the system with an increased load level and a large network size. Many works study the cascading failure phenomenon from a single network perspective, and there have also been recent studies of failure cascades in interdependent networks. Buldyrev et al. developed in paper[10] a one-to-one correspondence model to study the robustness of interconnected networks against cascading failures, and found that removal of a critical fraction of nodes could lead to a complete breakdown of the system. Since the work[10], many works have studied the robustness of interdependent networks from various perspectives[147–151], in which disruptions

[1]This chapter is a slightly modified version of our published article[60].

of components in one system may propagate and cause elements in the other system to fail.

In the competitive economic market, supply chain (SC) entities often build business relationships with outsourcing partners to reduce the overall cost and promote productivity. As a result, SCs have become more complicated and geographically dispersed, increasing the frequencies of SC disruptions[152]. Due to the increased dependencies among entities, disruptions of a company's operation can result in revenue losses in its business partners, and cascade to other components in the SC[153]. On the other hand, sustainability concerns have pushed for higher efficiency in the use of resources and reduction in protective redundancies in SCs, thus making SCs more susceptible to disruptions[154]. SC entities may suffer from financial losses due to delays in the flow of goods caused by natural disasters or intentional attacks. For example, heavily relying upon transportation services for timely delivery of animals among ranches, stockers, feedlots, and meat-processing plants, the beef industry can suffer substantial economic losses due to disruptions in transportation infrastructure caused by natural disasters and movement restrictions during disease outbreaks. During the 2011 Japan earthquake and tsunami, Toyota Motor Company suffered at least a 140,000-vehicle production loss. This adverse effect spread to other countries, which led to a massive collapse in the global automotive and electronics industry[155]. In the following weeks after the disaster, Toyota in North America experienced shortages of over 150 parts, resulting in curtailed operations at only 30% of capacity[156].

In light of these low probability and high impact disruptions, several studies have utilized the above overload failure models to analyze the SC robustness against cascading failure[19;20;157]. From a complex network perspective, a supply chain is also termed a supply network, in which network nodes and links refer to the SC entities and supply-demand relationships between the entities, respectively. Cluster SC network is a typical SC network based on industry clusters. Zeng and Xiao studied the dynamic robustness of cluster SC networks under overloaded cascading failures, and found that network load entropy can help identify the cascading failure phenomenon with large damage at its early stage, thereby avoiding the collapse of the whole network[19]. Tang et al.[20] examined the robustness of an interdependent SC network model, which consists of an undirected cyber layer and a directed physical layer, subject to different node removal strategies. However, the nature of cascading failures in SC systems is mostly underload-driven. When entities cannot fulfill the expected production requirement to overcome fixed production costs, they will fail to gain profit and possibly exit the market. When a node is disrupted, its downstream and upstream neighbors will be affected due to supply shortage and demand losses, respectively. If the neighboring node's remaining load drops below the lower bound constraint, i.e., cost, new failure occurs, and cascades to other nodes in the entire system[21;22]. Tang et al.[23] assessed the SC system robustness in the form of production capability losses, but they assumed that the failed node loads only propagate downstream without consideration of mitigation strategies. Wang et al.[21] attempted to improve the cluster SC network resilience against cascading failures, leveraging insights from the ant colony's spatial fidelity zones. In the model developed by Wang et al., a node can propagate the failure impact both upstream and downstream, and can dynamically change the strength of the business relationship with its neighbors[22]. Sun et al. proposed a multi-echelon supply chain evolutionary model and performed robustness analyses under different attack strategies. They assumed that node failures are caused by insufficient load, and successive failures happen only among nodes that have certain symbiotic relationships[24]. Huo et al. proposed a two-layer network to study the SC risk propagation under warning information diffusion. In their work, a risk propagation threshold is derived and found to have correlations with the network topology, the herd mentality, and the risk preference[158]. There also exists a series of studies focusing on the design of optimal recovery methods to cope with disturbance or disruptions in SC networks[159;160]. To the best of the authors' knowledge, there are few works considering underload-driven failures, and this work attempts to add a new element to this domain with a focus on the phase transition behavior.

Given the tremendous damages caused by the disruptions, understanding the nature of the systemic failure in SC that goes beyond a single component behavior is a significant problem to be addressed. The goal of this chapter is to build an underload cascade failure model and analyze its behavior against disruptive events. First, we will build a generalized underload cascade failure model with and without recovery strategies. The material flow of goods through an entity node defines its load. Second, we will examine the fraction of failed nodes in the system under scenarios of load decrease and load fluctuations. Third, we will provide analytic results based on the assumption of equal load redistribution upon failures for the studied scenarios.

The contributions of this chapter are: (i) Using the proposed model with recovery strategies, we confirm that strategies of backup suppliers and surplus inventories, often adopted in actual SCs, improve the system robustness. In addition, the system is relatively robust against load fluctuations but is more fragile to load decrease. (ii) Without the recovery process, we found numerically and analytically a discontinuous phase transition of the system under a load decrease scenario. Based on statistical physics, this indicates that a small fraction of failures can result in a sudden breakdown in the SC system. More specifically, the model is more robust under the power-law distribution than the uniform distribution of the lower bound load parameter for the studied scenarios. These findings indicate that underload driven systems have different behaviors against cascading failures compared with overload cascade models, and need to be further explored.

5.2 Underload cascading failure model

5.2.1 Load and load constraints

In multi-hierarchy SC networks, nodes are entities and edges denote the supply-demand relationships between the entities. SC entities are both demand-side and supply-side, and those in the same tier have similar network connections, core businesses, and competitive environments[161–163].

In this work, we represent the SC as follows:

$$G = (V,\ E,\ L,\ A,\ B), \tag{5.1}$$

where $V = \{v_1, v_2, \ldots,\ v_n\}$ is a set of nodes, and $E = \{(v_i, v_j)|e_{ij} = 1 \text{ or } 0\}$ is a set of edges. When $e_{ij} = 1$, there is a directed link between nodes v_i and v_j; otherwise, $e_{ij} = 0$.

$L = \{L_1, L_2, \ldots, L_n\}$ is a set of node loads. We define the load of a node $L_i(t)$ as the sum of material flows that go through an entity node, i.e., the total number of products that an entity has sold per time unit. $A = \{A_1, A_2, \ldots, A_n\}$ and $B = \{B_1, B_2, \ldots, B_n\}$ are sets of node load constraints. More specifically, A_i denotes the upper bound load for node i, which is the maximum number of products an entity can provide, i.e., inventory. B_i denotes the lower bound load for node i, and reflects costs such as labor costs and maintenance fees.

Suppose the SC network has T number of tiers, and the initial loads for nodes in the last tier T, equivalent to the demand for final customers, are known and equal. To initialize the node load and load constraints in the network, we first calculate weights on all edges, which reflect the business relationship strength between node entities. Weight on edge e_{ij} is calculated by $w_{ij} = (d_i \cdot d_j)^{\theta}$, with $\theta = 0.5$[21;22]. d_i denotes the node degree of node i, and is obtained by $d_i = d_i^+ + d_i^-$, where d_i^+ and d_i^- are the indegree and outdegree of node i, respectively.

Given initial node loads in tier T, we calculate all initial flows on edges between nodes in tier $T-1$ and tier T as follows:

$$F_{i,j}(0) = L_j(0) \cdot w_{ij} / \sum_{k \in \Gamma_j^U} w_{kj}, \tag{5.2}$$

where $F_{i,j}(t)$ is the flow on edge e_{ij} at time t and $w_{ij} / \sum_{k \in \Gamma_j^U} w_{kj}$ indicates the fraction of the supplies from supplier i to all suppliers of node j. Γ_j^U is the node collection consisting of upstream nodes connected to node j.

According to the node load definition, the initial load of each node in tier $T-1$ equals the sum of its outgoing flows, which is given by

$$L_i(0) = \sum_{j \in \Gamma_i^D} F_{i,j}(0), \tag{5.3}$$

where Γ_i^D is the node collection consisting of downstream nodes connected to node i.

After obtaining the initial loads of nodes in tier T-1, we calculate the initial node loads in tier T-2 using equations (5.2–5.3). Similarly, we sequentially calculate the initial loads of nodes in all tiers backward, i.e., T-3, ..., 2, 1. As a result, the sum of incoming flows equals the sum of outgoing flows for each node i, i.e., $L_i(t) = \sum_{m \in \Gamma_i^U(t)} F_{m,i}(t) = \sum_{j \in \Gamma_i^D(t)} F_{i,j}(t)$, with demand and supply balanced, which is in accordance with the node load definition.

In terms of node load constraints, we assume that A_i and B_i are proportional to the initial node load $L_i(0)$, and are given as follows

$$\begin{cases} A_i = aL_i(0) \\ B_i = bL_i(0) \end{cases}, \tag{5.4}$$

where a is the upper bound parameter, $a > 1$; b is the lower bound parameter, $0 < b < 1$.

5.2.2 Cascading failure process

In the normal state, the network is in the steady state and the load of node i at time t satisfies $B_i < L_i(t) < A_i$. When an SC network suffers from disruptive events, some nodes can be underloaded and fail initially. Caused by the connections between the entities, the impact of these initial failures could result in more failures and spread to the entire system. We consider the cascading failure processes with and without recovery measures as follows.

Step 1: We initialize the node load $L_i(0)$ for each node i in the network, and then calculate load constraints (A_i and B_i) based on the value of $L_i(0)$. Keeping the load constraints for each node unchanged, we decrease or fluctuate the initial node loads to simulate initial failures. The new initial load of node i after the load decrease or fluctuations is denoted as $L_i'(0)$.

Step 2: Caused by the new failures, node load loss propagates throughout the system, and all the loads and flows affected are updated.

Step 3: With recovery measures, the nodes affected but not yet failed can reduce load losses by altering flows with existing partners or by building new partners.

Then, if there are still nodes with loads below their lower bound load, i.e., $L_i(t) < B_i$, these nodes will be marked as failed and we continue the process from Step 2–3. Such a procedure is repeated until no new failure happens. Failure of a node indicates that the entity receives insufficient load and fails to gain profit in the competitive market.

Node load loss propagation scheme

We assume that if a node fails, it can neither receive supplies from upstream neighbors, nor ship products to downstream partners. Thus, once a node i fails at time t, both its load and the flows on its incoming and outgoing edges are set to zero. Here we use $\Delta_i^-(t)$ to denote the load loss of node i at time t, and $\Delta_{m,i}^-(t)$ to denote the load loss of node m influenced by node i at time t. $F_{i,j}(t)$ denotes the flow from node i to node j at time t.

We model the impact of the failed node i on its upstream nodes as follows. For node i failed at time t, its upstream neighboring node m in Γ_i^U will suffer load loss $\Delta_{m,i}^-(t)$. Accordingly, the load of node m, i.e., $L_m(t)$, and the flow $F_{m,i}(t)$ on edge e_{mi} are updated according to equation (5.5). Furthermore, the affected node m will lead to the load loss of node d in its upstream neighboring set, Γ_m^U.

$$\begin{cases} \Delta_i^-\left(t\right) = L_i\left(t-1\right) = \sum_{p\in\Gamma_i^U} F_{p,i}(t-1) \\ \Delta_{m,i}^-\left(t\right) = \Delta_i^-(t) F_{m,i}(t-1) / \sum_{p\in\Gamma_i^U} F_{p,i}\left(t-1\right) = F_{m,i}(t-1) \\ L_m\left(t\right) = L_m\left(t-1\right) - \Delta_{m,i}^-\left(t\right) \\ F_{m,i}\left(t\right) = F_{m,i}\left(t-1\right) - \Delta_{m,i}^-\left(t\right) = 0 \\ \Delta_{d,m}^-\left(t\right) = \Delta_{m,i}^-\left(t\right) F_{d,m}\left(t-1\right) / \sum_{q\in\Gamma_m^U} F_{q,m}\left(t-1\right) \\ L_d\left(t\right) = L_d\left(t-1\right) - \Delta_{d,m}^-\left(t\right) \\ F_{d,m}\left(t\right) = F_{d,m}\left(t-1\right) - \Delta_{d,m}^-\left(t\right) \end{cases}, \tag{5.5}$$

where $m \in \Gamma_i^U$ and $d \in \Gamma_m^U$. Summation $\sum_{p\in\Gamma_i^U} F_{p,i}\left(t-1\right)$ is the sum of flows on the incoming edges of node i, and $F_{m,i}\left(t-1\right) / \sum_{p\in\Gamma_i^U} F_{p,i}\left(t-1\right)$ indicates the fraction of the newly load loss allocated to node m with respect to the total load loss of node i.

In addition, the load loss of node i is propagated to downstream nodes. Due to the failure of node i, its downstream neighboring node s reduces load by $\Delta_{s,i}^-(t)$. The flow between nodes

i and s is also updated. As the load loss propagates further downstream, we also decrease the load of node r, which is the downstream neighboring of node s, and the corresponding flow $F_{s,r}(t)$ according to equation (5.6).

$$\begin{cases} \Delta_i^-(t) = L_i(t-1) = \sum_{g\in\Gamma_i^D} F_{i,g}(t-1) \\ \Delta_{s,i}^-(t) = \Delta_i^-(t) F_{i,s}(t-1) / \sum_{g\in\Gamma_i^D} F_{i,g}(t-1) = F_{i,s}(t-1) \\ L_s(t) = L_s(t-1) - \Delta_{s,i}^-(t) \\ F_{i,s}(t) = F_{i,s}(t-1) - \Delta_{s,i}^-(t) = 0 \\ \Delta_{r,s}^-(t) = \Delta_{s,i}^-(t) F_{s,r}(t-1) / \sum_{h\in\Gamma_s^D} F_{s,h}(t-1) \\ L_r(t) = L_r(t-1) - \Delta_{r,s}^-(t) \\ F_{s,r}(t) = F_{s,r}(t-1) - \Delta_{r,s}^-(t) \end{cases}, \tag{5.6}$$

where $s \in \Gamma_i^D$ and $r \in \Gamma_s^D$.

The node load loss propagation process continues upstream to tier 1 and downstream to tier T, mimicking the ripple effect spreading throughout the system.

To clearly illustrate the load loss propagation after nodes failed, we present a simplified example on a four-tier SC network, as shown in Fig 5.1. Assuming that nodes 9 and 13 fail at time t, the load they lose will affect their neighboring nodes 4, 14, 15 and 8, 18 through connectivity links. Then, affected nodes 14, 15 further impact their downstream nodes 18, 19 and 20 by reducing supply. Meanwhile, node 8 influences its upstream neighboring nodes 2, 3 and 4 by cutting back demand. It is worth noting that the load loss suffered by node 4 is affected by nodes 8 and 9 at the same time, thus its load at time t is decreased by $\Delta_{4,8}^-(t) + \Delta_{4,9}^-(t)$, where $\Delta_{4,9}^-(t) = L_9(t-1)$ and $\Delta_{4,8}^-(t) = \Delta_{8,13}^-(t) F_{4,8}(t-1) / \sum_{q\in\Gamma_8^U} F_{q,8}(t-1)$.

Load loss recovery scheme

In this section, the load loss recovery scheme is designed to simulate that entities can mitigate their losses by requesting rush orders or building new business partnerships during disruptive events. We define the residual load of node i at time t as $RL_i(t) = A_i - L_i(t)$, which indicates

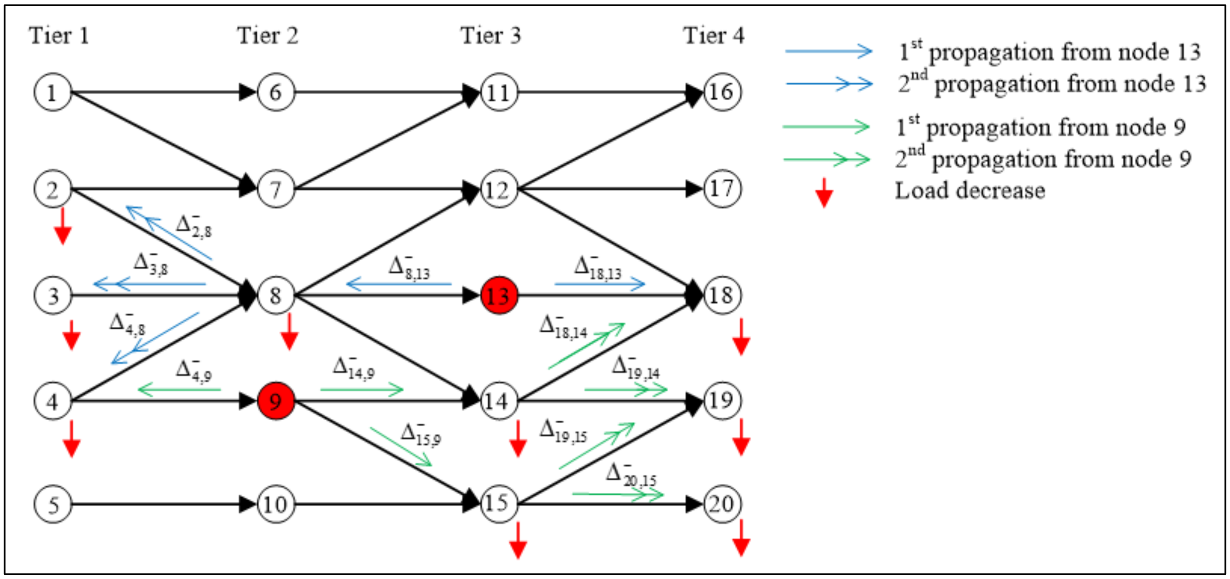

Figure 5.1: *An example of load loss propagation in a four-tier supply chain. Red circles represent the initial failures caused by load decrease or fluctuations..*

the additional available products an entity can provide, i.e., surplus inventory. Each node can at most provide its residual load when it helps its neighbor to recover losses.

When recovery measures are considered in the cascading failure model, only surviving nodes can recover their node load when suffering from load losses. Note that after the load loss propagation process, a node with $L_i(t) < B_i$ can recover its load if it is not marked as failed. If the node's load, $L_i(t)$, is still below its lower bound load, B_i, after the recovery process, this node will be marked as failed, and cause further load losses in the next step.

Since acquiring new partners will bring additional costs, we assume node i (not yet permanently failed) will first select from surviving nodes in its upstream neighboring set, Γ_i^U, and downstream neighboring set, Γ_i^D, to recover load losses. If all the neighboring nodes' residual load still cannot help it recover above B_i, node i will build links with surviving nodes in its upstream non-neighboring set, $\bar{\Gamma}_i^U(t)$, and downstream non-neighboring set, $\bar{\Gamma}_i^D(t)$.

According to the node load definition, each node's demand and supply are balanced in the steady state. Therefore, the impact of the increase in a node load will spread upstream to tier 1 and downstream to tier T. Then, it is easy to understand that the total load increase of nodes in each tier s, $\sum_{i\in\Omega_s}\Delta_i^+$ should always be equal, where Ω_s is the node collection consisting of surviving nodes in tier s and $s = 1, 2, \ldots, T$. In this section, we use $\Delta_i^+(t)$ to denote the load increase of node i, and $\Delta_{m,i}^+(t)$ to denote the load increase of node m influenced by node i.

Note that as the numbers of surviving nodes in each tier at time t are not necessarily the same, the total load loss for each tier, i.e., $\sum_{i\in\Omega_s}(L_i'(0) - L_i(t))$, are different. In addition, the total residual loads for each tier, i.e., $\sum_{i\in\Omega_s} RL_i(t)$, are also different.

The load loss recovery process is described as follows:

Due to the aforementioned reasons, we identify the tier γ_a with the minimum residual load, RL_{MIN}, and tier γ_b with the maximum loss, ΔL_{MAX} equation (5.7). The total load increase of each tier, $\sum_{i\epsilon \text{tier } s} \Delta_i^+(t)$, equals the smaller value of RL_{MIN} and ΔL_{MAX}.

$$\begin{cases} RL_{MIN} = \min\limits_{s}\left[\sum_{i\in\Omega_s} RL_i(t)\right],\ s = 1, 2, \ldots, T \text{ and } \gamma_a = s^* \\ \Delta L_{MAX} = \max\limits_{s}[\sum_{i\in\Omega_s}(L_i'(0) - L_i(t)]\ , s = 1, 2, \ldots, T \text{ and } \gamma_b = s^* \\ \sum_{i\in\Omega_s} \Delta_i^+ = \min(RL_{MIN}, \Delta L_{MAX}),\ s = 1, 2, \ldots, T \end{cases} \tag{5.7}$$

If $RL_{MIN} < \Delta L_{MAX}$, we first recover nodes in tier $\gamma = \gamma_a$ with the load of each node i increased by $\Delta_i^+(t) = RL_i(t)$, $i \in \Omega_{\gamma_a}$. Otherwise, if $RL_{MIN} \geq \Delta L_{MAX}$, we first recover node load in tier $\gamma = \gamma_b$, and each node load increases by $\Delta_i^+(t) = L_i'(0) - L_i(t)$, $i \in \Omega_{\gamma_b}$.

Similar to the load propagation process, the impact of load increase in tier γ will spread upstream and downstream to the entire system. Suppose node i is in tier γ, and its load gets increased by $\Delta_i^+(t)$. To imitate that node i requests a rush order from its supplier m, we increase $F_{m,i}(t)$ and the load of node m by $\Delta_{m,i}^+ = \min(\Delta_i^+(t),\ RL_m(t))$, $m \in \Gamma_i^U = \Omega_{\gamma-1}$. If the first randomly selected supplier m's residual load cannot satisfy the order request of node i ($RL_m(t) < \Delta_i^+(t)$), node i will continue to randomly select the next supplier in Γ_i^U. If all suppliers still fail to meet the request of node i, i.e., $\sum_{m\in\Gamma_i^U} RL_m(t) < \Delta_i^+(t)$, node i will build links with randomly selected nodes in the non-neighboring set $\bar{\Gamma}_i^U(t)$, until objective $\Delta_i^+(t) = \sum_{m\in\Gamma_i^{U\prime}} \Delta_{m,i}^+$ is met, where $\Gamma_i^{U\prime}$ is the new node collection consisting of all upstream neighboring nodes connected to node i .

Load increase of node m will further lead to load increase of its upstream nodes. This process continues until all related suppliers in tier 1 have increased their loads. Similarly, loads of surviving nodes downstream are updated.

5.3 Numerical simulation results

Researchers often study the phase transition behavior exhibited by the system through stressing external forces to it until the rupture point[164]. In this section, we examine the robustness of the SC networks under the stress of load decrease and fluctuations. Note that each node's load constraints, A_i and B_i, remained fixed as strength of the stress δ or σ changes under each scenario.

As the failures are underload-driven, we conduct extensive simulations with lower bound parameter b following (i) uniform and (ii) power-law distribution, which are two commonly used families of distributions[18;165]. Uniformly distributed over $[b_{min}, b_{max}]$, denoted by $U[b_{min}, b_{max}]$, the probability density function for a random variable b is given by $p\,(b) = 1/(b_{max} - b_{min}) \cdot 1_{b_{min} \leq b \leq b_{max}}$. Following a power-law distribution, the probability density function for a random variable b is of the form $p\,(b) = k \cdot (b)^{-\gamma}$ with $b \in [b_{min},\ 1]$.

5.3.1 Synthetic networks

Hernández and Pedroza-Gutiérrez[166] constructed random network models in bipartite graphs to model the theoretical SC networks. Similarly, we generate synthetic networks for a four-tier SC network, as shown in Fig. 5.1, representing suppliers, production centers, distribution centers, and customers. N nodes are generated and equally divided into four tiers, in which one enterprise node belongs only to one tier. Links are created randomly with a given connection probability p, which is the likelihood of existing business relationships between nodes in two tiers. Additional efforts are made to ensure the network created is without self-loops. Despite the random placement of links, most nodes will have approximately the same number of connections. For example, the average node outdegree of a network with 100 nodes in each tier ($N = 400$) and $p = 0.1$ will be around 10. Simulation results using synthetic networks are shown in Fig 5.2.

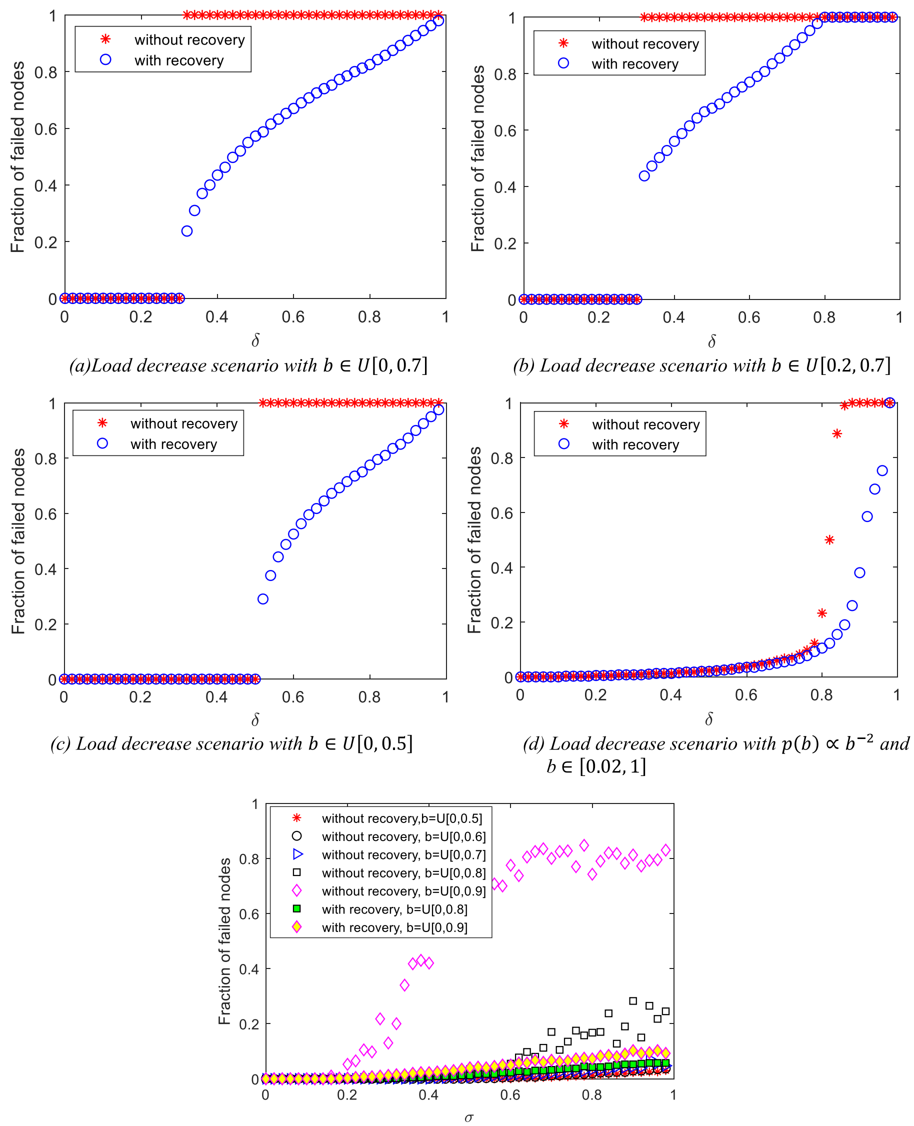

(a)Load decrease scenario with $b \in U[0, 0.7]$

(b) Load decrease scenario with $b \in U[0.2, 0.7]$

(c) Load decrease scenario with $b \in U[0, 0.5]$

(d) Load decrease scenario with $p(b) \propto b^{-2}$ *and* $b \in [0.02, 1]$

(e) Load fluctuation scenario

Figure 5.2: *Simulation results using synthetic networks.*

Load decrease

In this scenario, we consider a negative demand shock, in which demand for goods or services shrinkages suddenly. To model the load decrease, we simultaneously decrease the initial loads for all nodes in tier 4 by a factor δ, i.e., $L_i'(0) = (1 - \delta)\, L_i\,(0)$, and then calculate all the flows and node loads in tiers 1–3. Keeping the network topology unchanged, it is equivalent to a uniform decrease of all the nodes by a factor δ. In each realization, δ changes from 0 to 1 with a step size of 0.02. We record the fraction of failed nodes f at the end of the simulation, and the results are averaged over 100 realizations with network size $N = 400$ and connection probability $p = 0.1$.

In Fig. 5.2(a)–(c), we found a sharp collapse of the system when there are no recovery measures and b is uniformly distributed over $[b_{min}, b_{max}]$. More specifically, the critical point above which the failure occurs is only determined by b_{max}, the upper limit of the uniform distribution. For example, in Fig. 5.2(b), in which B_i ranges between $[0.2L_i\,(0),\ 0.7L_i\,(0)]$, when $\delta > 0.3$, i.e., $L_i'\,(0) < 0.7L_i\,(0)$, initial failures start to appear and will propagate throughout the system, resulting in the collapse of the whole system.

When recovery measures are included and $b \in \mathrm{U}[b_{min}, b_{max}]$, results in Fig. 5.2(a)–(c) show that the recovery strategy can reduce the scale of systemic failure, as the reconfiguration of the trade flows among alive nodes can absorb losses of nodes affected by the initial failures. In Fig. 5.2(b), when $\delta > 0.8$, i.e., $L_i'\,(0) < 0.2L_i\,(0)$, all the loads fail at the beginning and are marked as failed, so they will not mitigate losses under the recovery process.

With b in the form of power distribution, the system collapses when δ increases to 0.88 without recovery process in Fig. 5.2(d), indicating that the system becomes more robust compared to the uniform distribution case.

Load fluctuations

We mimic the load fluctuations by setting final customers' new initial load as $L_i'\,(0) = (1 + \sigma\ \xi_i)\,L_i\,(0)$, i.e., $L_i'\,(0) \in [(1-\sigma)\,L_i\,(0)\,,\quad (1+\sigma)\,L_i\,(0)]$, where ξ_i is a random variable uniformly distributed in $[-1, 1]$. Then, we calculate the new initial loads for the nodes in tier 1–3 and flows on the edges. It is equivalent to allowing all the initial loads to fluctuate by a fraction of σ. When σ varies between [0, 1], upper bound parameter a is set to be two to ensure $L_i'\,(0) < A_i$, with $A_i = aL_i\,(0)$. Results are averaged over 100 runs of the simulation, with network size $N = 400$ and connection probability $p = 0.1$.

Fig. 5.2(e) shows the changes in the fraction of failed nodes as variation size σ increases.

Compared with the load decrease scenario, the system collapse happens less abruptly. When recovery measures are not included and b is uniformly distributed over $[0, 0.9]$, the fraction of failed nodes reaches a plateau of around 80% as fluctuation escalates. In comparison, when b is uniformly distributed over $[0, 0.8]$, about 25% of nodes failed in the end, suggesting that the system is relatively robust.

5.3.2 Real-world example

The underload cascading model proposed in this work is independent of the network topologies and can be applied to other types of SC networks. In this section, we apply the proposed model to a European supply chain network obtained from Cardoso et al.[167], which includes 11 raw materials suppliers, 3 plants, 5 warehouses, and 18 markets.

As shown in Fig. 5.3, simulation results under load decrease/fluctuation scenarios coincide with previous simulation results obtained from synthetic networks. Regarding load decrease, we observe a discontinuous phase transition for the system without recovery measures, and this system becomes more robust with the addition of recovery measures. Also, the system is relatively robust in the case of load fluctuations. For instance, without recovery measures, the fraction of failed nodes varies between 40%–50% when the relative strength of load fluctuations σ is larger than 0.66.

5.4 Mean-field analysis

In this section, we forecast a discontinuous transition for the cascading failure model without the recovery process using mean-field analysis. In power systems, power flows can redistribute in the whole system upon failures according to the Kirchhoff's law, which is dependent on power line impedance. Similarly, the effects of disruptions can spread to the entire SC network, and the flow redistribution in the system is dependent on the business relationships among entities. This feature inspires us to leverage the equal load redistribution model that has been used in power systems[18;165;168;169]. The assumption is that when a node fails, the

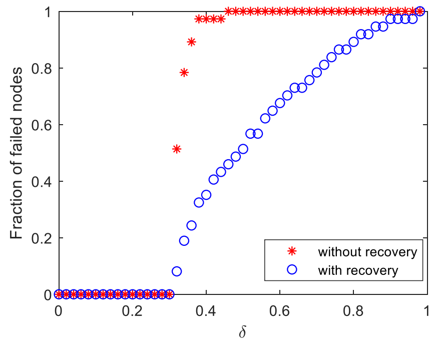

(a)Load decrease scenario with $b \in U[0, 0.7]$

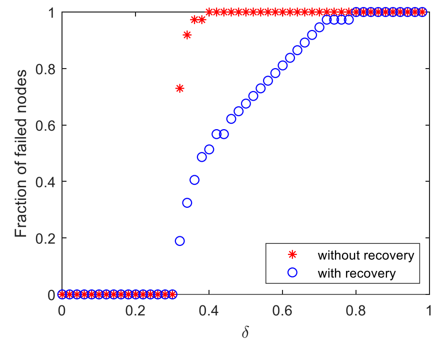

(b) Load decrease scenario with $b \in U[0.2, 0.7]$

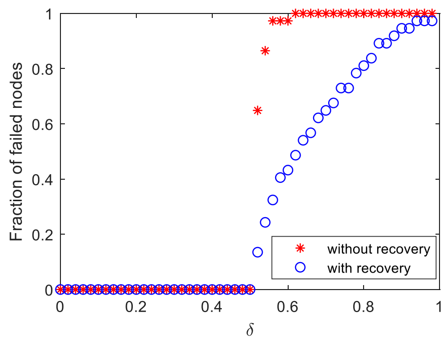

(c) Load decrease scenario with $b \in U[0, 0.5]$

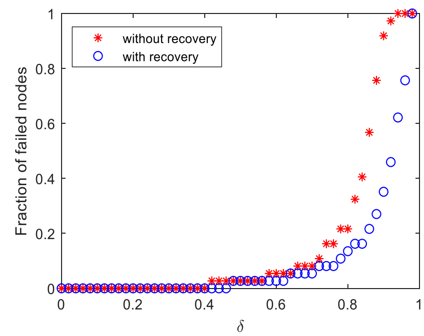

(d) Load decrease scenario with $p(b) \propto b^{-2}$ and $b \in [0.02, 1]$

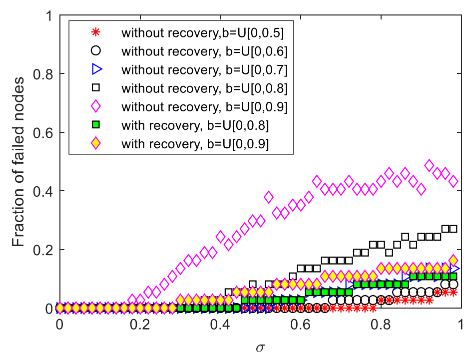

(e) Load fluctuation scenario

Figure 5.3: *Simulation results using the European supply chain network.*

load it carries before the failure will be redistributed equally among all the remaining nodes. The equal load redistribution assumption is originated from the widely used democratic fiber bundle model[170], in which N parallel fibers with different failure capacity share an applied force equally.

In the following, we analyze the load decrease scenario using a simple equal-load redistribution model. Suppose there are N nodes with a lower bound load B_i characterized by a probability distribution $p(B)$, and failures happen in discrete time steps $t = 0, 1, \ldots$ The fraction of failed nodes and the number of surviving nodes until cascade stage t is denoted as f_t and N_t respectively. When the load of a node goes below B_i, the node fails and its load gets redistributed equally among the remaining surviving nodes.

Suppose all the nodes initially carried the same load $\bar{L}'_0$. There is no failure before the disruptions, thus $f_0 = 0$ and $N_0 = N$. Under disruptions, a fraction of nodes $f_1 = \int_{\bar{L}'_0}^{\infty} p\,(B)\,dB$ immediately fails, since their load $\bar{L}'_0$ is below the lower bound load. After the first stage, the number of surviving nodes equals to $N_1 = (1 - f_1)\,N$, and the new load per node becomes $\bar{L}_1 = \bar{L}'_0 - \frac{f_1 \bar{L}'_0 N}{(1-f_1)N} = \left(1 - \frac{f_1}{1-f_1}\right)\bar{L}'_0$. The cascade failure process continues recursively, and the mean-field equations for the $(t+1)^{th}$ stage are as follows:

$$\begin{cases} f_{t+1} = \int_{\bar{L}_t}^{\infty} p\,(B)\,dB \\ N_{t+1} = (1 - f_{t+1})\,N \\ \bar{L}_{t+1} = \bar{L}_t - (f_{t+1}N - f_t N)\,\bar{L}_t/N_{t+1} = [1 - (f_{t+1} - f_t)/(1 - f_{t+1})]\bar{L}_t \end{cases}, \tag{5.8}$$

where $(f_{t+1}N - f_t N)/N_{t+1}$ is $\frac{\text{Number of lines that survive stage } t \text{ but fail at t+1}}{\text{Number of lines that survive stage } t+1}$.

Equation (5.8) can be simplified as

$$f_{t+1} = F(\bar{L}'_0 \prod_{t=1}^{t} (1 - \frac{f_t - f_{t-1}}{1 - f_t})) \tag{5.9}$$

where $F\,(x) = \int_x^{\infty} p\,(B)\,dB$.

From equation (5.9), we can see that the critical point f^* is mainly dependent on the distribution of B_i. To obtain the fraction of failed nodes, we provide analytic solutions by numerically solving equation (5.9) and verify them by simulating the above equal-load redistribution process under disruptions. We assume the initial node load $\bar{L}_0 = 1$ before the disruptions, and thus lower bound load $B_i = b\bar{L}_0 = b \cdot 1$ with $b \in [b_{min}, b_{max}]$. Under load decrease, the new initial load becomes $\bar{L}'_0 = (1 - \delta)\,\bar{L}_0 = (1 - \delta) \cdot 1$.

The results obtained from the simulation are averaged over 100 runs and compared with the results calculated from equations in Fig. 5.4, in which a discontinuous phase transition

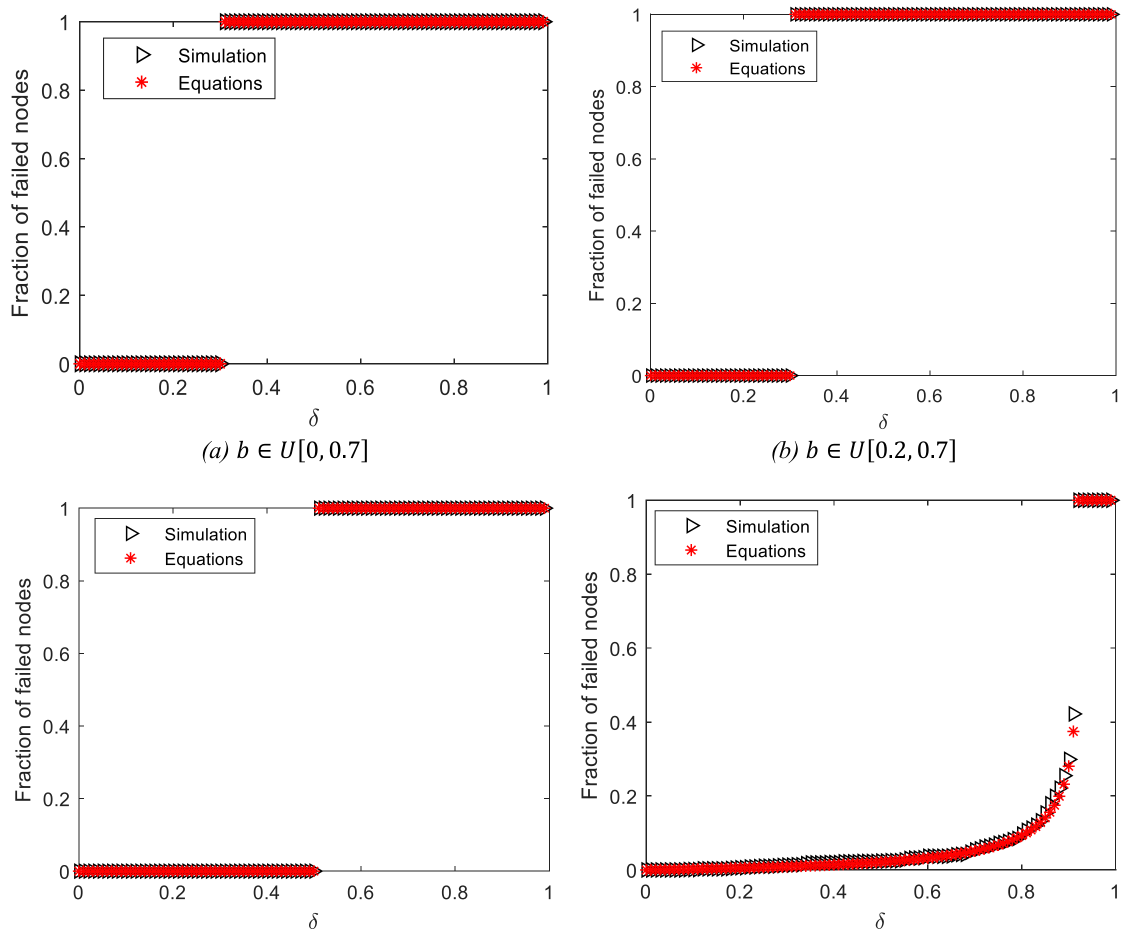

(a) $b \in U[0, 0.7]$ *(b)* $b \in U[0.2, 0.7]$

(c) $b \in U[0, 0.5]$ *d)* $p(b) \propto (b)^{-2}$ *with* $b \in [0.02, 1]$

Figure 5.4: *Plots of the fraction of failed nodes as a function of the relative load decrease* δ *using the mean-field model.*

occurs in all cases. In the uniform distribution case, the critical point below which a sudden collapse happens is only determined by b_{max}. When the new initial load $\bar{L}_0'$ is above B_i, there are no failures in the system. Once $\bar{L}_0'$ falls below B_i, the system collapses because the fraction of failed node obtained from the equation will increase to 1. When b follows a power-law distribution, the system is more robust, and there is an abrupt breakdown of the system at $\delta \approx 0.9$. Interestingly, this is contrary of the mean-field result for the overload cascade model[18], in which the discontinuous jump happens with no precursors in power-law distributions, and with precursors in line capacity following a uniform distribution. This indicates that the scale of cascade failures in SCs could be significantly affected by the shape of the b distribution, which is closely related to a company's cost.

5.5 Summary

In this chapter, we constructed an underload cascading failure model to study the robustness of SC networks under load decrease and load fluctuation scenarios. Most real-world SCs are equipped with redundancies such as surplus inventory and backup suppliers, and our simulation results from both synthetic networks and real network topologies show that the recovery strategies can significantly reduce the scale of the systemic failure when disruptive events happen. In addition, the system is relatively robust under the load fluctuation scenario, as the fraction of failed nodes escalates only when variation size σ is very high without considering recovery measures, which rarely happens in reality. Compared to the load fluctuations, the system appears more vulnerable against disruptive events such as load decrease, i.e., demand shock, and SC decision-makers need to take proactive protection measures to reduce or avoid the impact of such disruptive events.

Since many cascading failure models do not consider the recovery process, we also studied the behavior of the proposed underload-driven model without the recovery measures. We found that the model exhibits a discontinuous phase transition behavior under load decrease scenario as predicted by the mean-field analysis. More specifically, under different distributions of lower bound parameter b, i.e., cost per output, the system is more robust when b follows a power distribution compared to the uniform distribution for the studied scenarios. These emergent behaviors observed are different from the analytic results derived from the overload-driven system by Pahwa et al.[18], in which the power-law distribution of capacity results in a more abrupt system breakdown.

Chapter 6

Analysis of mitigation strategies against COVID spreading[1]

In the United States, the 2019 novel coronavirus disease (COVID-19) pandemic could result in \$13.6 billion of economic losses to the beef industry[6]. Several slaughterhouses were forced to stop operations temporarily due to outbreaks identified in the workforce. In this chapter, we use network-based modeling to examine the impact of non-pharmaceutical interventions on the COVID spreading with various scenarios. Although the method is applied to simulate the early stage of epidemic dynamics in Hubei province, China, the model developed can be easily adapted to other regions.

6.1 Introduction

The COVID-19 emerged in Wuhan City, Hubei Province of China, in the late fall of 2019[171]. The highly contagious virus outbreak during the Chinese Spring festival period made containment an unprecedented challenge. The risks of human-to-human transmission, long persistence on surfaces, and asymptomatic infections increased spread and made case detection difficult[172;173]. Increasing case reports saturated hospitals in Hubei Province, overwhelming

[1]Parts of this chapter are extracted and adapted from our published article[61].

medical resources. Despite the high case reports, the true infection rate was likely underreported, as infected individuals with only mild symptoms might have recovered without being detected[174;175].

To stop the viral spread, a series of strict control measures have been implemented in mainland China, including the enforcement of the tourism ban, suspension of the school, and extension of the Spring Festival holiday. From January 23rd to April 8th, 2020, the Chinese government implemented a metropolitan-wide quarantine of Wuhan and nearby cities, suspending all public transportation and advising residents to stay at home[176;177]. Since February 8th, a door-to-door check was started in Wuhan to take all confirmed and suspected people into medical care, which ended at around February 19th[178]. Since February 10th, Wuhan City started to close the community.

Understanding the impact of non-pharmaceutical interventions on the epidemic dynamics is crucial for decision-makers to take proper actions to contain the COVID-19. Since the beginning of the outbreak, scientists have been actively retrieving the epidemiological characteristics such as the time from infection to illness onset (incubation period) and the time from illness onset to hospital admission or isolation (infectious period)[171;179;180]. Researchers have used the reported cases during the early stage of the epidemic and predicted the epidemic trajectory, the basic reproductive number R_0 from which ranges from 2.2 to 6.6[175;178;181]. Several studies explored the effects of the quarantine of Wuhan[182;183], travel restrictions[184], and other non-pharmaceutical intervention strategies[185;186] on the future transmission dynamics at different geographical scales.

China's aggressive and prompt measures have led to a dramatic decrease in the number of new cases. Those measures saved many lives, although at a high economic cost. As of March 18th, 2020, the cumulative number of confirmed cases in China was 81,186. Compared to the previous day, the number of new cases was only 70, most of which were imported from outside the country[187]. In the meantime, COVID-19 spread further around the world, and parts of Italy, South Korea, the United States, and Iran struggled to contain the epidemic.

In this chapter, we build an individual-level based network model and perform stochastic simulations to reconstruct the epidemics in Hubei Province at its early stage and examine the epidemic dynamics under different scenarios. We consider four scenarios: keeping the early-stage trend without any mitigation, reducing the average node through social distancing, reducing the infection rate by adopting protective measures, and decreasing the infection rate through both social distancing and protective measures. The findings of this work can be a reference for policy recommendations regarding COVID-19 in other countries.

6.2 Model

6.2.1 Generalized epidemic modeling framework

To simulate COVID spreading, we apply the generalized epidemic modeling framework (GEMF) developed by the Network Science and Engineering group at Kansas State University[188;189]. In GEMF, nodes represent individuals and links denote interactions among individuals in the complex network. The state of node i at time t is a random variable denoted by $x_i(t)$. It is assumed that each node has only one node state among M possible states at time t, labeled with an index from 1 to M (i.e., $x_i(t) \in 1, \ldots, M$). A node can change its node state either through nodal transitions or edge-based transitions. Nodal transitions of a node do not depend on the states of its neighbors in the network. Edge-based transitions of a node are caused by interactions between neighbors in the network.

To describe the epidemiology of COVID-19 pneumonia, we use the Susceptible-Exposed-Infectious-Removed (SEIR) compartmental model, which has been frequently used in the study of the COVID-19[176;178;181;182]. Each node is either in one of the compartments susceptible, exposed, infectious, or removed. Susceptible nodes refer to people free of the virus and can become infected due to contact with infectious nodes. Exposed nodes have been infected by the disease, but have not yet shown symptoms or become infectious. Removed nodes represent those individuals who are recovered, isolated, hospitalized, or dead due to the disease. The node-level description of transitions in GEMF can be expressed as follows:

$$
\begin{cases}
P_r[x_i\,(t+\Delta t)=1|x_i\,(t)=0,\;\;X\,(t)]=\beta'(t)Y_i\Delta t+o(\Delta t) \\
P_r\,[x_i\,(t+\Delta t)=2|x_i\,(t)=1,X\,(t)]=\lambda\Delta t+o(\Delta t) \\
P_r\,[x_i\,(t+\Delta t)=3|x_i\,(t)=2,X\,(t)]=\delta'\Delta t+o(\Delta t)
\end{cases}, \tag{6.1}
$$

where $X\,(t)$ is the joint state of all individual nodes at time t; $x_i\,(t) = 0, 1, 2, 3$ means that the state of node i at time t is in susceptible, exposed, infectious and removed compartment, respectively; Y_i is the number of infectious neighbors of node i; $\beta'(t)$ is the rate for one node transitions from susceptible state to the exposed state; λ is the rate from the exposed state to the infectious state, and δ' is the removal rate from infectious state to the removed state, which is the inverse of the infectious period.

6.2.2 Application to Hubei Province

Right after the COVID-19 outbreak in China, many studies have estimated the epidemiological parameters, which are essential to calibrate the epidemic models. However, we noticed that there exists a variety regarding the epidemiological parameters. Based on 1099 patients in 31 provincial municipalities through January 29th, 2020, Guan et al.[179] estimated that the median incubation period was 4.0 days (interquartile range 2 to 7 days). Based on a smaller sample size of 425 patients, Li et al.[190] estimated the mean incubation period to be 5.2 days (95% confidence interval, 4.1 to 7.0 days). Du et al.[177] considered the delay from symptom onset to case detection as 4–5 days. Considering the possibility of asymptomatic infections, we adopt a relatively short mean incubation (latent) period as 3 days and mean infectious period as 4 days[191].

In the network, nodes represent people and are divided to 17 groups to represent the 17 prefecture-level cities in Hubei Province (each group is called a city hereafter). Links are generated to reflect both the effects of person-to person contacts within a city and population flows between the cities on the spread of COVID-19. More specifically, we generate intra-city links for each city in two steps. First, we further divide nodes in each city into multiple communities to make it more realistic. Inside each community, links are generated based on the degree distribution given in Zhang et al.[192] using the configuration model. Second, on average each node is connected to another node in the same city based on Erdős–Rényi model such that these communities have connections with each other.

Then, we generate inter-city links based on the number of people that traveled between the cities obtained from Baidu Migration data. For example, if the daily population flow from city i to city j is K number of people, directed links will be generated between K randomly selected nodes in city i to Kd_t nodes in city j, where d_t is the network average node degree at time t. More specifically, the average daily population movement from January 1st–22nd is used to build inter-city links before the Wuhan City lockdown on January 23rd. Since the value of population flows between cities remain stable during the quarantine period, we use the average daily population movement from January 23rd–29th to build inter-city links after the Wuhan City lockdown.

In GEMF simulations, we consider the COVID-19 epidemic outbreak starting in Wuhan City from January 19th, because all confirmed cases reported in Hubei Province were in Wuhan City before January 19th, 2020. To reduce the computational cost, the population of each city and population flows among the cities are scaled by 198, which is the number of cumulative confirmed cases in Hubei Province up to January 19th. After scaling, the total number of nodes in the network N equals 298,838. In total, we generate three adjacency lists of the network topology, which are imported to GEMF and changed according to time during simulation. More specifically, the first adjacency list A_1 corresponds to the network with $d_t = 15$ and inter-city links before the Wuhan City lockdown, and is used during simulation up to January 22nd. The second adjacency list A_2 refers to the network with $d_t = 15$ and inter-city links after the Wuhan City lockdown, and is used during simulation up to February 9th. The third adjacency list A_3 incorporates $d_t = 3$ and inter-city links after the Wuhan City lockdown, and is used during simulation on and after February 10th when community closure was implemented.

To fit the model, we take the number of confirmed cases as the number of people in the removed state. By keeping $\lambda = 1/3\ day^{-1}$ and $\delta' = 1/4\ day^{-1}$ unchanged, we estimate the infection rate β' as a piecewise constant function of the time. The β' function and time intervals are both tuned to minimize the error between the number of removed people from our simulations and the number of cumulative confirmed cases in Hubei Province[193]. The total period from January 19th to April 15th is separated into three phases (January 19th–January 27th, January 28th–February 9th, and after February 9th). During the first phase, Wuhan city lockdown happened, and hospitals were short of beds. During the second phase, Thunder God Mountain Hospital and Fire God Mountain Hospital were put into use, and door-to-door screening was implemented. In the third phase, community closure was enacted.

GEMF is available in MATLAB, R, Python, and C programming language, and we performed extensive stochastic simulations by adapting the GEMF toolbox with MATLAB during the experiment. We track the number of nodes in each compartment and demonstrate the simulation results with confidence intervals. The number of simulation runs is 1500 in all scenarios.

6.2.3 Data collection

The population size of each city in Hubei Province is obtained from the Hubei Statistical Yearbook. We collected Baidu Migration data (https://qianxi.baidu.com/) for the 17 cities in the Hubei Province from January 1st to January 29th, 2020. The daily Baidu migration data contain two types of data. First type: the data include the immigration index and emigration index of each city, which are linearly related to the human traffic volume moving in and out of individual cities. Second type: for each city i, the data also contain the composition of city i's incoming flow, namely the fraction of flows coming from every other city j to city i (flow from city j to i divided by the total flow coming into city i). Similarly, the data contain the fraction of flows going out of city i to city m (flow from city i to m divided by the total flow going out of city i).

Based on the fact that around 5 million people have moved out of Wuhan before the city lockdown on January 23rd, we obtain the number of people that traveled between the cities using the following approach. First, we estimate value of α, which equals 5 million divided by the sum of Wuhan's emigration indexes from January 1st to January 23rd. Then, we can calculate the population flow moving in or out of each individual city by α times the immigration or emigration index. In addition, the population flow multiplied by the flow fraction going to or coming from a specific city gives us the number of daily travelers to or from a particular individual city to another.

6.3 Results

In this section, we present results based on GEMF stochastic simulations. To reconstruct the epidemics in Hubei province, we continuously tune the infection rate parameter β' to minimize the error between the number of nodes in the removed compartment from GEMF simulations and the number of cumulative confirmed cases from the data, as shown in Fig. 6.1.

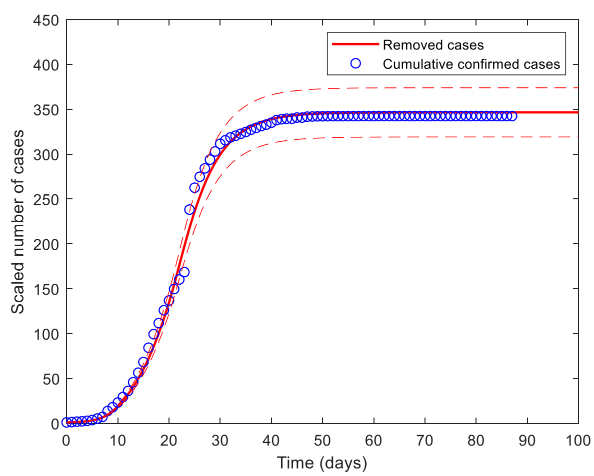

Figure 6.1: *Fitting the model to the cumulative confirmed cases from January 19th to April 15th.*

By performing GEMF stochastic simulations, we obtain that β' is equal to 0.06 for day 0–8 (January 19th–January 27th), and then becomes 0.0169 for day 9–21 (January 28th–February 9th), and equals 0.01 on and after day 22 (February 10th). The infection rate dramatically drops, indicating that public health interventions implemented in Hubei Province have considerably controlled the epidemic development since the nascent stage of the outbreak. Based on the fitted parameter β', we estimate the basic reproduction number ($R_0 = \beta' d_t/\delta$) decreases from 3.6 before January 27th, to 1.014 between January 27th–February 9th, and to 0.12 on and after February 10th.

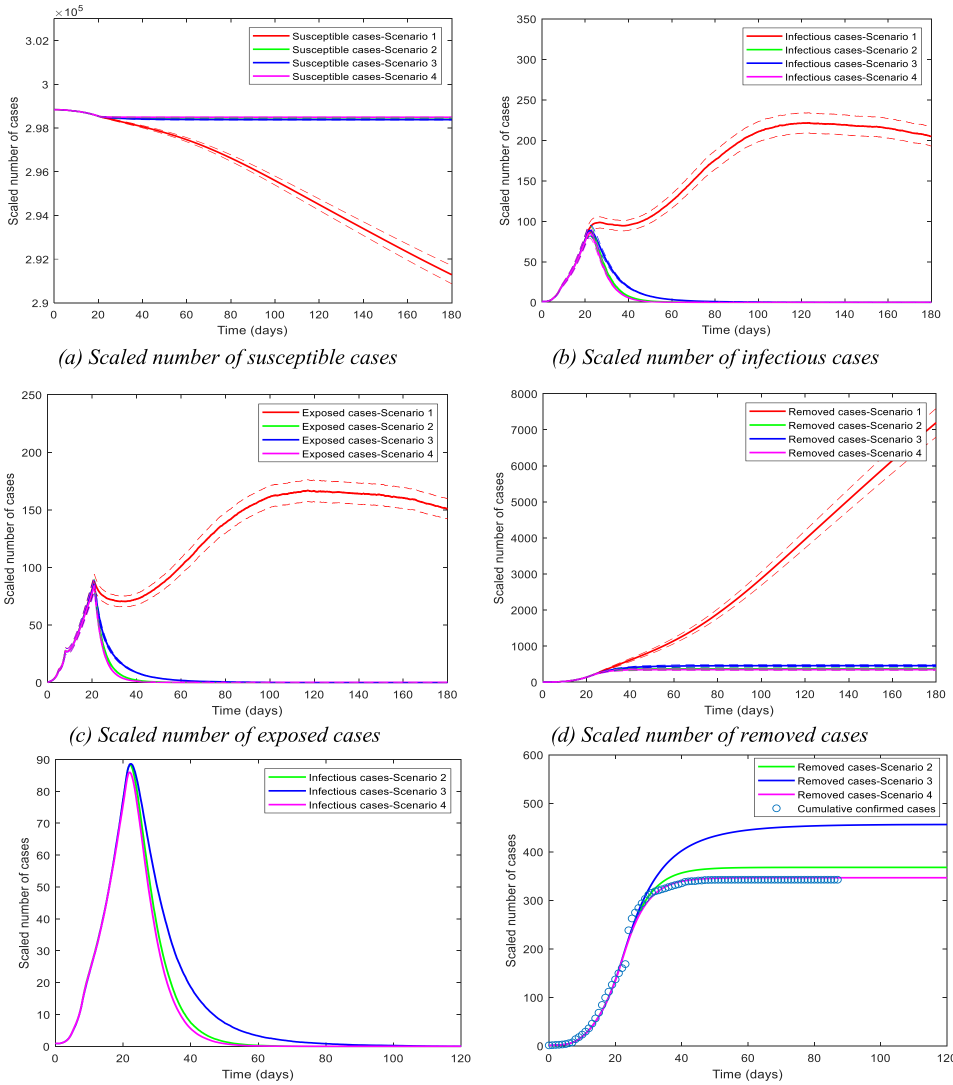

(a) Scaled number of susceptible cases

(b) Scaled number of infectious cases

(c) Scaled number of exposed cases

(d) Scaled number of removed cases

(e) Scaled average number of infectious cases after zooming in

(f) Scaled average number of removed cases compared to the cumulative confirmed cases

Figure 6.2: *Epidemic dynamics under four scenarios (red, green, blue, and magenta) from GEMF stochastic simulations. Note that the magenta curves almost overlap perfectly with the green curves in Fig. 6.2(b), so Figs. 6.2(e–f) are provided to zoom in and show the differences.*

Fig. 6.2 shows the epidemic trajectories under four scenarios, in which different mitigation strategies are implemented after February 9th: continuing the current trend with $\beta' = 0.0169$ and the network average node degree $d_t = 15$ (Scenario 1); reducing d_t from 15 to 3 (Scenario

2); decreasing β' by 75% (Scenario 3); reducing β' from 0.0169 to 0.01 and d_t from 15 to 3 (Scenario 4). Preventive measures such as wearing masks can help reduce the infection rate. On the other hand, the average node degree refers to the possible contacts a person may have in daily life, and this can be reduced by contact reduction and social distancing.

In Fig. 6.2, if the current trend as of February 9th had continued, the epidemic spreading could have become more severe than what happened in Hubei Province. Reducing the average node degree from 15 to 3 (Scenario 2), the epidemic would reach the peak at around day 21.85 and fade out at around day 66.80 with the final epidemic size 367.86 (95% 339.55–396.18). When β' is reduced by 75% in Scenario 3, the number of removed cases in the steady-state would reach 456.47 on average (95% CI: 423.34–489.59), and the epidemic would fade out at day 110.90 on average. When a combination of reducing β' and average node degree is conducted in Scenario 4, the epidemic dynamics would approximate the actual epidemic trajectory in Hubei Province in the steady-state with mean scaled number of removed cases 346.54 (95% CI: 319.12–373.96). In addition, the epidemic would reach the peak at day 21.50 and fade out at day 61.55 on average.

Overall, GEMF simulation results suggest that more strict prevention and control measures have been taken since February 9th to achieve the current cumulative confirmed cases in Hubei Province. Preventive measures and social distancing measures need to be taken in combination by the government to speed up the containment of the epidemic and reduce the peak infection dramatically.

6.4 Summary

In this work, we test and confirm the effectiveness of non-pharmaceutical interventions on the containment of the epidemic dynamics by performing GEMF stochastic simulations. The daily cases of the COVID-19 epidemic in Hubei Province peaked at over 15,000 on February 12th and became almost zero in mid-March. Our simulation results indicate that the containment of this highly contagious disease was achieved by stringent control measures by the Chinese government. Without continued and aggressive control measures, the epidemic in Hubei Province would have become more severe. Only with combined implementation of enhanced protective measures and social distancing measures, the epidemic dynamics would peak at around mid-February and approximate the actual epidemic trajectory in March. This can be an important message for countries going through the exponential growth of the epidemic in the current days. In addition, the model developed can be easily adapted to simulate the COVID epidemic dynamics in other regions.

Chapter 7

Conclusion and future work

7.1 Summary

In this dissertation, we have investigated complex system behaviors facing biosecurity challenges from different perspectives. In modern society, infrastructure systems have become increasingly interconnected. Although this interdependence enables the economic functioning of the interdependent system, it also brings vulnerabilities to the system amplifying disease spreading and natural disaster consequences. With this background, this dissertation addresses five research questions that aim to assess the behavior of complex systems in face of biosecurity challenges. The answers to these research questions can help policymakers to identify vulnerabilities in the system and benefit existing disaster preparedness. The accomplishments of this dissertation are summarized as follows:

- Chapters 2–4 describe the development of an agent-based model focused on southwest Kansas, United States. The model mirrors the beef cattle production and transportation based on regular business operating principles and assumed conditions obtained from the literature review, beef cattle experts, and field studies. It is capable of capturing the complicated interactions between disease spreading and individuals' responsiveness on biosecurity measures, considering individuals' heterogeneous risk attitudes.
- In Chapter 2, we evaluate the robustness of the interdependent system by constructing

hypothetical disruptions in both the cattle industry and the transportation industry. We find that the system is robust to random failures but vulnerable to the targeted shutdown of cattle premises or truck premises. In addition, disruptions in the trucks serving packers have the worst impact on cattle production, as compared to other transportation disruptions. In disaster preparations, policymakers and system designers need to consider vulnerabilities caused by the interdependent infrastructure and pay particular attention to one of its critical components, meat packers.

- In Chapter 3, we assess the impact of truck contamination on the foot-and-mouth disease transmission with the truck agent following an independent clean-infected-clean cycle. Scenario analyses results show that including indirect contact routes between premises via truck movements can significantly increase the disease spread amplitude, compared with equivalent scenarios that only consider direct contact routes via animal movement. We add an information-sharing functionality such that producers/packers can trace back and forward their trade records to inform their trade partners during outbreaks. We find that mitigation strategies informed by information sharing can effectively mitigate epidemics, highlighting the benefit of promoting information sharing in the cattle industry.

- In Chapter 4, we integrate the human decision-making process into epidemiological processes, and examine the impact of human behavior factors on a hypothetical foot-and-mouth disease outbreak. In the model, human behaviors related to biosecurity practices change following an increase in the regional disease incidence. Here, biosecurity is referred to as implementing control measures to decrease the chance of animal disease spreading. With the same initial biosecurity status, the number of infected producer locations and cattle losses can be more effectively reduced with an increase in the percentage of risk-averse producers selecting large producers first compared to randomly selecting producers. In addition, the reduction in epidemic size caused by the shifting of producers' risk attitudes towards risk-aversion is heavily dependent on the distribution of the initial biosecurity level. A comprehensive investigation of the initial biosecurity status is recommended to inform the design of risk communication strategies.

- In Chapter 5, we study the robustness of supply chain networks against cascading failures. Considering the upper and lower bound load constraints, i.e., inventory and cost, we examine the fraction of failed entities under load decrease and load fluctuation scenarios. The simulation results obtained from synthetic networks and a European supply chain network confirm that the recovery strategies of surplus inventory and backup suppliers often adopted in actual supply chains can enhance the system robustness, compared with the system without the recovery process. In addition, the system is relatively robust against load fluctuations but is more fragile to demand shocks. For the underload-driven model without the recovery process, we find the existence of a discontinuous phase transition. Unlike other systems studied under overload cascading failures, this system is more robust for power-law distributions than uniform distributions of the lower bound parameter for the studied scenarios.

- As an emerging infectious disease, the 2019 coronavirus disease has developed into a global pandemic. In Chapter 6, we use a network-based model to reconstruct the epidemic dynamics in Hubei Province and examine the effectiveness of non-pharmaceutical interventions on the epidemic spreading with various scenarios. We reveal that without continued control measures, the epidemic in Hubei Province could have become persistent. Only by continuing to decrease the infection rate through protective measures and social distancing can the actual epidemic trajectory that happened in Hubei Province be reconstructed in simulation.

7.2 Limitations and directions for future work

This section provides several recommendations for future work based on the limitations of this dissertation. The research scope of Chapters 2–4 only focuses on the beef cattle industry in southwest Kansas, which has many feedlots and few numbers of ranches and packers. As a result, some of our conclusions depend on this system particularity, and may not be applicable to beef cattle industry at other locations. However, the model developed can be readily adapted to other regions as soon as relevant data sets become available. In addition, actual cattle and truck movement data are not accessible in southwest Kansas due to privacy issues. The availability of high-quality actual cattle and truck movement data in the future may result in different outcomes and lead to a better understanding of the system behavior. However, one of the main goal of the project is to generate realistic cattle and truck movement data under this data unavailability, and we provided these data sets for the community studying interconnected complex systems.

In the agent-based model, producers/packers randomly select other producers to trade cattle, and we disregard price factors and seasonal fluctuations. Future work can analyze the disease spread under various contact network structures by altering the current trade pattern. For simplicity, we assume that once control measures are implemented in packers, packers stop requesting cattle and do not go back to normal operations during the epidemic period, while this may not be what happens in practice. Future work may impart greater realism to the packer agent and further analyze the economic impact caused by different control strategies.

In addition, we include only truck movement and disregard other forms of indirect contact, such as the movement of personnel or equipment. As the truck movement occurs for the shipment of cattle, indirect contact is always associated with direct contact. Therefore, we compare the disease spread under the scenario of direct contact only and scenario of indirect and direct contact in Chapter 3, without considering the indirect contact only scenario. Nonetheless, it would be interesting to include other potential indirect transmission routes such as feed transporters and veterinarians to investigate the role of indirect contact in the disease spreading thoroughly. This can be the topic of future analyses.

Moreover, the duration of a truck or a loading/unloading area of premises remaining contaminated, i.e., the contamination period, is affected by not only the ability of the pathogen to survive in fomites, but also by environmental factors such as temperature and by the frequency of the disinfection operations[128]. The exact value of the contamination period is not available and is assumed to be 14 days similar to the work in papers[8;128;130]. However, sensitivity analyses results show that epidemic sizes are sensitive to variations in the contamination period. This highlights the need for a more accurate estimation of this parameter.

Cattle producers are reluctant to share their information due to privacy concerns. Over the past decades, many studies have focused on the usage of information sharing as a method to improve supply chain performance and resilience to disruptions[194;195]. The information shared, such as demand and inventory level, can foster the operation control and decision making about supply chain disruptions. To enhance food security by sharing the authentic data while maintaining privacy, several recent studies have analyzed food supply chain traceability using blockchain technology[120;122;122;196], which is promising to result in more information sharing. Chapter 3 assumes that all producers participate in the information-sharing process. Another area of future work is to investigate how acceptance rate of the information infrastructure will affect the epidemic size, and how to enhance the acceptance of information sharing infrastructure considering economic and social factors. Sensitivity analysis shows that the number of days to trace back and forward during information sharing has a significant influence on the epidemic size and is worth further studying considering the economic impacts of the related mitigation strategies.

In Chapter 5, we mainly focus on qualitatively showing the dynamic behavior of general supply chain networks against disruptions. Thus, providing practical implications on the specific beef supply chain is not our primary focus. However, this work paves the foundation for future research in modeling beef supply chains in the face of cascading failures, which could hopefully shed light on policy recommendations for decision-makers to make the beef industry more robust. We find that strategies such as surplus inventories can reduce the scale of systemic failure during disruptions. Nonetheless, the best approach to protecting the beef cattle industry is a tradeoff between the cost and benefit of these protection measures, which require more investigation. What's more, links are randomly generated based on a connection probability, and all nodes are disrupted with a factor in the supply chain synthetic network. Therefore, the initial failures triggered in this work can be seen as caused by random attacks. Future work can examine the system behavior under targeted attacks with various network topologies. With appropriate data available, we can also use the agent-based modeling method to validate the theoretical results in this chapter.

Bibliography

[1] World Health Organization. Biosecurity: An integrated approach to manage risk to human, animal and plant life and health, March 2010. URL https://www.who.int/foodsafety/fs_management/No_01_Biosecurity_Mar10_en.pdf.

[2] Laura A Meyerson and Jamie K Reaser. Biosecurity: Moving toward a comprehensive approach: A comprehensive approach to biosecurity is necessary to minimize the risk of harm caused by non-native organisms to agriculture, the economy, the environment, and human health. *BioScience*, 52(7):593–600, 2002.

[3] Nesrein M Hashem, Antonio González-Bulnes, and Alfonso J Rodriguez-Morales. Animal welfare and livestock supply chain sustainability under the COVID-19 outbreak: An overview. *Frontiers in Veterinary Science*, 7:679, 2020.

[4] Christian Gortázar and José de la Fuente. COVID-19 is likely to impact animal health. *Preventive Veterinary Medicine*, 180:105030, 2020.

[5] Jeremy N Marchant-Forde and Laura A Boyle. COVID-19 effects on livestock production: A one welfare issue. *Frontiers in Veterinary Science*, 7:734, 2020.

[6] DS Peel, D Aherin, R Blach, K Burdine, D Close, A Hagerman, J Maples, J Robb, and G Tonsor. Economic damages to the US beef cattle industry due to COVID-19. *Oklahoma Cooperative Extension Service*, 2020.

[7] Shauhrat S Chopra and Vikas Khanna. Interconnectedness and interdependencies of critical infrastructures in the US economy: Implications for resilience. *Physica A: Statistical Mechanics and its Applications*, 436:865–877, 2015.

[8] Alba Bernini, Luca Bolzoni, and Renato Casagrandi. When resolution does matter:

Modelling indirect contacts in dairy farms at different levels of detail. *PLoS ONE*, 14 (10):e0223652, 2019.

[9] Kristi Miley. Global health biosecurity in a vulnerable world–an evaluation of emerging threats and current disaster preparedness strategies for the future. In *Global Health Security*, pages 79–102. Springer, 2020.

[10] Sergey V Buldyrev, Roni Parshani, Gerald Paul, H Eugene Stanley, and Shlomo Havlin. Catastrophic cascade of failures in interdependent networks. *Nature*, 464(7291):1025–1028, 2010.

[11] Xuqing Huang, Jianxi Gao, Sergey V Buldyrev, Shlomo Havlin, and H Eugene Stanley. Robustness of interdependent networks under targeted attack. *Physical Review E*, 83 (6):065101, 2011.

[12] Fei Tan, Yongxiang Xia, Wenping Zhang, and Xinyu Jin. Cascading failures of loads in interconnected networks under intentional attack. *Europhysics Letters*, 102(2):28009, 2013.

[13] Yakup Koç, Martijn Warnier, Piet Van Mieghem, Robert E Kooij, and Frances MT Brazier. A topological investigation of phase transitions of cascading failures in power grids. *Physica A: Statistical Mechanics and its Applications*, 415:273–284, 2014.

[14] Yakup Koç, Martijn Warnier, Piet Van Mieghem, Robert E Kooij, and Frances MT Brazier. The impact of the topology on cascading failures in a power grid model. *Physica A: Statistical Mechanics and its Applications*, 402:169–179, 2014.

[15] Yueyi Hou, Xiaoyun Xing, Menghui Li, An Zeng, and Yougui Wang. Overload cascading failure on complex networks with heterogeneous load redistribution. *Physica A: Statistical Mechanics and its Applications*, 481:160–166, 2017.

[16] Fei Xue, Ettore Bompard, Tao Huang, Lin Jiang, Shaofeng Lu, and Huaiying Zhu. Interrelation of structure and operational states in cascading failure of overloading

lines in power grids. *Physica A: Statistical Mechanics and its Applications*, 482:728–740, 2017.

[17] JunJie Wu, HJ Sun, and ZY Gao. Cascading failures on weighted urban traffic equilibrium networks. *Physica A: Statistical Mechanics and its Applications*, 386(1):407–413, 2007.

[18] Sakshi Pahwa, Caterina Scoglio, and Antonio Scala. Abruptness of cascade failures in power grids. *Scientific Reports*, 4(1):1–9, 2014.

[19] Yu Zeng and Renbin Xiao. Modelling of cluster supply network with cascading failure spread and its vulnerability analysis. *International Journal of Production Research*, 52 (23):6938–6953, 2014.

[20] Liang Tang, Ke Jing, Jie He, and H Eugene Stanley. Complex interdependent supply chain networks: Cascading failure and robustness. *Physica A: Statistical Mechanics and its Applications*, 443:58–69, 2016.

[21] Yingcong Wang and Renbin Xiao. An ant colony based resilience approach to cascading failures in cluster supply network. *Physica A: Statistical Mechanics and its Applications*, 462:150–166, 2016.

[22] Yingcong Wang and Fengpeng Zhang. Modeling and analysis of under-load-based cascading failures in supply chain networks. *Nonlinear Dynamics*, 92(3):1403–1417, 2018.

[23] Liang Tang, Ke Jing, Jie He, and H Eugene Stanley. Robustness of assembly supply chain networks by considering risk propagation and cascading failure. *Physica A: Statistical Mechanics and its Applications*, 459:129–139, 2016.

[24] Junyan Sun, Jianming Tang, Weiping Fu, Zhirui Chen, and Yaru Niu. Construction of a multi-echelon supply chain complex network evolution model and robustness analysis of cascading failure. *Computers & Industrial Engineering*, 144:106457, 2020.

[25] Jens Seedorf and Ralf-Gunther Schmidt. The simulated air flow pattern around a moving animal transport vehicle as the basis for a prospective biosecurity risk assessment. *Heliyon*, 3(8):e00358, 2017.

[26] Matt J Keeling, Mark EJ Woolhouse, Darren J Shaw, Louise Matthews, Margo Chase-Topping, Dan T Haydon, Stephen J Cornell, Jens Kappey, John Wilesmith, and Bryan T Grenfell. Dynamics of the 2001 UK foot and mouth epidemic: stochastic dispersal in a heterogeneous landscape. *Science*, 294(5543):813–817, 2001.

[27] DM Green, IZ Kiss, and RR Kao. Modelling the initial spread of foot-and-mouth disease through animal movements. *Proceedings of the Royal Society B: Biological Sciences*, 273(1602):2729–2735, 2006.

[28] A Ortiz-Pelaez, DU Pfeiffer, RJ Soares-Magalhaes, and FJ Guitian. Use of social network analysis to characterize the pattern of animal movements in the initial phases of the 2001 foot and mouth disease (FMD) epidemic in the UK. *Preventive Veterinary Medicine*, 76(1-2):40–55, 2006.

[29] Thomas W Bates, Mark C Thurmond, and Tim E Carpenter. Direct and indirect contact rates among beef, dairy, goat, sheep, and swine herds in three California counties, with reference to control of potential foot-and-mouth disease transmission. *American Journal of Veterinary Research*, 62(7):1121–1129, 2001.

[30] RL Sanson, G Struthers, P King, JF Weston, and RS Morris. The potential extent of transmission of foot-and-mouth disease: a study of the movement of animals and materials in Southland, New Zealand. *New Zealand Veterinary Journal*, 41(1):21–28, 1993.

[31] Paolo Bajardi, Alain Barrat, Fabrizio Natale, Lara Savini, and Vittoria Colizza. Dynamical patterns of cattle trade movements. *PLoS ONE*, 6(5):e19869, 2011.

[32] Hartmut HK Lentz, Andreas Koher, Philipp Hövel, Jörn Gethmann, Carola Sauter-Louis, Thomas Selhorst, and Franz J Conraths. Disease spread through animal move-

ments: a static and temporal network analysis of pig trade in Germany. *PLoS ONE*, 11(5):e0155196, 2016.

[33] Gianluigi Rossi, Giulio A De Leo, Stefano Pongolini, Silvano Natalini, Simone Vincenzi, and Luca Bolzoni. Epidemiological modelling for the assessment of bovine tuberculosis surveillance in the dairy farm network in Emilia-Romagna (Italy). *Epidemics*, 11:62–70, 2015.

[34] Kathrin Schemann, Melanie R Taylor, J-ALML Toribio, and Navneet K Dhand. Horse owners' biosecurity practices following the first equine influenza outbreak in Australia. *Preventive Veterinary Medicine*, 102(4):304–314, 2011.

[35] Arata Hidano, Gareth Enticott, Robert M Christley, and M Carolyn Gates. Modeling dynamic human behavioral changes in animal disease models: challenges and opportunities for addressing bias. *Frontiers in Veterinary Science*, 5:137, 2018.

[36] Aditi Mankad. Psychological influences on biosecurity control and farmer decision-making. A review. *Agronomy for Sustainable Development*, 36(2):1–14, 2016.

[37] Ângelo J Mendes, Daniel T Haydon, Emma McIntosh, Nick Hanley, and Jo EB Halliday. Socially vs. privately optimal control of livestock diseases: A case for integration of epidemiology and economics. *Frontiers in Veterinary Science*, 7:937, 2020.

[38] Melissa Tracy, Magdalena Cerdá, and Katherine M Keyes. Agent-based modeling in public health: current applications and future directions. *Annual Review of Public Health*, 39:77–94, 2018.

[39] Dimitris Kremmydas, Ioannis N Athanasiadis, and Stelios Rozakis. A review of agent based modeling for agricultural policy evaluation. *Agricultural Systems*, 164:95–106, 2018.

[40] Christophe Schinckus. Agent-based modelling and economic complexity: a diversified perspective. *Journal of Asian Business and Economic Studies*, 2019.

[41] Donald L DeAngelis and Stephanie G Diaz. Decision-making in agent-based modeling: A current review and future prospectus. *Frontiers in Ecology and Evolution*, 6:237, 2019.

[42] Uwe Clausen, Matthias Brueggenolte, Marc Kirberg, Christoph Besenfelder, Moritz Poeting, and Mustafa Gueller. Agent-based simulation in logistics and supply chain research: Literature review and analysis. In *Proceedings of the Interdisciplinary Conference on Production, Logistics and Traffic*, pages 45–59. Springer, 2019.

[43] Philipp Ringler, Dogan Keles, and Wolf Fichtner. Agent-based modelling and simulation of smart electricity grids and markets–a literature review. *Renewable and Sustainable Energy Reviews*, 57:205–215, 2016.

[44] Oded Cats and Erik Jenelius. Planning for the unexpected: the value of reserve capacity for public transport network robustness. *Transportation Research Part A: Policy and Practice*, 81:47–61, 2015.

[45] Volker Grimm, Uta Berger, Finn Bastiansen, Sigrunn Eliassen, Vincent Ginot, Jarl Giske, John Goss-Custard, Tamara Grand, Simone K Heinz, Geir Huse, et al. A standard protocol for describing individual-based and agent-based models. *Ecological Modelling*, 198(1-2):115–126, 2006.

[46] Hsiao-Hsuan Wang and William E Grant. Alternative ecological modeling formats: Commonalities from a systems perspective. *Developments in Environmental Modelling*, 31:249–264, 2019.

[47] Erik Cuevas. An agent-based model to evaluate the COVID-19 transmission risks in facilities. *Computers in Biology and Medicine*, 121:103827, 2020.

[48] Kevin E Jablonski, Randall B Boone, and Paul J Meiman. An agent-based model of cattle grazing toxic Geyer's larkspur. *PLoS ONE*, 13(3):e0194450, 2018.

[49] C Athena Aktipis, Lee Cronk, and Rolando de Aguiar. Risk-pooling and herd survival:

an agent-based model of a Maasai gift-giving system. *Human Ecology*, 39(2):131–140, 2011.

[50] AJ Romera, ST Morris, J Hodgson, WD Stirling, and SJR Woodward. A model for simulating rule-based management of cow–calf systems. *Computers and Electronics in Agriculture*, 42(2):67–86, 2004.

[51] Marleen Schouten, Tim Verwaart, and Wim Heijman. Comparing two sensitivity analysis approaches for two scenarios with a spatially explicit rural agent-based model. *Environmental Modelling & Software*, 54:196–210, 2014.

[52] Andrew M Bate, Glyn Jones, Adam Kleczkowski, Rebecca Naylor, Jon Timmis, Piran CL White, and Julia Touza. Livestock disease management for trading across different regulatory regimes. *EcoHealth*, 15(2):302–316, 2018.

[53] Sebastian Rasch, Thomas Heckelei, Roelof Oomen, and Christiane Naumann. Cooperation and collapse in a communal livestock production SES model–a case from South Africa. *Environmental Modelling & Software*, 75:402–413, 2016.

[54] Shaobin Li, Yuwei Qin, Jeyamkondan Subbiah, and Bruce Dvorak. Life cycle assessment of the US beef processing through integrated hybrid approach. *Journal of Cleaner Production*, 265:121813, 2020.

[55] USDA ERS. Sector at a Glance, January 2021. URL https://www.ers.usda.gov/topics/animal-products/cattle-beef/sector-at-a-glance/.

[56] Kansas Department of Agriculture. Kansas agriculture and agriculture related industries economic contribution report, August 2020. URL https://www.agriculture.ks.gov/about-kda/kansas-agriculture.

[57] James S Drouillard. Current situation and future trends for beef production in the United States of America—A review. *Asian-Australasian Journal of Animal Sciences*, 31(7):1007, 2018.

[58] Qihui Yang, Don Gruenbacher, Jessica L Heier Stamm, Gary L Brase, Scott A DeLoach, David E Amrine, and Caterina Scoglio. Developing an agent-based model to simulate the beef cattle production and transportation in southwest Kansas. *Physica A: Statistical Mechanics and its Applications*, 526:120856, 2019.

[59] Qihui Yang, Don M Gruenbacher, Jessica L Heier Stamm, David E Amrine, Gary L Brase, Scott A DeLoach, and Caterina M Scoglio. Impact of truck contamination and information sharing on foot-and-mouth disease spreading in beef cattle production systems. *PLoS ONE*, 15(10):e0240819, 2020.

[60] Qihui Yang, Caterina M Scoglio, and Don M Gruenbacher. Robustness of supply chain networks against underload cascading failures. *Physica A: Statistical Mechanics and its Applications*, 563:125466, 2021.

[61] Qihui Yang, Chunlin Yi, Aram Vajdi, Lee W Cohnstaedt, Hongyu Wu, Xiaolong Guo, and Caterina M Scoglio. Short-term forecasts and long-term mitigation evaluations for the COVID-19 epidemic in Hubei Province, China. *Infectious Disease Modelling*, 5:563–574, 2020.

[62] Shuliang Wang, Liu Hong, and Xueguang Chen. Vulnerability analysis of interdependent infrastructure systems: A methodological framework. *Physica A: Statistical Mechanics and its applications*, 391(11):3323–3335, 2012.

[63] Defense Use Case. Analysis of the cyber attack on the Ukrainian power grid. *Electricity Information Sharing and Analysis Center (E-ISAC)*, 388, 2016.

[64] Bo Liu and Hongyu Wu. Optimal D-FACTS placement in moving target defense against false data injection attacks. *IEEE Transactions on Smart Grid*, 11(5):4345–4357, 2020.

[65] Hang Zhang, Bo Liu, and Hongyu Wu. Smart grid cyber-physical attack and defense: A review. *IEEE Access*, 9:29641–29659, 2021.

[66] National Centers for Environmental Information. Billion-dollar weather and climate disasters: Overview. 2017.

[67] Réka Albert, Hawoong Jeong, and Albert-László Barabási. Error and attack tolerance of complex networks. *Nature*, 406(6794):378–382, 2000.

[68] Sakshi Pahwa, M Youssef, P Schumm, C Scoglio, and N Schulz. Optimal intentional islanding to enhance the robustness of power grid networks. *Physica A: Statistical Mechanics and its Applications*, 392(17):3741–3754, 2013.

[69] Ali Sydney, Caterina Scoglio, and Don Gruenbacher. Optimizing algebraic connectivity by edge rewiring. *Applied Mathematics and Computation*, 219(10):5465–5479, 2013.

[70] Xiao Fan Wang and Jian Xu. Cascading failures in coupled map lattices. *Physical Review E*, 70(5):056113, 2004.

[71] US DHS. Critical infrastructure sectors. *US Department of Homeland Security*, 2019.

[72] Kortney E Craft, Rezaul Mahmood, Stephen A King, Gregory Goodrich, and Jun Yan. Droughts of the twentieth and early twenty-first centuries: Influences on the production of beef and forage in Kentucky, USA. *Science of the Total Environment*, 577:122–135, 2017.

[73] Ted C Schroeder, Dustin L Pendell, Michael W Sanderson, and Sara Mcreynolds. Economic impact of alternative FMD emergency vaccination strategies in the midwestern United States. *Journal of Agricultural and Applied Economics*, 47(1):47–76, 2015.

[74] TG O'Quinn, DR Woerner, TE Engle, PL Chapman, JF Legako, JC Brooks, KE Belk, and JD Tatum. Identifying consumer preferences for specific beef flavor characteristics in relation to cattle production and postmortem processing parameters. *Meat Science*, 112:90–102, 2016.

[75] Temple Grandin. Recommended animal handling guidelines and audit guide. *A systematic approach to animal welfare. American Industry Foundation: USA*, 2010.

[76] KS Schwartzkopf-Genswein, Luiggi Faucitano, Samira Dadgar, Phillys Shand, LA González, and TG Crowe. Road transport of cattle, swine and poultry in North

America and its impact on animal welfare, carcass and meat quality: A review. *Meat Science*, 92(3):227–243, 2012.

[77] GC Miranda-De La Lama, Morris Villarroel, and Gustavo A María. Livestock transport from the perspective of the pre-slaughter logistic chain: a review. *Meat Science*, 98(1): 9–20, 2014.

[78] SM Huertas, AD Gil, JM Piaggio, FJCM Van Eerdenburg, et al. Transportation of beef cattle to slaughterhouses and how this relates to animal welfare and carcase bruising in an extensive production system. *Animal Welfare*, 19(3):281–285, 2010.

[79] AR Barham, BL Barham, AK Johnson, DM Allen, JR Blanton Jr, and MF Miller. Effects of the transportation of beef cattle from the feedyard to the packing plant on prevalence levels of Escherichia coli o157 and salmonella spp. *Journal of Food Protection*, 65(2):280–283, 2002.

[80] Yong Bai, Pat C Oslund, Thomas E Mulinazzi, Shyamala Tamara, Chunxiao Liu, Michael M Barnaby, and Christine E Atkins. Transportation logistics and economics of the processed meat and related industries in Southwest Kansas. 2007.

[81] Paolo Motta, Thibaud Porphyre, Ian Handel, Saidou M Hamman, Victor Ngu Ngwa, Vincent Tanya, Kenton Morgan, Rob Christley, M Barend, et al. Implications of the cattle trade network in Cameroon for regional disease prevention and control. *Scientific Reports*, 7(1):1–13, 2017.

[82] Mike J Jeger, Marco Pautasso, Ottmar Holdenrieder, and Mike W Shaw. Modelling disease spread and control in networks: implications for plant sciences. *New Phytologist*, 174(2):279–297, 2007.

[83] Istvan Z Kiss, Darren M Green, and Rowland R Kao. The network of sheep movements within Great Britain: network properties and their implications for infectious disease spread. *Journal of the Royal Society Interface*, 3(10):669–677, 2006.

[84] Paolo Bajardi, Alain Barrat, Lara Savini, and Vittoria Colizza. Optimizing surveillance for livestock disease spreading through animal movements. *Journal of the Royal Society Interface*, 9(76):2814–2825, 2012.

[85] Gianluigi Rossi, Giulio A De Leo, Stefano Pongolini, Silvano Natalini, Luca Zarenghi, Matteo Ricchi, and Luca Bolzoni. The potential role of direct and indirect contacts on infection spread in dairy farm networks. *PLoS Computational Biology*, 13(1):e1005301, 2017.

[86] Marnie L Brennan, R Kemp, and Robert M Christley. Direct and indirect contacts between cattle farms in north-west England. *Preventive Veterinary Medicine*, 84(3-4): 242–260, 2008.

[87] Brandon J Dominguez. *Characterization of livestock herds in extensive agricultural settings in southwest Texas*. PhD thesis, Texas A&M University, 2010.

[88] Michael G Buhnerkempe, Daniel A Grear, Katie Portacci, Ryan S Miller, Jason E Lombard, and Colleen T Webb. A national-scale picture of US cattle movements obtained from Interstate Certificate of Veterinary Inspection data. *Preventive Veterinary Medicine*, 112(3-4):318–329, 2013.

[89] Erin E Gorsich, Angela D Luis, Michael G Buhnerkempe, Daniel A Grear, Katie Portacci, Ryan S Miller, and Colleen T Webb. Mapping US cattle shipment networks: Spatial and temporal patterns of trade communities from 2009 to 2011. *Preventive Veterinary Medicine*, 134:82–91, 2016.

[90] Hong Liu, Phillip Schumm, Anton Lyubinin, and Caterina Scoglio. Epirur_cattle: a spatially explicit agent-based simulator of beef cattle movements. *Procedia Computer Science*, 9:857–865, 2012.

[91] Aristides Moustakas and Matthew R Evans. Coupling models of cattle and farms with models of badgers for predicting the dynamics of bovine tuberculosis (TB). *Stochastic Environmental Research and Risk Assessment*, 29(3):623–635, 2015.

[92] Chrysm Watson Ross, Robert J Glass, John Harger, Stephen H Conrad, Aldo A Zagonel, Walter E Beyeler, and Melissa Finley. Development of an agent-based epidemiological model of beef cattle. In *Proceedings of the 19th International Conference of the System Dynamics Society*, 2011.

[93] Hyeyoung Kim, Ningchuan Xiao, Mark Moritz, Rebecca Garabed, and Laura W Pomeroy. Simulating the transmission of foot-and-mouth disease among mobile herds in the far north region, Cameroon. *Journal of Artificial Societies and Social Simulation*, 19(2), 2016.

[94] Elise Dion, Louis VanSchalkwyk, and Eric F Lambin. The landscape epidemiology of foot-and-mouth disease in South Africa: A spatially explicit multi-agent simulation. *Ecological Modelling*, 222(13):2059–2072, 2011.

[95] Jessica Robins, Sarah Bogen, Auldon Francis, Annet Westhoek, Andrew Kanarek, Suzanne Lenhart, and Shigetoshi Eda. Agent-based model for Johne's disease dynamics in a dairy herd. *Veterinary Research*, 46(1):1–9, 2015.

[96] Sameera Abar, Georgios K Theodoropoulos, Pierre Lemarinier, and Gregory MP O'Hare. Agent based modelling and simulation tools: A review of the state-of-art software. *Computer Science Review*, 24:13–33, 2017.

[97] Robert L Larson and Brad J White. Reproductive systems for North American beef cattle herds. *Veterinary Clinics: Food Animal Practice*, 32(2):249–266, 2016.

[98] Alejandro Ramirez, Dan Whitney, and Danelle A Bickett-Weddle. Foreign animal disease preparedness & response plan. 2011.

[99] Federal Motor Carrier Safety Administration. Summary of hours-of-service regulations, 2013.

[100] Scott A DeLoach and Juan Carlos Garcia-Ojeda. O-MaSE: a customisable approach to designing and building complex, adaptive multi-agent systems. *International Journal of Agent-Oriented Software Engineering*, 4(3):244–280, 2010.

[101] Scott A DeLoach. Omacs: A framework for adaptive, complex systems. In *Handbook of research on multi-agent systems: Semantics and dynamics of organizational models*, pages 76–104. IGI Global, 2009.

[102] Miranda R Bertram, Le T Vu, Steven J Pauszek, Barbara P Brito, Ethan J Hartwig, George R Smoliga, Bui H Hoang, Nguyen T Phuong, Carolina Stenfeldt, Ian H Fish, et al. Lack of transmission of foot-and-mouth disease virus from persistently infected cattle to naïve cattle under field conditions in Vietnam. *Frontiers in Veterinary Science*, 5:174, 2018.

[103] Y Hayama, T Yamamoto, S Kobayashi, N Muroga, and T Tsutsui. Mathematical model of the 2010 foot-and-mouth disease epidemic in Japan and evaluation of control measures. *Preventive Veterinary Medicine*, 112(3-4):183–193, 2013.

[104] Alice Namatovu, Kirsten Tjørnehøj, Graham J Belsham, Moses T Dhikusooka, Sabenzia N Wekesa, Vincent B Muwanika, Hans R Siegismund, and Chrisostom Ayebazibwe. Characterization of foot-and-mouth disease viruses (FMDVs) from Ugandan cattle outbreaks during 2012-2013: Evidence for circulation of multiple serotypes. *PLoS ONE*, 10(2):e0114811, 2015.

[105] Thomas W Bates, Mark C Thurmond, and Tim E Carpenter. Description of an epidemic simulation model for use in evaluating strategies to control an outbreak of foot-and-mouth disease. *American Journal of Veterinary Research*, 64(2):195–204, 2003.

[106] Dustin L Pendell, Thomas L Marsh, Keith H Coble, Jayson L Lusk, and Sara C Szmania. Economic assessment of FMDv releases from the national bio and agro defense facility. *PLoS ONE*, 10(6):e0129134, 2015.

[107] Anette Boklund, T Halasa, Lasse Engbo Christiansen, and Claes Enøe. Comparing control strategies against foot-and-mouth disease: will vaccination be cost-effective in Denmark? *Preventive Veterinary Medicine*, 111(3-4):206–219, 2013.

[108] Tariq Halasa, Anette Boklund, Anders Stockmarr, Claes Enøe, and Lasse E Christiansen. A comparison between two simulation models for spread of foot-and-mouth disease. *PLoS ONE*, 9(3):e92521, 2014.

[109] Leonard M Mansley, Alex I Donaldson, Michael V Thrusfield, N Honhold, et al. Destructive tension: mathematics versus experience—the progress and control of the 2001 foot and mouth disease epidemic in Great Britain. *Revue Scientifique et Technique-OIE*, 30(2):483, 2011.

[110] Krishna K Thakur, Javier Sanchez, Daniel Hurnik, Zvonimir Poljak, Sheldon Opps, and Crawford W Revie. Development of a network based model to simulate the between-farm transmission of the porcine reproductive and respiratory syndrome virus. *Veterinary microbiology*, 180(3-4):212–222, 2015.

[111] Serge W Wiltshire. Using an agent-based model to evaluate the effect of producer specialization on the epidemiological resilience of livestock production networks. *PLoS ONE*, 13(3):e0194013, 2018.

[112] Fernanda C Dórea, Maria Nöremark, Stefan Widgren, Jenny Frössling, Anette Boklund, Tariq Halasa, and Karl Ståhl. Evaluation of strategies to control a potential outbreak of foot-and-mouth disease in Sweden. *Frontiers in veterinary science*, 4:118, 2017.

[113] Neil Harvey, Aaron Reeves, Mark A Schoenbaum, Francisco J Zagmutt-Vergara, Caroline Dubé, Ashley E Hill, Barbara A Corso, W Bruce McNab, Claudia I Cartwright, and Mo D Salman. The North American Animal Disease Spread Model: A simulation model to assist decision making in evaluating animal disease incursions. *Preventive Veterinary Medicine*, 82(3-4):176–197, 2007.

[114] M Graeme Garner and SD Beckett. Modelling the spread of foot-and-mouth disease in Australia. *Australian Veterinary Journal*, 83(12):758–766, 2005.

[115] MA Stevenson, RL Sanson, MW Stern, BD O'Leary, M Sujau, N Moles-Benfell, and RS Morris. InterSpread Plus: a spatial and stochastic simulation model of disease in animal populations. *Preventive Veterinary Medicine*, 109(1-2):10–24, 2013.

[116] Richard A Bradhurst, Sharon E Roche, IJ East, P Kwan, and MG Garner. Improving the computational efficiency of an agent-based spatiotemporal model of livestock disease spread and control. *Environmental Modelling & Software*, 77:1–12, 2016.

[117] Martin Sterchi, Céline Faverjon, Cristina Sarasua, Maria Elena Vargas, John Berezowski, Abraham Bernstein, Rolf Grütter, and Heiko Nathues. The pig transport network in Switzerland: Structure, patterns, and implications for the transmission of infectious diseases between animal holdings. *PLoS ONE*, 14(5):e0217974, 2019.

[118] World Perspectives, Inc. Comprehensive feasibility study: U.S. beef cattle identification and traceability systems: Evaluation of opportunities, obstacles and incentives across the U.S. beef industry value chain, January 2018. URL https://www.ncba.org/CMDocs/BeefUSA/NCBA%20feasibility%20study%20on%20traceability_WPI%20report%2001302018.pdf.

[119] Dustin L Pendell, Gary W Brester, Ted C Schroeder, Kevin C Dhuyvetter, and Glynn T Tonsor. Animal identification and tracing in the United States. *American Journal of Agricultural Economics*, 92(4):927–940, 2010.

[120] Feng Tian. An agri-food supply chain traceability system for china based on RFID & blockchain technology. In *Proceedings of 2016 13th International Conference on Service Systems and Service Management*, pages 1–6. IEEE, 2016.

[121] Feng Tian. A supply chain traceability system for food safety based on HACCP, blockchain & Internet of things. In *Proceedings of 2017 International Conference on Service Systems and Service Management*, pages 1–6. IEEE, 2017.

[122] Miguel Pincheira Caro, Muhammad Salek Ali, Massimo Vecchio, and Raffaele Giaffreda. Blockchain-based traceability in Agri-Food supply chain management: A practi-

cal implementation. In *2018 IoT Vertical and Topical Summit on Agriculture-Tuscany*, pages 1–4. IEEE, 2018.

[123] Jun Lin, Zhiqi Shen, Anting Zhang, and Yueting Chai. Blockchain and IoT based food traceability for smart agriculture. In *Proceedings of the 3rd International Conference on Crowd Science and Engineering*, pages 1–6, 2018.

[124] USDA. SDA APHIS foot-and-mouth response plan: The red book, October 2014. URL https://www.aphis.usda.gov/animal_health/emergency_management/downloads/fmd_responseplan.pdf.

[125] Kansas Department of Agriculture. Secure beef supply plan: A foot and mouth disease preparedness and continuity of business plan, October 2019. URL https://agriculture.ks.gov/docs/default-source/rc-ah-large-animal/draft_ks_sbs_summary_plan_.pdf?sfvrsn=687783c1_12.

[126] Shankar Yadav, Carolina Stenfeldt, Matthew A Branan, Karla I Moreno-Torres, Lindsey K Holmstrom, Amy H Delgado, and Jonathan Arzt. Parameterization of the durations of phases of foot-and-mouth disease in cattle. *Frontiers in Veterinary Science*, 6:263, 2019.

[127] Emily Walz, Jamie Middleton, Fernando Sampedro, Kimberly VanderWaal, Sasidhar Malladi, and Timothy Goldsmith. Modeling the transmission of foot and mouth disease to inform transportation of infected carcasses to a disposal site during an outbreak event. *Frontiers in Veterinary Science*, 6:501, 2020.

[128] Gianluigi Rossi, Rebecca L Smith, Stefano Pongolini, and Luca Bolzoni. Modelling farm-to-farm disease transmission through personnel movements: from visits to contacts, and back. *Scientific Reports*, 7(1):1–11, 2017.

[129] Fabrizio Natale, Armando Giovannini, Lara Savini, Diana Palma, Luigi Possenti, Gianluca Fiore, and Paolo Calistri. Network analysis of Italian cattle trade patterns and

evaluation of risks for potential disease spread. *Preventive Veterinary Medicine*, 92(4): 341–350, 2009.

[130] Thibaud Porphyre, Barend M de C Bronsvoort, George J Gunn, and Carla Correia-Gomes. Multilayer network analysis unravels haulage vehicles as a hidden threat to the British swine industry. *Transboundary and Emerging Diseases*, 67(3):1231–1246, 2020.

[131] Clara Granell, Sergio Gómez, and Alex Arenas. Dynamical interplay between awareness and epidemic spreading in multiplex networks. *Physical Review Letters*, 111(12): 128701, 2013.

[132] Chunyuan Zheng, Chengyi Xia, Quantong Guo, and Matthias Dehmer. Interplay between SIR-based disease spreading and awareness diffusion on multiplex networks. *Journal of Parallel and Distributed Computing*, 115:20–28, 2018.

[133] FD Sahneh, FN Chowdhury, G Brase, and CM Scoglio. Individual-based information dissemination in multilayer epidemic modeling. *Mathematical Modelling of Natural Phenomena*, 9(2):136–152, 2014.

[134] Faryad Darabi Sahneh, Fahmida N Chowdhury, and Caterina M Scoglio. On the existence of a threshold for preventive behavioral responses to suppress epidemic spreading. *Scientific Reports*, 2(1):1–8, 2012.

[135] Sebastian Funk, Marcel Salathé, and Vincent AA Jansen. Modelling the influence of human behaviour on the spread of infectious diseases: a review. *Journal of the Royal Society Interface*, 7(50):1247–1256, 2010.

[136] Nicolò Gozzi, Daniela Perrotta, Daniela Paolotti, and Nicola Perra. Towards a data-driven characterization of behavioral changes induced by the seasonal flu. *PLoS Computational Biology*, 16(5):e1007879, 2020.

[137] Yang Ye, Qingpeng Zhang, Zhongyuan Ruan, Zhidong Cao, Qi Xuan, and Daniel Dajun Zeng. Effect of heterogeneous risk perception on information diffusion, behavior change, and disease transmission. *Physical Review E*, 102(4):042314, 2020.

[138] Amy C Kinsley, Gianluigi Rossi, Matthew J Silk, and Kimberly VanderWaal. Multilayer and multiplex networks: An introduction to their use in veterinary epidemiology. *Frontiers in Veterinary Science*, 7:596, 2020.

[139] Ho Fai Chan, Ahmed Skali, David A Savage, David Stadelmann, and Benno Torgler. Risk attitudes and human mobility during the COVID-19 pandemic. *Scientific Reports*, 10(1):1–13, 2020.

[140] Samuel Tomczyk, Maxi Rahn, and Silke Schmidt. Social distancing and stigma: Association between compliance with behavioral recommendations, risk perception, and stigmatizing attitudes during the COVID-19 outbreak. *Frontiers in Psychology*, 11: 1821, 2020.

[141] Damian Tago, James K Hammitt, Alban Thomas, and Didier Raboisson. The impact of farmers' strategic behavior on the spread of animal infectious diseases. *PLoS ONE*, 11(6):e0157450, 2016.

[142] Antonino Marvuglia, Sameer Rege, Tomas Navarrete Gutierrez, Laureen Vanni, Didier Stilmant, and Enrico Benetto. A return on experience from the application of agent-based simulations coupled with life cycle assessment to model agricultural processes. *Journal of Cleaner Production*, 142:1539–1551, 2017.

[143] Shaheen A Abdulkareem, Ellen-Wien Augustijn, Tatiana Filatova, Katarzyna Musial, and Yaseen T Mustafa. Risk perception and behavioral change during epidemics: Comparing models of individual and collective learning. *PLoS ONE*, 15(1):e0226483, 2020.

[144] Gabriela Bucini, Scott C Merrill, Eric Clark, Susan M Moegenburg, Asim Zia, Christopher J Koliba, Serge Wiltshire, Luke Trinity, and Julia M Smith. Risk attitudes affect

livestock biosecurity decisions with ramifications for disease control in a simulated production system. *Frontiers in Veterinary Science*, 6:196, 2019.

[145] Jaap Sok and Egil AJ Fischer. Farmers' heterogeneous motives, voluntary vaccination and disease spread: an agent-based model. *European Review of Agricultural Economics*, 47(3):1201–1222, 2020.

[146] Sakshi Pahwa, Amelia Hodges, Caterina Scoglio, and Sean Wood. Topological analysis of the power grid and mitigation strategies against cascading failures. In *Proceedings of 2010 IEEE International Systems Conference*, pages 272–276. IEEE, 2010.

[147] Lin Zhang, Jian Lu, Bai-bai Fu, and Shu-bin Li. A cascading failures model of weighted bus transit route network under route failure perspective considering link prediction effect. *Physica A: Statistical Mechanics and its Applications*, 523:1315–1330, 2019.

[148] Malgorzata Turalska, Keith Burghardt, Martin Rohden, Ananthram Swami, and Raissa M D'Souza. Cascading failures in scale-free interdependent networks. *Physical Review E*, 99(3):032308, 2019.

[149] Yi Shen, Gang Ren, Ning Zhang, Guohao Song, Qin Wang, and Bin Ran. Effects of mutual traffic redistribution on robustness of interdependent networks to cascading failures under fluctuant load. *Physica A: Statistical Mechanics and its Applications*, 560:125138, 2020.

[150] Cristian E La Rocca, H Eugene Stanley, and Lidia A Braunstein. Strategy for stopping failure cascades in interdependent networks. *Physica A: Statistical Mechanics and its Applications*, 508:577–583, 2018.

[151] Jilong Zhong, FengMing Zhang, Shunkun Yang, and Daqing Li. Restoration of interdependent network against cascading overload failure. *Physica A: Statistical Mechanics and its Applications*, 514:884–891, 2019.

[152] Christoph Bode and Stephan M Wagner. Structural drivers of upstream supply chain

complexity and the frequency of supply chain disruptions. *Journal of Operations Management*, 36:215–228, 2015.

[153] Dmitry Ivanov, Boris Sokolov, and Alexandre Dolgui. The ripple effect in supply chains: trade-off 'efficiency-flexibility-resilience' in disruption management. *International Journal of Production Research*, 52(7):2154–2172, 2014.

[154] Rodrigo Reyes Levalle and Shimon Y Nof. Resilience by teaming in supply network formation and re-configuration. *International Journal of Production Economics*, 160: 80–93, 2015.

[155] Seyedmohsen Hosseini, Nazanin Morshedlou, Dmitry Ivanov, MD Sarder, Kash Barker, and Abdullah Al Khaled. Resilient supplier selection and optimal order allocation under disruption risks. *International Journal of Production Economics*, 213:124–137, 2019.

[156] Bill Canis. *Motor vehicle supply chain: effects of the Japanese earthquake and tsunami.* DIANE publishing, 2011.

[157] Yu Zeng, Renbin Xiao, and Xiangmei Li. A resilience approach to symbiosis networks of ecoindustrial parks based on cascading failure model. *Mathematical Problems in Engineering*, 2013, 2013.

[158] Liangan Huo, Hongyuan Guo, Yingying Cheng, and Xiaoxiao Xie. A new model for supply chain risk propagation considering herd mentality and risk preference under warning information on multiplex networks. *Physica A: Statistical Mechanics and its Applications*, 545:123506, 2020.

[159] Nils Goldbeck, Panagiotis Angeloudis, and Washington Ochieng. Optimal supply chain resilience with consideration of failure propagation and repair logistics. *Transportation Research Part E: Logistics and Transportation Review*, 133:101830, 2020.

[160] Liang Geng and Renbin Xiao. Outer synchronization and parameter identification

approach to the resilient recovery of supply network with uncertainty. *Physica A: Statistical Mechanics and its Applications*, 482:407–421, 2017.

[161] Haiyang Fang, Dali Jiang, Tinghong Yang, Ling Fang, Jian Yang, Wu Li, and Jing Zhao. Network evolution model for supply chain with manufactures as the core. *PLoS ONE*, 13(1):e0191180, 2018.

[162] Dmitry Ivanov, Boris Sokolov, and Joachim Kaeschel. A multi-structural framework for adaptive supply chain planning and operations control with structure dynamics considerations. *European Journal of Operational Research*, 200(2):409–420, 2010.

[163] Julie Drzymalski, Nicholas G Odrey, and George R Wilson. Aggregating performance measures of a multi-echelon supply chain using the analytical network and analytical hierarchy process. *International Journal of Services, Economics and Management*, 2 (3-4):286–306, 2010.

[164] Stefano Zapperi, Purusattam Ray, H Eugene Stanley, and Alessandro Vespignani. First-order transition in the breakdown of disordered media. *Physical Review Letters*, 78(8):1408, 1997.

[165] Yingrui Zhang and Osman Yağan. Optimizing the robustness of electrical power systems against cascading failures. *Scientific Reports*, 6(1):1–15, 2016.

[166] Juan M Hernández and Carmen Pedroza-Gutiérrez. Estimating the influence of the network topology on the agility of food supply chains. *PLoS ONE*, 14(7):e0218958, 2019.

[167] Sónia R Cardoso, Ana Paula Barbosa-Póvoa, Susana Relvas, and Augusto Q Novais. Resilience metrics in the assessment of complex supply-chains performance operating under demand uncertainty. *Omega*, 56:53–73, 2015.

[168] Osman Yağan. Robustness of power systems under a democratic-fiber-bundle-like model. *Physical Review E*, 91(6):062811, 2015.

[169] Antonio Scala and Pier Giorgio De Sanctis Lucentini. The equal load-sharing model of cascade failures in power grids. *Physica A: Statistical Mechanics and its Applications*, 462:737–742, 2016.

[170] Henry Ellis Daniels. The statistical theory of the strength of bundles of threads. i. *Proceedings of the Royal Society of London. Series A. Mathematical and Physical Sciences*, 183(995):405–435, 1945.

[171] Nanshan Chen, Min Zhou, Xuan Dong, Jieming Qu, Fengyun Gong, Yang Han, Yang Qiu, Jingli Wang, Ying Liu, Yuan Wei, et al. Epidemiological and clinical characteristics of 99 cases of 2019 novel coronavirus pneumonia in Wuhan, China: a descriptive study. *The Lancet*, 395(10223):507–513, 2020.

[172] Jasper Fuk-Woo Chan, Shuofeng Yuan, Kin-Hang Kok, Kelvin Kai-Wang To, Hin Chu, Jin Yang, Fanfan Xing, Jieling Liu, Cyril Chik-Yan Yip, Rosana Wing-Shan Poon, et al. A familial cluster of pneumonia associated with the 2019 novel coronavirus indicating person-to-person transmission: a study of a family cluster. *The Lancet*, 395(10223): 514–523, 2020.

[173] Camilla Rothe, Mirjam Schunk, Peter Sothmann, Gisela Bretzel, Guenter Froeschl, Claudia Wallrauch, Thorbjörn Zimmer, Verena Thiel, Christian Janke, Wolfgang Guggemos, et al. Transmission of 2019-nCoV infection from an asymptomatic contact in Germany. *New England Journal of Medicine*, 382(10):970–971, 2020.

[174] Hiroshi Nishiura, Sung-mok Jung, Natalie M Linton, Ryo Kinoshita, Yichi Yang, Katsuma Hayashi, Tetsuro Kobayashi, Baoyin Yuan, and Andrei R Akhmetzhanov. The extent of transmission of novel coronavirus in Wuhan, China, 2020. *Journal of Clinical Medicine*, 2020.

[175] Steven Sanche, Yen Ting Lin, Chonggang Xu, Ethan Romero-Severson, Nicolas W Hengartner, and Ruian Ke. The novel coronavirus, 2019-nCoV, is highly contagious and more infectious than initially estimated. *arXiv preprint arXiv:2002.03268*, 2020.

[176] Joseph T Wu, Kathy Leung, and Gabriel M Leung. Nowcasting and forecasting the potential domestic and international spread of the 2019-nCoV outbreak originating in Wuhan, China: a modelling study. *The Lancet*, 395(10225):689–697, 2020.

[177] Zhanwei Du, Lin Wang, Simon Cauchemez, Xiaoke Xu, Xianwen Wang, Benjamin J Cowling, and Lauren Ancel Meyers. Risk for transportation of coronavirus disease from Wuhan to other cities in China. *Emerging Infectious Diseases*, 26(5):1049, 2020.

[178] Shi Zhao, Qianyin Lin, Jinjun Ran, Salihu S Musa, Guangpu Yang, Weiming Wang, Yijun Lou, Daozhou Gao, Lin Yang, Daihai He, et al. Preliminary estimation of the basic reproduction number of novel coronavirus (2019-nCoV) in China, from 2019 to 2020: A data-driven analysis in the early phase of the outbreak. *International Journal of Infectious Diseases*, 92:214–217, 2020.

[179] Wei-jie Guan, Zheng-yi Ni, Yu Hu, Wen-hua Liang, Chun-quan Ou, Jian-xing He, Lei Liu, Hong Shan, Chun-liang Lei, David SC Hui, et al. Clinical characteristics of coronavirus disease 2019 in China. *New England Journal of Medicine*, 382(18): 1708–1720, 2020.

[180] Chaolin Huang, Yeming Wang, Xingwang Li, Lili Ren, Jianping Zhao, Yi Hu, Li Zhang, Guohui Fan, Jiuyang Xu, Xiaoying Gu, et al. Clinical features of patients infected with 2019 novel coronavirus in Wuhan, China. *The Lancet*, 395(10223):497–506, 2020.

[181] Jonathan M Read, Jessica RE Bridgen, Derek AT Cummings, Antonia Ho, and Chris P Jewell. Novel coronavirus 2019-nCoV: early estimation of epidemiological parameters and epidemic predictions. *MedRxiv*, 2020.

[182] Xinhai Li, Xumao Zhao, and Yuehua Sun. The lockdown of Hubei Province causing different transmission dynamics of the novel coronavirus (2019-nCoV) in Wuhan and Beijing. *MedRxiv*, 2020.

[183] Mingwang Shen, Zhihang Peng, Yuming Guo, Yanni Xiao, and Lei Zhang. Lockdown

may partially halt the spread of 2019 novel coronavirus in Hubei province, China. *MedRxiv*, 2020.

[184] Matteo Chinazzi, Jessica T Davis, Marco Ajelli, Corrado Gioannini, Maria Litvinova, Stefano Merler, Ana Pastore y Piontti, Kunpeng Mu, Luca Rossi, Kaiyuan Sun, et al. The effect of travel restrictions on the spread of the 2019 novel coronavirus (COVID-19) outbreak. *Science*, 368(6489):395–400, 2020.

[185] Shengjie Lai, Nick W Ruktanonchai, Liangcai Zhou, Olivia Prosper, Wei Luo, Jessica R Floyd, Amy Wesolowski, Mauricio Santillana, Chi Zhang, Xiangjun Du, et al. Effect of non-pharmaceutical interventions to contain COVID-19 in China. *Nature*, 585(7825): 410–413, 2020.

[186] Xiaolin Zhu, Aiyin Zhang, Shuai Xu, Pengfei Jia, Xiaoyue Tan, Jiaqi Tian, Tao Wei, Zhenxian Quan, and Jiali Yu. Spatially explicit modeling of 2019-nCoV epidemic trend based on mobile phone data in mainland China. *MedRxiv*, 2020.

[187] Tianzhi Wu, Xijin Ge, Guangchuang Yu, and Erqiang Hu. Open-source analytics tools for studying the COVID-19 coronavirus outbreak. *MedRxiv*, 2020.

[188] Faryad Darabi Sahneh, Caterina Scoglio, and Piet Van Mieghem. Generalized epidemic mean-field model for spreading processes over multilayer complex networks. *IEEE/ACM Transactions on Networking*, 21(5):1609–1620, 2013.

[189] Qihui Yang, Haiyan Lu, Caterina Scoglio, Martin de Jong, and Don Gruenbacher. A network-based approach to model the development of city branding in China. *Computers, Environment and Urban Systems*, 72:161–176, 2018.

[190] Qun Li, Xuhua Guan, Peng Wu, Xiaoye Wang, Lei Zhou, Yeqing Tong, Ruiqi Ren, Kathy SM Leung, Eric HY Lau, Jessica Y Wong, et al. Early transmission dynamics in Wuhan, China, of novel coronavirus–infected pneumonia. *New England Journal of Medicine*, 2020.

[191] Qianying Lin, Shi Zhao, Daozhou Gao, Yijun Lou, Shu Yang, Salihu S Musa, Maggie H Wang, Yongli Cai, Weiming Wang, Lin Yang, et al. A conceptual model for the coronavirus disease 2019 (COVID-19) outbreak in Wuhan, China with individual reaction and governmental action. *International Journal of Infectious Diseases*, 93: 211–216, 2020.

[192] Juanjuan Zhang, Maria Litvinova, Yuxia Liang, Yan Wang, Wei Wang, Shanlu Zhao, Qianhui Wu, Stefano Merler, Cécile Viboud, Alessandro Vespignani, et al. Changes in contact patterns shape the dynamics of the COVID-19 outbreak in China. *Science*, 368(6498):1481–1486, 2020.

[193] Hubei Provincial Bureau of Statistics. Hubei Province Statistical Yearbook 2019, March 2020. URL http://tjj.hubei.gov.cn/tjsj/sjkscx/tjnj/qstjnj/.

[194] Nguyen Quoc Viet, Behzad Behdani, and Jacqueline Bloemhof. The value of information in supply chain decisions: A review of the literature and research agenda. *Computers & Industrial Engineering*, 120:68–82, 2018.

[195] Minkyun Kim and Sangmi Chai. The impact of supplier innovativeness, information sharing and strategic sourcing on improving supply chain agility: Global supply chain perspective. *International Journal of Production Economics*, 187:42–52, 2017.

[196] Zhaojing Wang, Tengyu Wang, Hao Hu, Jie Gong, Xu Ren, and Qiying Xiao. Blockchain-based framework for improving supply chain traceability and information sharing in precast construction. *Automation in Construction*, 111:103063, 2020.